Reconnaissance geochemical mapping of map sheets 67 V.1 and 68 V.1 (66° to 68°N, 51°40′ to 54°W), West Greenland

Agnete Steenfelt, Else Dam
and Jens Peter Nielsen

Open File Series 93/1

January 1993

GRØNLANDS GEOLOGISKE UNDERSØGELSE
Ujarassiortut Kalaallit Nunaanni Misissuisoqarfiat
GEOLOGICAL SURVEY OF GREENLAND

GRØNLANDS GEOLOGISKE UNDERSØGELSE
Ujarassiortut Kalaallit Nunaanni Misissuisoqarfiat
GEOLOGICAL SURVEY OF GREENLAND
Øster Voldgade 10, DK-1350 Copenhagen K, Denmark

The Geological Survey of Greenland (GGU) is a research institute affiliated to the Mineral Resources Administration for Greenland (MRA) within the Danish Ministry of Energy. As with all other activities involving the non-living resources in Greenland, GGU's investigations are carried out within the framework of the policies decided jointly by the Greenland Home Rule Authority and the Danish State.

Open File Series

The Open File Series consists of unedited reports and maps that are made available quickly in limited numbers to the public. They are a non-permanent form of publication that may be cited as sources of information. Certain reports may be replaced later by edited versions.

Citation form

Open File Series Grønlands Geologiske Undersøgelse

conveniently abbreviated to:

Open File Ser. Grønlands geol. Unders.

GGU's Open File Series består af uredigerede rapporter og kort, som publiceres hurtigt og i et begrænset antal. Disse publikationer er midlertidige og kan anvendes som kildemateriale. Visse af rapporterne vil evt. senere blive erstattet af redigerede udgaver.

ISSN 0903-7322

GRØNLANDS GEOLOGISKE UNDERSØGELSE
Open File Series 93/1

Reconnaissance geochemical mapping of map sheets 67 V. 1 and 68 V. 1 (66° to 68°N, 51°40′ to 54° W), West Greenland

Agnete Steenfelt, Else Dam and Jens Peter Nielsen

January 1993

Abstract

Geochemical mapping by means of stream sediment and water collected at a density of 1 sample per c. 20 km^2 has been carried out over two map sheets covering the western part of the Proterozoic Nagssugtoqidian mobile belt in West Greenland. The <0.1 mm fraction of the sediment samples were analysed by X-ray fluorescence and instrumental neutron activation techniques and results are reported for 44 major and trace elements. The conductivity and fluoride content of the water samples were determined.

The distribution of geochemical anomalies in the survey area indicates that the most promising setting for base metal and gold mineralisation is where shear zones affect supracrustal enclaves in the gneisses.

Geochemical provinces are recognised in many of the element distribution maps which may be related to lithotectonic units and the intrusion of magmas of shonkinitic and lamprophyric affinities. The main geochemical boundary coincides with a pronounced zone of Proterozoic ductile shearing and thrusting (the Ikertooq shear zone).

Introduction

The sampling carried out in map sheets 67 V 1 and 68 V 1 is part of the Geological Survey of Greenland (GGU)'s geochemical mapping programme based on drainage samples. The purpose of this programme is to provide reconnaissance geochemical data which may be used together with geophysical and geological information to outline provinces or zones with potential for mineral resources.

Samples were collected during the period 2th to 21th of July by A.Steenfelt and E. Dam and from 22th of July to 15th of August 1992 by J.P. Nielsen and P. Wulff. The two sampling teams were based in Sisimiut (Holsteinsborg) and used a Bell 206 (Jet Ranger) helicopter for transportation. A part of the 1992 sampling programme was financially supported by the Mineral Resource Administration for Greenland under the Danish Ministry of Energy.

Administratively the surveyed area is divided between the communities of Kangaatsiaq, Sisimiut (Holsteinsborg) and Maniitsoq (Sukkertoppen).

Geology

The survey area lies within the Nagssugtoqidian mobile belt of the Precambrian Laurentian shield (Escher et al., 1976; Korstgaard, 1979a). The belt consists mainly of Archaean basement (gneiss with subordinate supracrustal sequences) which was reworked during the Proterozoic c. 1850 Ma ago (Figs 1 and 2). In the inner fjord zone south of Arfersiorfik (east of the survey area) some units of calc-alkaline volcanic and plutonic rocks have been shown to be of Proterozoic juvenile origin (Kalsbeek et al., 1987); Proterozoic metasediments also occur.

Most of the Nagssugtoqidian (Proterozoic) deformation and magma generation is presently believed to be related to a collision between two Archaean continents about 1850 Ma ago (Kalsbeek et al., 1987; Bridgwater et al., 1990; Larsen & Rex, 1992). However, geological field work has been very limited in the Nagssuqtoqidian belt since the recognition of the Proterozoic age and juvenile origin of some of the rocks, and the exact character and location of a suture has not yet been established.

The coastal section of this region and the fjord zones was first mapped geologically by Noe-Nygaard & Ramberg (1961), and was later covered by GGU's geological maps at 1:500 000 sheet 2 and 3 which join at 66° 45'N (Escher, 1971; Allaart, 1982). The northern quarter part of the survey area (67 V 1 N) was mapped at 1:100 000 scale (Olesen, 1984).

The Archaean basement gneisses are granodioritic or tonalitic in composition and are metamorphosed to amphibolite or granulite facies (Fig. 2). The enclaves of supracrustal rocks comprise sequences of semi-pelitic metasediments and marble as well as of basic and intermediate volcanic rocks (amphibolites and metaandesites). The individual supracrustal rock types are not distinguished in Fig. 2.

Structurally, the Nagssugtoqidian mobile belt is characterised by a number of ENE trending straight belts separating areas where large scale open fold structures are preserved (Escher et al., 1976; see Fig. 1). Pronounced shear movements took place in the Nordre Strømfjord shear zone (NSSZ; Sørensen, 1983) which transects the northern part of the survey area (Fig. 2). Two other conspicuous shear zones or belts have been recognised in the area, the Ikertooq and Itilleq belts (see Korstgård, 1979a; Bak et al., 1975). The southern Itilleq is probably Archaean (Kalsbeek & Zeck, 1978) whereas the Ikertooq belt contains Archaean shearing overprinted by Proterozoic ductile thrusting (Korstgård, 1979; Korstgård et al, 1987).

The latest shear movements in the Nagssugtoqidian mobile belt are Proterozoic as they affect the Kangâmiut dykes (1950 Ma of age, Kalsbeek et al., 1978) and the Arfersiorfik quartz diorite (1920 Ma of age, Kalsbeek et al., 1987), and so are some large open folds which involve Proterozoic supracrustals south of the NSSZ.

Physiography

The relief of the surveyed area is moderate in the northern part to steep in the southern with elevations reaching 1400-1500 m above sea level. The streams are generally running from May to September, although those being sustained by melting snow commonly dry up during July. The spring of 1992 had been unusually cold and the snow cover had just started to melt at the beginning of July. The onset of summer produced high melting rates and high flow rates in the streams throughout the sampling period, which reduced the deposition of fine grained stream sediment. As a result a number of the samples did not contain enough fine fraction material for the entire analytical programme.

The bedrock exposure is generally good except in valleys and on gentle slopes where the surface is covered by talus and vegetation (herbs, grass, low scrubs).

Sampling

Thirty working days and 83 helicopter flying-hours were spent during the sampling of 706 sites distributed over 14500 square km. On average 23 samples were collected per day at a density of 1 site per 20.5 square km; 7 flying minutes were spent per sampling site, which corresponds to 20 flying seconds per square km.

The sample sites were selected and marked on air photos prior to the sampling using criteria such as even distribution of the sites, a reasonable size of upstream drainage area, and a reasonable slope dip.

At each station c. 500 g of stream sediment was collected in a paper bag and 100 ml of stream water in a polyethylene bottle. In addition the radioactivity (total gamma-radiation) was measured on the surface of outcrops or stream boulders using a scintillometer (Table 1). To increase the representativity each stream sediment sample was composed of subsamples from 3 to 7 different sites of sand and silt deposits in the stream bed or banks. Duplicate samples of both sediment and water were collected at 21 sites which corresponds to 3 % of the total number of sites.

The central part of the Nordre Strømfjord region (Fig. 2) was sampled during a uranium exploration programme in 1977 (Watt, 1977), where stream sediment and water samples were collected at higher density (1 sample per 4 km^2 on average). As these samples were archived, there was no need to resample this area.

Sample preparation and analysis

Sediment. The sample bags were dried at room temperature at the base-camp in Sisimiut and then sent by ship to GGU, Copenhagen. Here the samples were further dried at 65° C and sieved into three grain size fractions using sieve apertures of 1 mm and 0.1 mm. The coarse fraction was discarded, the medium fraction archived, and the fine fraction submitted for analysis to Activation Laboratories Ltd., Canada.

The samples were analysed by instrumental neutron activation (INA) method for Au and 34 other elements, by X-ray fluorescence using pressed powder pellets for 14 trace elements (XRF-trace) and by X-ray fluorescence on fused discs, using Li-borate, for major elements (XRF-major). Some samples did not contain sufficient amounts of the fine fraction to permit all three types of analysis, and this explains the decreasing number of samples analysed: 653 INA, 638 XRF-trace, and 542 XRF-major. The samples from the Nordre Strømfjord uranium exploration programme were analysed by INA at Activation Laboratories Ltd.

Water. The water samples (totalling 665) were sent by ship to GGU, Copenhagen, where they were analysed c. 2 months after collection. The conductivity and fluoride concentration were measured (Table 1).

Data presentation

The analytical results from 67 V 1 and 68 V 1 are shown in this report as element distribution maps at the scale of 1:1 000 000 together with summary statistical parameters and histograms of the frequency distribution for each element (Figs 3 to 47). A total of 59 samples were selected with a density of c. 1 per 20 km^2 from the detailed uranium exploration sample collection and the analytical results were included in the data set presented. However, the additional samples are not yet analysed for XRF-major and XRF-trace elements, and in the corresponding element distribution maps the area is left blank. A total of 41 samples collected in the 1992 field season outside the map frame are not displayed.

Elements with insignificant concentrations, i.e. at or below the detection limit (Table 2), are not presented. In cases where an element has been determined by more than one method only one of the data sets is presented: the one regarded as the most reliable or determined at the lowest detection limit. The major elements are expressed as oxides and the plots represent analytical values recalculated as volatile free components. The amount of volatiles (as determined by loss on ignition) is on average 6.5 %, 95th percentile is 18 %, and maximum value 42 %. The high amounts of volatiles were obtained in samples with high proportions of organic matter.

In the element distribution maps the size of a dot is proportional to the concentration in the sample. The scaling of the dot size is chosen so that regional variations in the geochemical background are displayed as clearly as possible. Maximum values are found in the statistical parameters in the figures, and values regarded as geochemical anomalies are shown on the anomaly maps (Figs 46 and 47).

Comments on the element distribution patterns

In general the element distribution patterns reflect the lithogeochemical variation over the survey area and high values for some elements can often be interpreted to indicate mineralisation. In the present map sheets the main contributors to the lithogeochemical variation are the gneisses, the supracrustal enclaves and the granite/pegmatite intrusions.

The supracrustal rock group which has not been subdivided in Fig. 2, comprises basic metavolcanics ("amphibolites"), and metasediments including marble. Enclaves of these rocks occur frequently in the basement gneisses, also as abundant smaller units which cannot be shown on the simplified geological map of Fig. 2. The presence of amphibolites in the gneisses is reflected by scattered elevated values of Mg, Co, and Cu whereas the metasediments, having a gross chemical composition similar to the surrounding gneisses, are only reflected by higher concentrations of elements, such as Zn, Pb, Cu, As, derived from eventual mineralisation within the metasediments. The marble occurrences are too small to influence the element distribution patterns.

In Table 3 the means for element concentrations over the whole of map sheets 67 V 1 + 68 V 1 are compared with average values for upper and lower crust according to Taylor and McLennan (1985). With regard to most of the elements the survey area corresponds to a position between upper and lower crust which is in agreement with the predominance of granodioritic to dioritic gneisses with supracrustal rocks metamorphosed under amphibolite to granulite facies conditions. Exceptions are Ba, Sr, and REE, particularly light REE, which are enriched in the survey area even beyond the level corresponding to upper crust, see the discussion below.

Element distribution indicating mineralisation

High values of ore forming elements may be indicative of mineralisation. In the neighbouring areas the most promising geochemical and field indications of mineralisation were found to be associated with sheared supracrustal rocks (Steenfelt & Dam, 1991; Steenfelt et al., 1992). In Fig. 46 the location of the highest values for Au, As, Cu, Pb, Zn, Ni and Cr are shown together with the prominent shear zones. It appears that there is some clustering of anomalies associated with NSSZ, IKSZ, and the Proterozoic thrust north of Sukkertoppen ice cap but there are also scattered anomalies, particularly in the southern region.

The Cu anomalies occur in a province which is characterised by an elevated background for Cu (Fig. 20 and 47). The Cu-province is interpreted to reflect that the supracrustals within this province are dominated by basic metavolcanics possibly of oceanic origin. The highest Cu values in this province indicate that Cu mineralisation may have occurred within these rocks. The high Ni and Cr values may be indicative of inclusions of ultramafic rocks in the gneisses, as such are shown in the geological map south of ITSZ (Allaart, 1982).

Geochemical variation related to crustal structure

Many of maps display element variations in which distinct provinces are recognised. These are displayed in Fig. 47. The most conspicuous geochemical boundary coincides with the thrust belt separating the granulite belt (province III) and the amphibolite facies terrain (province IV). As a general feature the area north of the boundary is higher in Zr, Hf and Th than the terrain south of the boundary.

The northernmost province (I) has elevated SiO_2, K_2O, Rb and U reflecting the predominance of granodioritic to granitic gneisses (Henderson, 1969). The blank area (province II) in Fig. 47 has concentration levels corresponding to the total survey medians for most elements except those just mentioned, which are higher in both province I and II. The levels for MnO, MgO, Na_2O, Cu, Nb and Ni are slightly lower than the medians.

Province III is very pronounced, see element characteristics in Fig. 47. The northern and southern boundaries of the province are distinct whereas the eastern boundary is not defined by the maps. However, it is known from the geochemical mapping of the map sheet 67 V 2 that such high concentrations of Ba, Sr, P_2O_5 and REE do not continue towards the east (Steenfelt & Dam, 1991). The province is underlain by granulite facies gneiss interleaved with garnet rich quartz-feldspar gneiss termed granulite (s.s.) by Noe-Nyegaard and Ramberg (1960). The granulite is most abundant in the northwestern part of this province which is characterised by high Al_2O_3, K_2O and Ga (Figs 5, 11 and 22). The geological observations during the stream sampling confirmed that brown granulite facies gneiss is common throughout the province but also revealed that light coloured feldspar and garnet rich intrusive veins or pegmatitic schlieren are common. The geochemical response over the remaining hypersthene gneiss terrain to the north and east is less pronounced, and the enrichment in Ba, Sr etc. is ascribed to the leucocratic garnetiferous phase. A small cluster of c. 10 samples close to longitude 53°W is high in Th, U, and Rb (Figs 36, 37 and 31). It is interpreted to reflect the occurrence of pegmatites, as pegmatites were observed at some of the sample sites in this area.

Six samples have extreme compositions as seen in Table 3. Their location is shown in Fig. 47. They cluster at two sites, of which the western is the most enriched in Ba, Sr, REE and P_2O_5. The geochemical signature suggest that the rock type drained by the streams is akin to alkaline-ultramafic rocks or carbonatites. A large number of dykes including lamprophyres, kimberlites, shonkinites and monchiquites has been registered in this region (reviewed by Larsen & Rex, 1992) as well as the Sarfartoq carbonatite complex immediately southeast of the survey area (Secher & Larsen, 1980). Three of the dyke analyses in Larsen & Rex (1992) were selected as the closest in composition to the anomalous stream sediments and are shown in Table 3: two shonkinites from the surroundings of the Sarfartoq carbonatite and a monchiquite from the north shore of Itilleq.

Based on the chemical similarities it is suggested that the geochemical anomalies between Nordre Isortoq and Ikertooq reflects intrusion of magma with shonkinitic affinity into the hypersthene gneiss terrain. The volume of such magma must be more than just one dyke to account for the anomalies of which the western cluster represents a total drainage area of c. 5 km^2. The elevated background for Ba, Sr, P_2O_5, etc in the geochemical province surrounding the anomalies may reflect that the entire province is intruded by dykes or veins of a magmatic rock, but there may also be other explanations and further speculations should await further investigations. Near the coast at latitude 66° 30'N there is a N-S elongate cluster of samples enriched in P_2O_5, CaO, Sr, and LREE which may also indicate a dyke? occurrence of lamprophyric or kimberlitic affinity. Such dykes occur on the north shore of Itilleq

(Larsen & Rex, 1992).

The area south of the thrust belt is divided into two provinces (IV and V). The southernmost is the Archean terrain which escaped Proterozoic deformation, and which comprises granulite facies gneiss with few enclaves of supracrustal rocks. This terrain is intruded by the Kangamiut dyke swarm. Geochemically, the province is characterised by low level of most lithophile elements and high level of Cr and ferro-magnesian elements. The chemical signature agrees with a low crustal level (Taylor & McLennan, 1985), particularly in the western part of the area. At either side of Søndre Strømfjord the granodiorite is reflected by elevated K_2O, Lu, Rb, Sc, Y and lower Ni compared to the surrounding gneiss terrain.

The remaining geochemical province (IV) coincides roughly with the Archaean terrain affected by Proterozoic deformation (deformation of Kangâmiut dykes) and in amphibolite facies. The province displays an uneven pattern for many elements with scattered high values in a background of low values. The province is particularly distinguished by unevenly distributed high U values (Fig. 37), but the same type of pattern is displayed by the other elements noted as high in Fig. 47 (Th, Nb, Rb, LREE, Cu). The element association is suggestive of alkaline to carbonatitic magmatic rocks and the scattered anomalous samples may reflect the occurrence of dykes or veins and associated fenitisation related to the intrusion of the Sarfartoq carbonatite complex situated only 25 km east of the map area at latitude 66° 30'N. In reconnaissance geochemical maps the Sarfartoq carbonatite complex, which hosts a pyrochlore mineralisation, is particularly characterised by Nb anomalies (Steenfelt, 1991).

Supplementary investigations

In the course of the stream sediment programme samples were also collected to examine the geochemical response from rust zones in the Ikertooq shear belt, localities A and B in Fig. 46.

At loc. A, altitude 200 to 250 m, within the granulite facies terrain the rust zones were found to be associated with sheared supracrustal rocks close to a mylonite, 15 metres wide, the trend of which is indicated with a fault signature in Fig. 46. Two samples of stream sediment and 8 soil samples were collected across the valley hosting the mylonite. Most of the valley is covered by thin overburden soil supporting dense low vegetation. At each soil sample site 4 pits were dug and soil was collected from the horizon below the plant and humus layer, which is usually immediately above the weathered bedrock.

At loc. B, altitude 650 to 700 m, situated in the amphibolite facies terrain, rust zones are extensive and also here associated with sheared supracrustal sequences. The bedrock exposure is much better at this locality, being at higher altitude, than at loc. A, and the 9 number of soil samples were collected as composite samples directly from the surface of the soil formed by weathering bedrock. The samples were preferably collected from the rust zones.

The analyses of the samples from loc. A and B are shown in Table 4. The highest values of ore forming elements Cu, Ni, Cr, V, Mo, As are associated with loc. B in the Ikertooq shear zone. One sample derived from weathering products of bleached gneiss is enriched in Pb, Cu and Ni which indicates that mineralisation was probably associated with hydrothermal activity. The difference in overall chemistry of the soil samples between the two localities reflect the their location in two different lithological provinces. Loc. A is generally higher in SiO_2, CaO, Na_2O, Sr and Ba than loc.B whereas loc. B has higher TiO_2, Fe_2O_3, MgO, K_2O, Nb, Rb in addition to the metals already mentioned. The differences are in agreement with the variation displayed by the stream sediment maps.

Conclusion

The distribution of high values for Au, As, Cu, Pb, Zn, Ni seems indicative of mineralisation where supracrustal sequences are affected by Proterozoic shear zones. The supracrustal enclaves south of the Itilleq shear zone are characterised by high Cu which is suggested to reflect predominance of basaltic metavolcanics which may be Cu mineralised.

The variations in geochemical bakground over the survey area defines geochemical provinces which are interpreted to reflect a change in crustal level from higher in the north to lower in the south. The boundaries between some of the provinces are sharp suggesting that they may be of tectonic nature.

Anomaly patterns for Ba, Sr, P_2O_5, and REE indicate that a large area of reworked Archaean basement may be intruded by dykes of alkaline-ultramafic kind. Dykes of such magma types have been recorded along the coasts, particularly between Itilleq and Sisimiut.

Acknowledgment. The sampling benefitted greatly from the skill and keen cooperation of the GLACE helicopter pilot Olle Westlund.

References

Allaart, J. H. 1982: Geological map of Greenland. 1:500 000 sheet 2, Frederikshåb Isblink to Søndre Strømfjord. Copenhagen: Geol. Surv. Greenland.

Bak, J., Sørensen, K., Grocott, J., Korstgård, J.A., Nash, D. & Watterson, J. 1975: Tectonic implications of Precambrian shear belts in western Greenland. *Nature*, 254, 566-569.

Bridgwater, D., Austrheim, H., Hansen, B.T., Mengel, F., Pedersen, S. & Winter, J. 1990: The Proterozoic Nagssugtoqidian mobile belt of southeast Greenland: A link between the eastern Canada and Baltic shields. *Geosci. Can.* 17, 305-310.

Escher, A. 1971: Geological map of Greenland. 1:500 000 sheet 3, Søndre Strømfjord - Nûgssuaq. Copenhagen: Geol. Surv. Greenland.

Escher, A., Sørensen, K. & Zeck, H.P. 1976: Nagssugtoqidian mobile belt in West Greenland. *In* Escher, A. & Watt, W. S. (ed.) *Geology of Greenland,* 77-95. Copenhagen: Geol. Surv. Greenland.

Grocott, J. 1979: Controls of metamorphic grade in shear belts. *Rapp. Grønlands geol. Unders.* 89, 47-62.

Henderson, G. 1969: The Precambrian rocks of the Egedesminde-Christianshåb area, West Greenland. *Rapp. Grønlands geol. Unders.* 23, 37 pp.

Kalsbeek, F. & Zeck, H. 1978: Preliminary Rb-Sr whole-rock data for Archaean and Nagssugtoqidian rocks from the Søndre Strømfjord area, West Greenland. *Rapp. Grønlands geol. Unders.* 90, 129-134.

Kalsbeek, F., Bridgwater, D.B. & Zeck, H. 1978: A 1950+/-60 Ma Rb-Sr whole rock isochron age from two Kangâmiut dykes and the timing of the Nagssugtoqidian (Hudsonian) orogeny in West Greenland. *Can. J. Earth Sci.* 15, 1122-1128.

Kalsbeek, F., Pidgeon, R.T. & Taylor, P. 1987: Nagssugtoqidian mobile belt of West Greenland: a cryptic suture between two Archaean continents - chemical and isotopic evidence. *Earth Planet. Sci. Lett.* 85, 365-385.

Korstgård, J.A. (ed.) 1979a: Nagssugtoqidian geology. *Rapp. Grønlands geol. Unders.* 89. 146 pp.

Korstgård, J.A. 1979b: Metamorphism of the Kangâmiut dykes and the metamorphic and structural evolution of the southern Nagssugtoqidian boundary in the Itivdleq-Ikertôq region, West Greenland. *Rapp. Grønlands geol. Unders.* 89, 63-75.

Korstgård, J.A., Ryan, B. & Wardle, R. 1987: The boundary between Proterozoic and Archaean crustal blocks in central West Greenland and northern Labrador. *In* R.G. Park & J. Tarney (eds) *Evolution of the Lewisian and comparable Precambrian terrains*, Geological Society Special Publication 27, 247-259.

Larsen, L.M. & Rex, D.C. 1992: A review of the 2500 span of alkaline-ultramafic, potassic and carbonatitic magmatism in West Greenland. *Lithos* 28, 367-402.

Noe-Nygaard, A. & Ramberg, H. 1961: Geological reconnaissance map of the country between latitudes 69°N and 63°45' N, West Greenland. *Meddr Grønland,* 123 (5), 1 map, 9pp.

Olesen, N.Ø. 1984: Geologisk kort over Grønland 1:100 000, Agto 67 V.1 Nord. Copenhagen: Geol. Surv. Greenland.

Secher, K. & Larsen, L.M. 1980: Geology and mineralogy of the Sarfartôq carbonatite complex, southern West Greenland. *Lithos* 13, 199-212.

Steenfelt, A. 1991: High-technology metals in alkaline and carbonatitic rocks in Greenland: recognition and exploration. *J. Geochem. Explor.* 40, 263-279.

Steenfelt, A. & Dam, E. 1991: Reconnaissance geochemical exploration of map sheet 67 V 2 (67° to 68°N, 49°30′ to 52°W), West Greenland. *Open File Ser. Grønlands geol. Unders.* 91/8. 13 pp. 42 Figs.

Steenfelt, A., Dam, E. & Nielsen, J.P. 1992: Reconnaissance geochemical exploration of map sheet 68 V 2 (67°55' to 68°45'N, 50°15' to 52°45'W), West Greenland. *Open File Ser. Grønlands geol. Unders.* 92/7. 20 pp. 42 Figs.

Sørensen, K. 1983: Growth and dynamics of the Nordre Strømfjord shear zone. *J. Geophys. Res.* 88, 3419-3437.

Taylor, S. R. & McLennan, S. M. 1985: *The Continental Crust: its Composition and Evolution.* Oxford: Blackwell Scientific Publications, 312 pp.

Watt, M. 1977: Geokemisk prøveindsamling i Nordre Strømfjord og 'Sarfartoq', centrale Vestgrønland. Int. rep. Grønlands geol. Unders., 11 pp.

Table 1. Instrumentation at the Geological Survey of Greenland

Field measurement of gamma-radiation: Saphymo-Srat SPP-2 scintillometer
Water samples:
Conductivity: Chemotest JK 8800
Fluoride concentration: Orion EA 920 pH/ion analyzer

Table 2. Analytical detection limits.

Instrumental Neutron Activation Analysis (Activation Laboratories Ltd.)

Au	5.0 ppm	Ag	5.0 ppm	As	2.0 ppm	Ba	100.0 ppm
Br	1.0 ppm	Ca	1.0 %	Co	5.0 ppm	Cr	10.0 ppm
Cs	2.0 ppm	Fe	0.02 %	Hf	1.0 ppm	Hg	1.0 ppm
Ir	5.0 ppm	Mo	5.0 ppm	Na	500.0 ppm	Ni	50.0 ppm
Rb	30.0 ppm	Sb	0.2 ppm	Sc	0.1 ppm	Se	5.0 ppm
Sn	0.01 %	Sr	0.05 %	Ta	1.0 ppm	Th	0.5 ppm
U	0.05 ppm	W	4.0 ppm	Zn	50.0 ppm	La	1.0 ppm
Ce	3.0 ppm	Nd	5.0 ppm	Sm	0.1 ppm	Eu	0.2 ppm
Tb	0.5 ppm	Yb	0.05 ppm	Lu	0.05 ppm		

X-ray Fluorescence Spectrometry (pressed powder pellets) (Activation Laboratories Ltd.)

Ba	5.0 ppm	Co	5.0 ppm	Cr	5.0 ppm	Cu	5.0 ppm
Ga	5.0 ppm	Nb	2.0 ppm	Ni	5.0 ppm	Pb	5.0 ppm
Rb	2.0 ppm	Sr	2.0 ppm	V	5.0 ppm	Y	2.0 ppm
Zn	5.0 ppm	Zr	5.0 ppm				

Table 3. Selected average element concentrations in the survey area, 67 V 1 & 68 V 1 compared with estimates for upper and lower crust by Taylor & McLennan (1985). Major elements in %, trace elements in ppm.

	SiO_2	TiO_2	Al_2O_3	Fe_2O_3	MnO	MgO	CaO	Na_2O	K_2O %
Survey mean	61.1	0.96	15.8	7.8	0.13	3.2	5.5	3.6	1.6
Upper crust	66.0	0.5	15.2	5.0	0.06	2.2	4.2	3.9	3.4
Lower crust	54.4	1.0	16.1	11.8	0.17	6.3	8.5	2.8	0.34

	Sc	V	Cr	Co	Ni	Cu	Zn	Rb	Sr	Ba	Th	U
Survey mean	19	104	112	26	64	63	89	38	416	590	8	1.5
Upper crust	11	60	35	10	20	25	71	112	350	550	11	3
Lower crust	36	285	235	35	135	90	83	5	230	150	1	0.3

	La	Ce	Nd	Sm	Eu	Yb	Lu
Survey mean	66	106	48	7.3	1.8	2.4	0.33
Upper crust	30	64	26	4.5	0.88	2.2	0.32
Lower crust	11	23	13	3.2	1.17	2.2	0.29

Table 4. Selected element concentrations of two clusters of REE anomalous stream sediment samples northeast of Sisimiut with compositions of some mafic potassic dykes for comparison. Western cluster 381038-040, eastern 380548-381053. shonk1 and shonk2 are shonkinite dykes from the surroundings of the Sarfartoq carbonatite complex southeast of the survey area. monch is a monchiqite dyke from the north coast of Itilleq, south of Sisimiut. Rock analyses from Larsen & Rex (1992). Major elements in %, trace elements in ppm.

GGU-no	SiO_2	TiO_2	Al_2O_3	Fe_2O_3	MnO	MgO	CaO	Na_2O	K_2O	P_2O_5
381038	50.50	1.24	14.70	11.00	0.14	4.66	8.46	2.92	2.47	2.41
381040	51.70	1.21	15.20	9.72	0.13	4.15	7.61	3.23	2.38	2.02
381041	49.80	1.83	14.60	13.20	0.15	4.12	7.41	2.91	2.16	1.88
380548	53.70	0.63	16.20	7.57	0.13	3.42	6.05	3.99	2.29	0.73
381024	53.40	1.13	14.70	9.71	0.13	4.24	7.23	3.39	2.06	1.37
381053	51.90	1.12	14.20	9.69	0.15	3.58	5.92	3.12	1.98	0.81
shonk1	37.64	1.43	9.69	9.60	0.16	8.77	14.99	1.56	4.79	3.95
shonk2	45.52	1.42	11.31	9.31	0.12	7.09	10.09	2.25	5.64	3.16
monch	39.79	2.69	9.08	13.91	0.21	10.52	12.62	2.05	1.55	0.52

GGU-no	Rb	Ba	Sr	La	Nd	Y	Zr	Nb	Pb
381038	45	3056	1962	710	390	43	461	9	24
381040	42	2778	1920	620	320	42	440	9	25
381041	36	2315	1453	530	300	41	761	15	20
380548	30	2282	1731	250	130	21	324	3	29
381024	36	1997	1344	300	200	31	331	12	20
381053	40	1633	951	200	120	31	406	10	19
shonk1	102	6992	3580	684	676	48	476	21	83
shonk2	121	5573	4987	378	421	36	640	22	65
monch	32	945	881	129		26	277		

GGU-no	Th	Zn	Cu	Sc	V	Cr	Ni	Ga
381038	20	130	54	29	180	79	59	22
381040	17	118	41	27	158	84	48	22
381041	18	132	45	33	211	146	64	22
380548	5	127	107	18	110	37	62	22
381024	12	104	50	24	141	86	58	19
381053	11	127	55	23	147	83	53	16
shonk1	28	139	119	11	116	176	177	14
shonk2	30	161	9	8	96	167	153	19
monch	10	82	27	22	165	800	1260	16

Table 5. Chemical composition of soil samples collected around rusty metasediments in shear zones. Major elements, Pb, Zn, Cu, Ni, Co, Cr, V, Sr, Rb, Ba, Ga, Y, Zr, Nb by X-ray fluorescence; Au, As, Sb, Mo, Th, U by instrumental neutron activation. Analyses by Activation Laboratories Ltd.

GGU no.	SiO_2 %	TiO_2 %	Al_2O_3 %	Fe_2O_3 %	MnO %	MgO %	CaO %	Na_2O %	K_2O %	P_2O_5 %
Loc. A										
380727	55.60	0.954	14.90	6.80	.10	2.97	4.90	3.47	1.43	.23
380728	56.40	0.852	15.10	7.00	.10	2.82	4.95	3.46	1.63	.31
380729	56.40	0.961	15.20	7.85	.11	2.92	5.57	3.72	1.36	.28
380730	39.90	0.925	11.50	16.90	.66	2.59	4.25	2.08	1.03	.35
380732	52.80	0.945	15.00	9.88	.16	3.37	4.57	3.12	1.72	.25
380733	56.90	0.984	15.60	8.42	.14	3.55	6.47	3.87	1.34	.41
380734	57.40	0.880	14.40	6.82	.10	2.45	4.60	3.45	1.52	.11
380735	53.40	0.718	13.30	6.12	.09	2.24	4.24	3.13	1.42	.20
380736	52.90	0.933	14.00	7.16	.10	2.44	4.79	3.37	1.32	.17
380737	54.00	1.180	14.70	9.71	.12	2.95	5.30	3.45	1.35	.28
Loc. B										
380738	43.20	1.230	12.70	20.20	.19	3.59	2.33	1.63	2.33	.27
380739	30.80	1.690	8.13	32.60	.06	4.60	1.49	.86	3.01	.45
380740	49.70	0.996	12.10	12.20	.12	6.09	7.62	2.54	1.39	.39
380741	46.60	1.120	12.30	17.50	.09	3.44	3.25	2.28	1.87	.27
380742	45.80	1.320	12.60	14.60	.15	6.11	4.43	2.11	1.92	.33
380743	51.00	0.905	14.80	11.20	.12	3.30	3.88	2.52	1.69	.28
380744	37.40	1.310	12.50	21.00	.08	4.31	2.30	1.36	2.95	.36
380745	46.20	1.290	16.50	13.20	.09	4.16	2.85	2.08	2.64	.23
380746	35.70	1.230	10.10	29.30	.06	3.07	2.24	1.72	2.41	.20

GGU no.	Au ppb	As ppm	Sb ppm	Mo ppm	Pb ppm	Zn ppm	Cu ppm	Ni ppm	Co ppm	Cr ppm	V ppm
Loc. A											
380727	0	2	0	7	6	77	26	39	20	95	108
380728	6	0	0	0	89	76	42	41	23	101	108
380729	0	0	0	0	0	80	38	36	24	84	120
380730	8	0	0	0	0	141	75	64	68	51	133
380732	0	0	0	0	56	133	57	48	35	70	135
380733	0	0	0	0	49	92	46	43	27	90	122
380734	0	0	0	0	13	23	23	30	18	96	109
380735	0	0	0	0	5	57	24	32	16	95	88
380736	0	0	0	0	8	60	27	26	18	69	106
380737	5	0	0	0	0	82	42	43	26	93	138
Loc. B											
380738	36	0	0	26	92	345	153	34	17	231	342
380739	0	38	1	26	42	63	51	9	13	390	377
380740	0	0	0	0	165	55	461	269	54	122	163
380741	0	4	0	7	0	80	52	31	20	170	207
380742	0	5	0	6	13	158	164	269	50	525	259
380743	0	0	0	8	12	238	123	84	31	146	172
380744	0	6	0	23	29	198	123	47	22	205	273
380745	0	4	0	14	15	178	82	36	20	196	300
380746	0	7	0	15	20	99	97	18	14	191	291

GGU no.	Sr ppm	Rb ppm	Ba ppm	Ga ppm	Nb ppm	Zr ppm	Y ppm	Th ppm	U ppm
Loc. A									
380727	502	31	769	21	11	284	18	4.5	0.0
380728	512	37	841	20	9	266	24	4.7	0.0
380729	602	27	812	21	8	325	27	4.7	0.0
380730	349	23	796	12	5	223	32	6.5	2.0
380732	428	39	725	21	9	329	29	10.0	1.7
380733	556	23	716	21	10	298	23	5.0	0.8
380734	405	31	623	19	10	267	15	3.1	0.0
380735	386	31	590	20	10	237	15	3.4	0.0
380736	484	23	683	19	9	296	15	4.0	1.2
380737	508	23	708	21	10	428	21	6.6	0.9
Loc. B									
380738	173	81	612	23	16	356	20	16.0	5.3
380739	86	91	317	20	20	294	7	15.0	5.0
380740	278	43	378	17	9	214	18	1.4	2.0
380741	243	61	433	19	10	279	11	8.9	2.8
380742	210	59	464	18	13	294	23	12.0	3.2
380743	286	62	544	19	12	376	22	13.0	3.2
380744	139	97	458	20	15	324	21	19.0	15.0
380745	216	98	506	29	16	444	24	19.0	5.5
380746	150	64	427	19	16	314	9	15.0	2.5

380727 soil under vegetation, sheared gneiss
380728 soil, do
380729 soil, do
380730 stream sediment, small stream
380732 rusty top soil, supracrustals
380733 stream sediment, main valley stream
380734 soil, no exposures
380735 soil, under vegetation, no exposures
380736 soil, do
380737 soil, under vegetation, supracrustals and gneiss

380738 top soil, sheared gneiss
380739 rusty top soil, felsic metavolcanic rock
380740 top soil, bleached gneis
380741 rusty top soil, felsic graphite bearing muscovite schist
380742 garnet amphibolite
380743 top soil, felsic garnetiferous metavolcanic rock
380744 do
380745 rusty top soil, felsic metavolcanic rock
380746 do

List of figures

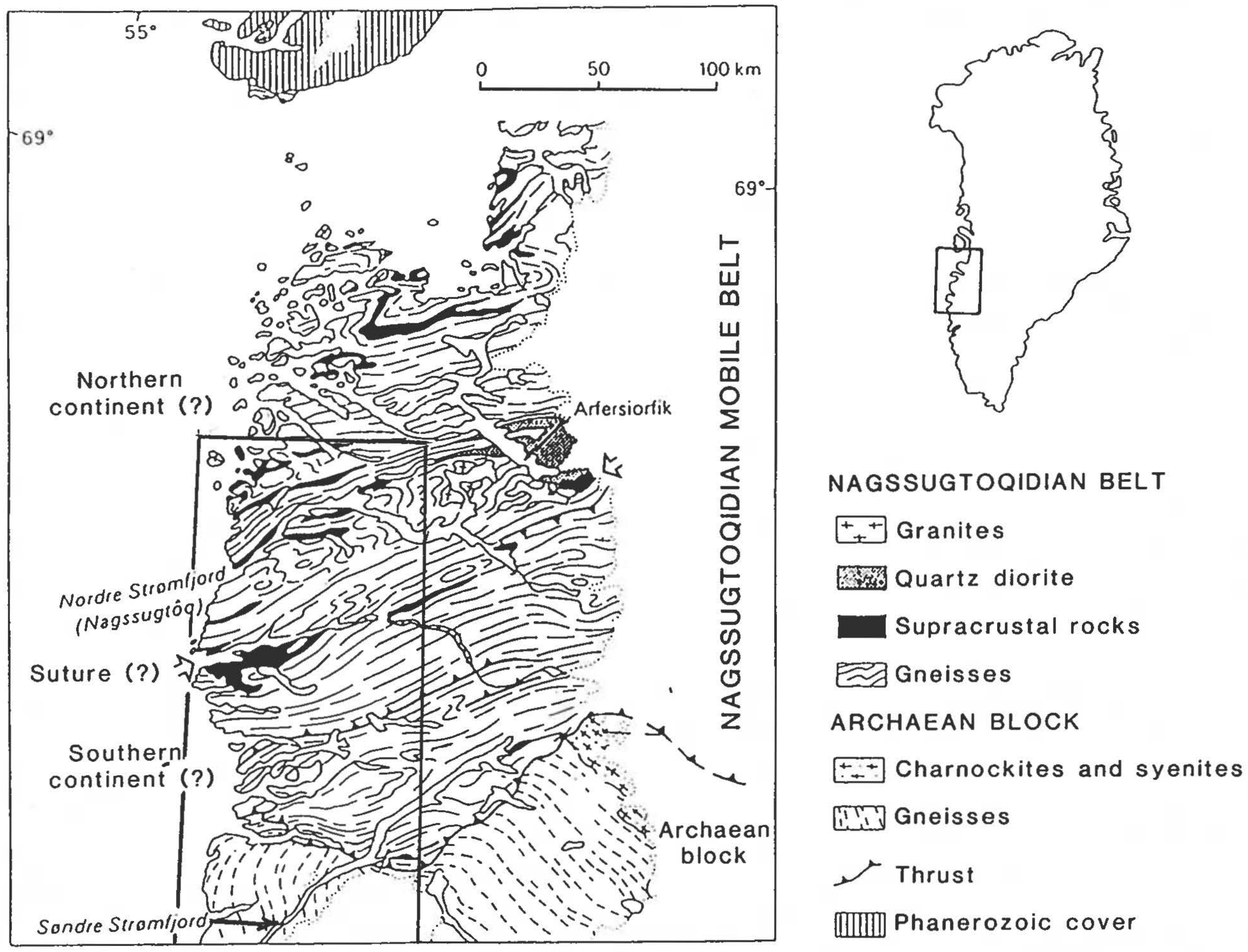
55°
69°
0
50
100 km
69°
NAGSSUGTOQIDIAN MOBILE BELT
Northern
continent (?)
Arfersiorfik
Nordre Strømfjord
(Nagssugtôq)
Suture (?)
Southern
continent (?)
Archaean
block
Søndre Strømfjord
NAGSSUGTOQIDIAN BELT
Granites
Quartz diorite
Supracrustal rocks
Gneisses
ARCHAEAN BLOCK
Charnockites and syenites
Gneisses
Thrust
Phanerozoic cover

Fig. 1

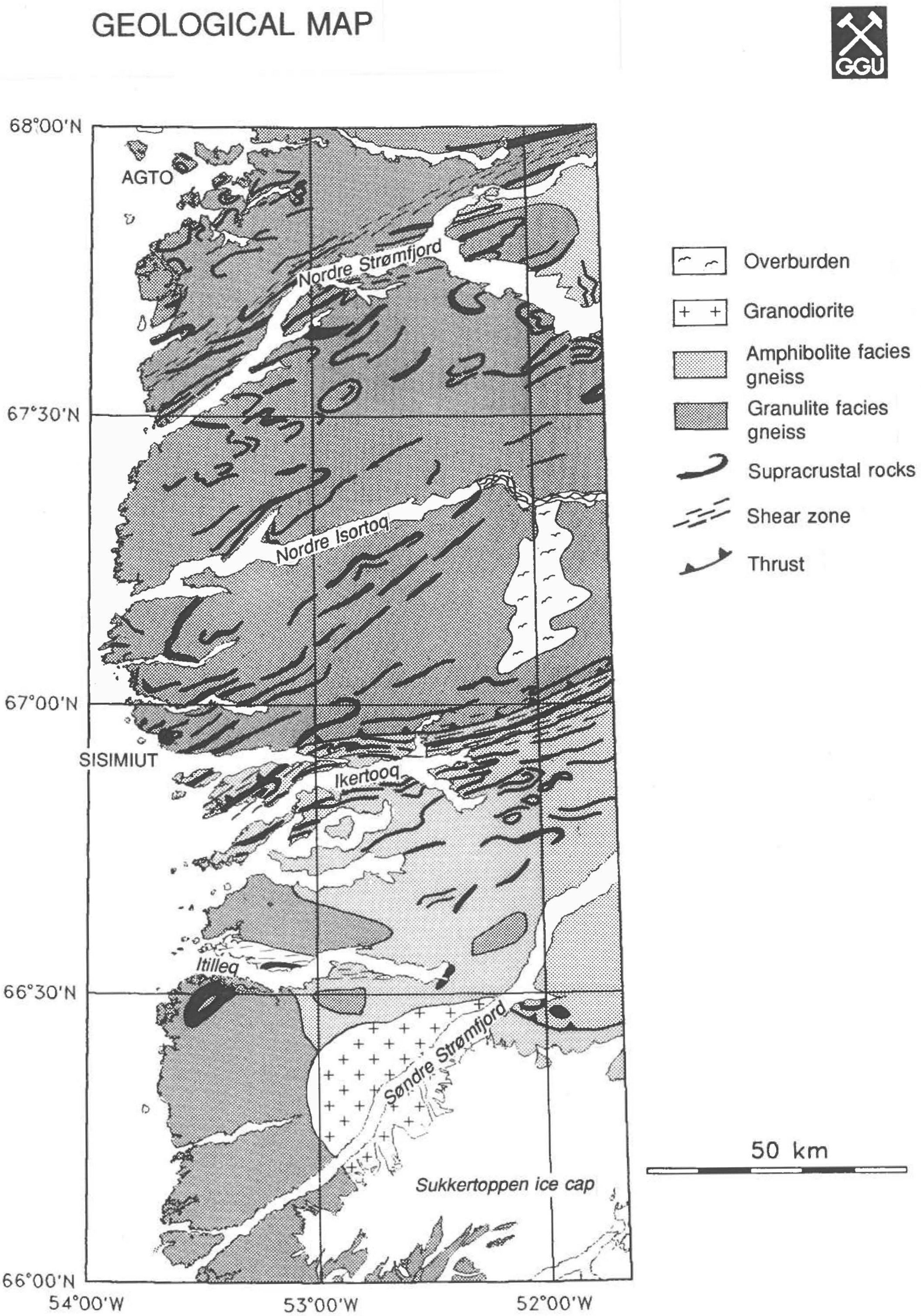
GEOLOGICAL MAP
GGU
68°00'N
67°30'N
67°00'N
66°30'N
66°00'N
54°00'W
53°00'W
52°00'W
AGTO
Nordre Strømfjord
Nordre Isortoq
SISIMIUT
Ikertooq
Itilleq
Søndre Strømfjord
Sukkertoppen ice cap
Overburden
Granodiorite
Amphibolite facies gneiss
Granulite facies gneiss
Supracrustal rocks
Shear zone
Thrust
50 km

Fig. 2

SiO_2 in stream sediment

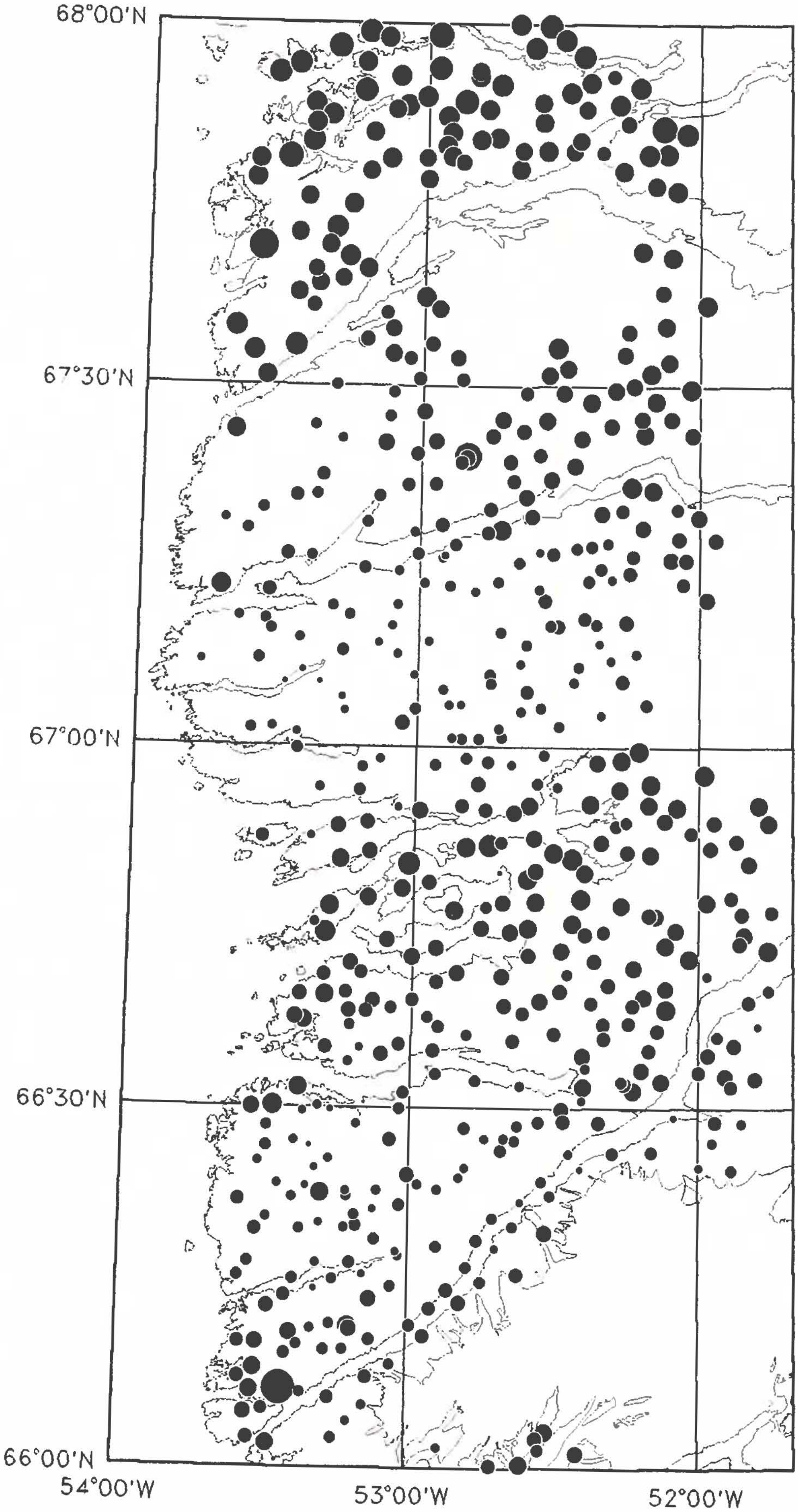

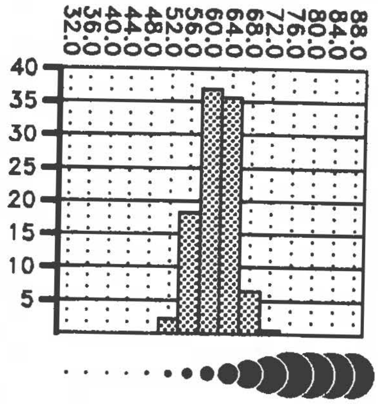

pct

X-ray Fluorescence

Number of samples:	542
Min. value:	50.2
Max. value:	73.2
Mean:	61.1
Median:	61.3
Variance:	13.0
Std. Dev.:	3.6

50 km

Fig. 3

TiO2 in stream sediment

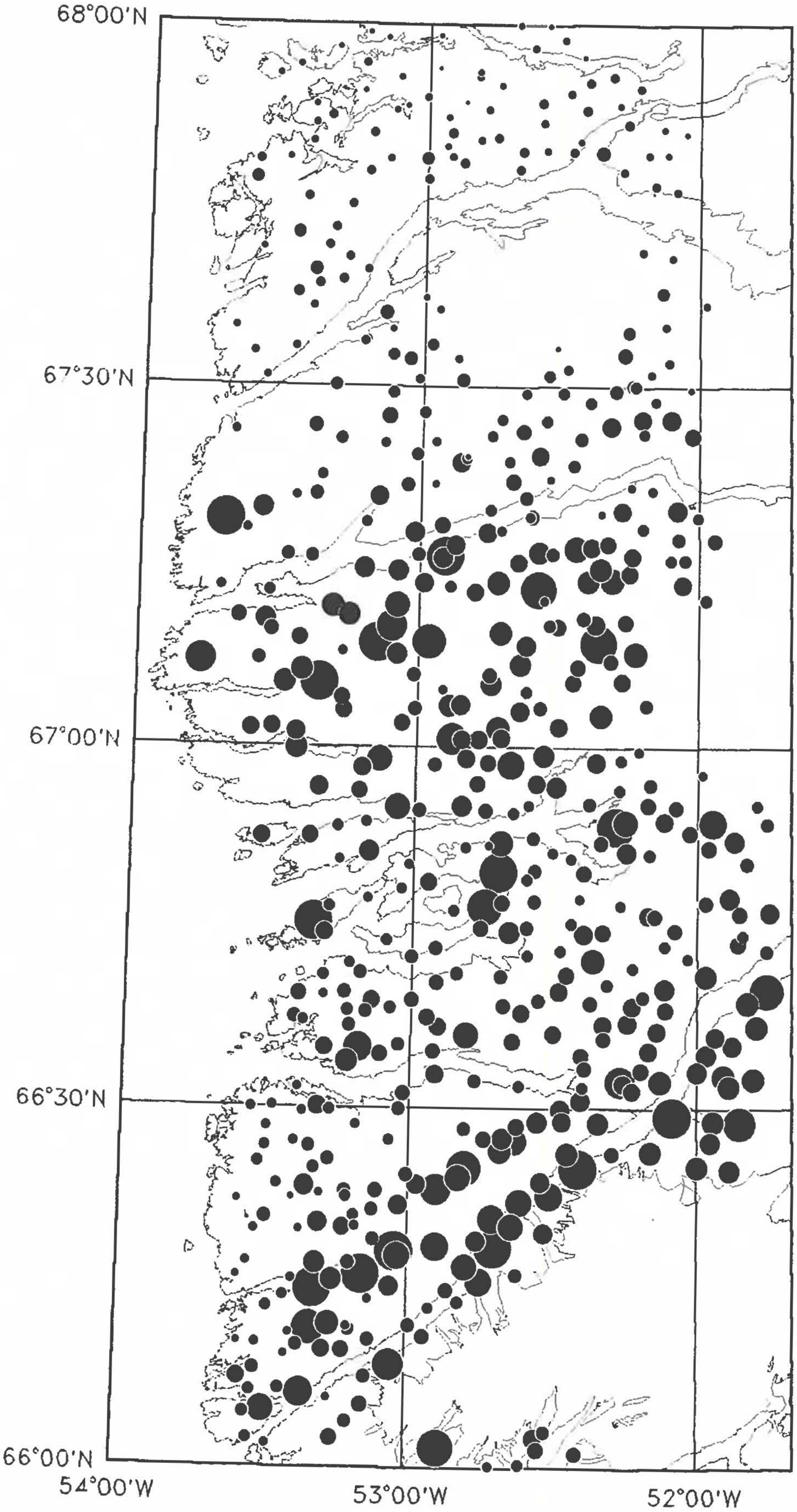

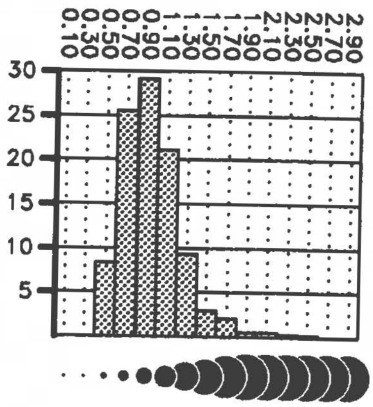

pct

X-ray Fluorescence

Number of samples:	542
Min. value:	0.40
Max. value:	3.93
Mean:	0.96
Median:	0.90
Variance:	0.11
Std. Dev.:	0.34

50 km

Fig. 4

Al2O3 in stream sediment

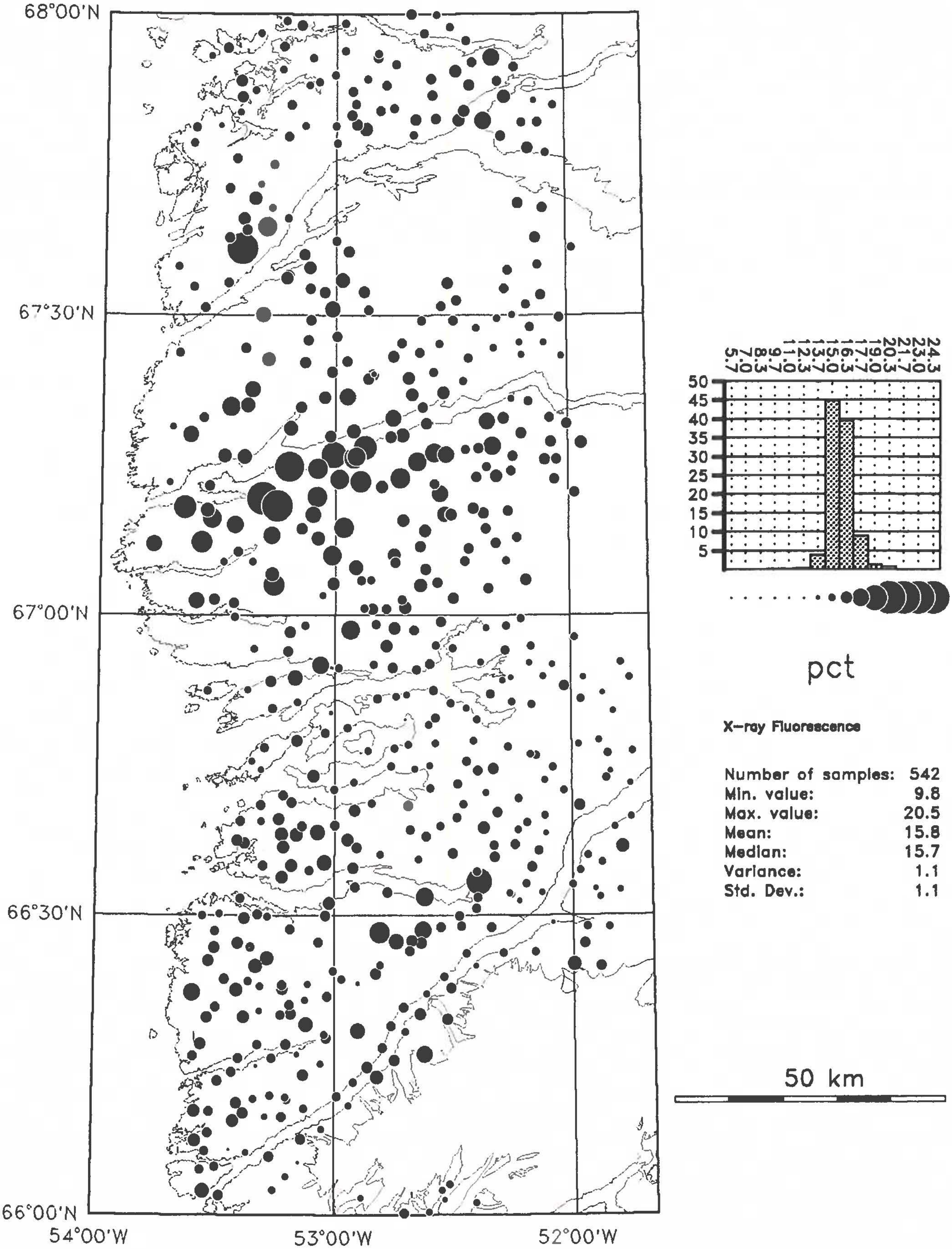

X-ray Fluorescence

Number of samples:	542
Min. value:	9.8
Max. value:	20.5
Mean:	15.8
Median:	15.7
Variance:	1.1
Std. Dev.:	1.1

50 km

Fig. 5

Fe2O3 in stream sediment

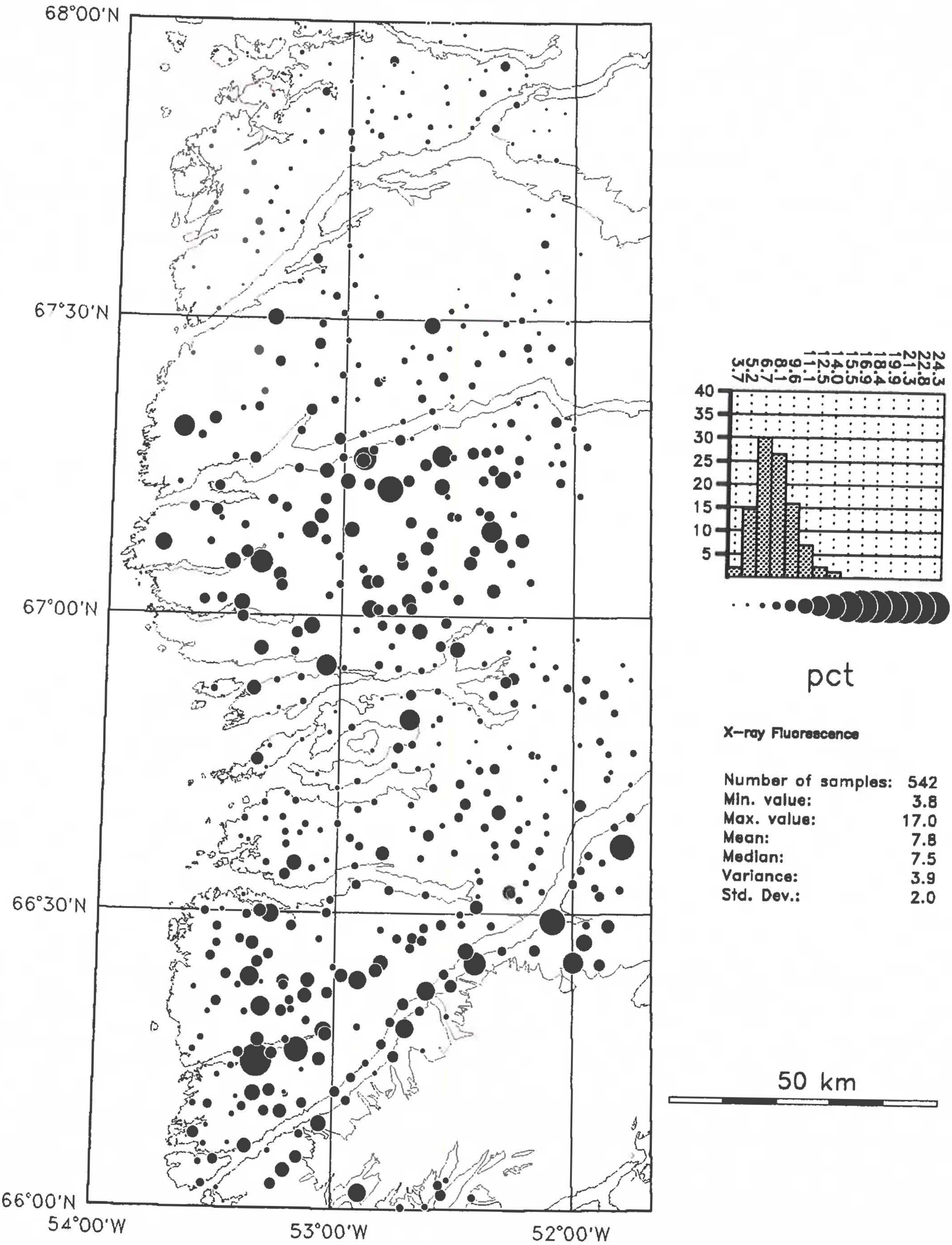

Fig. 6

MnO in stream sediment

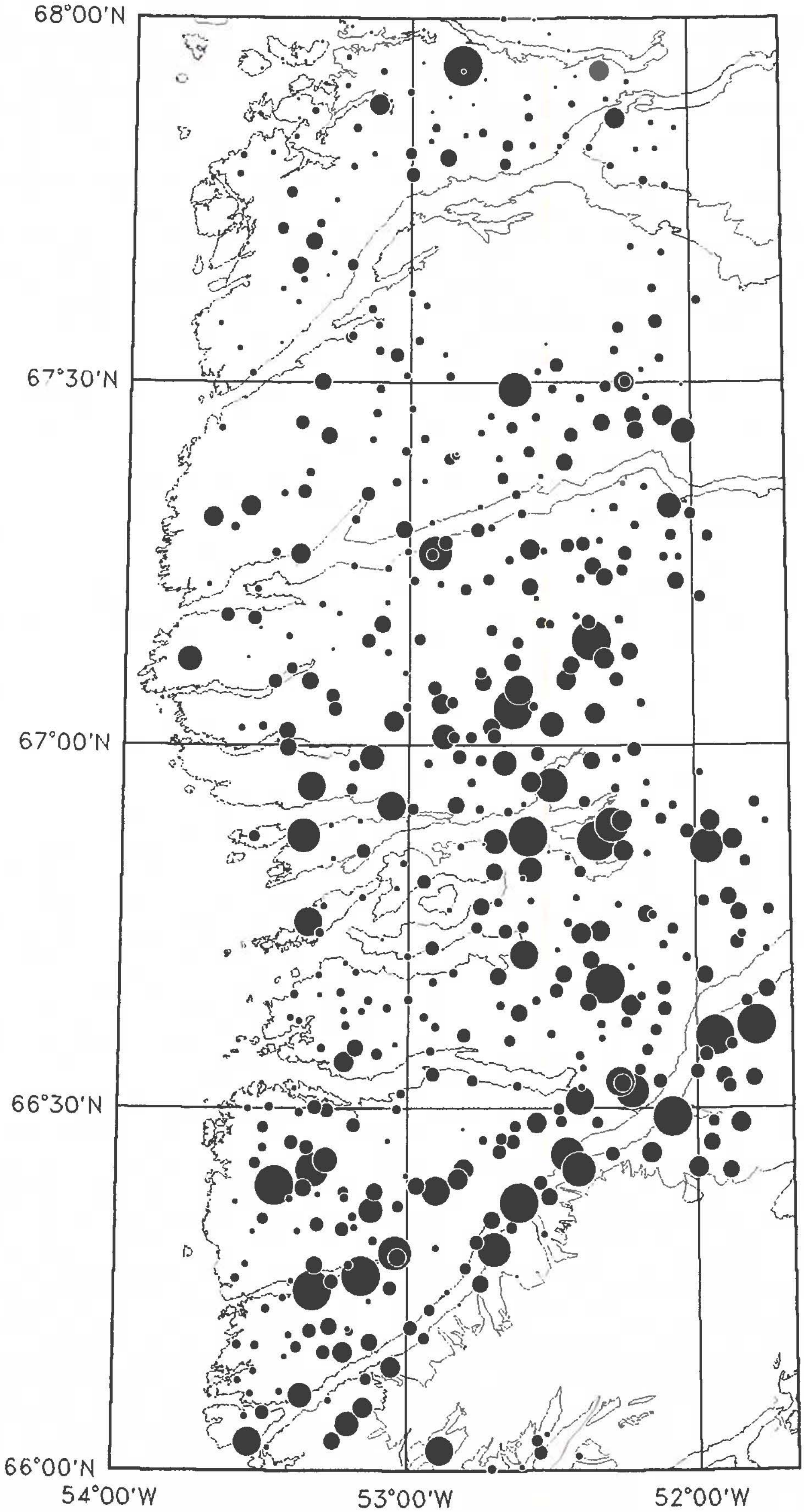

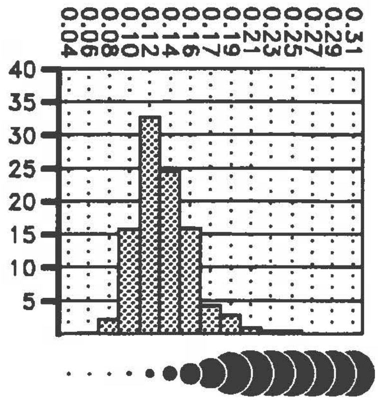

pct

X-ray Fluorescence

Number of samples:	542
Min. value:	0.06
Max. value:	0.34
Mean:	0.13
Median:	0.12
Variance:	0.00
Std. Dev.:	0.03

50 km

Fig. 7

MgO in stream sediment

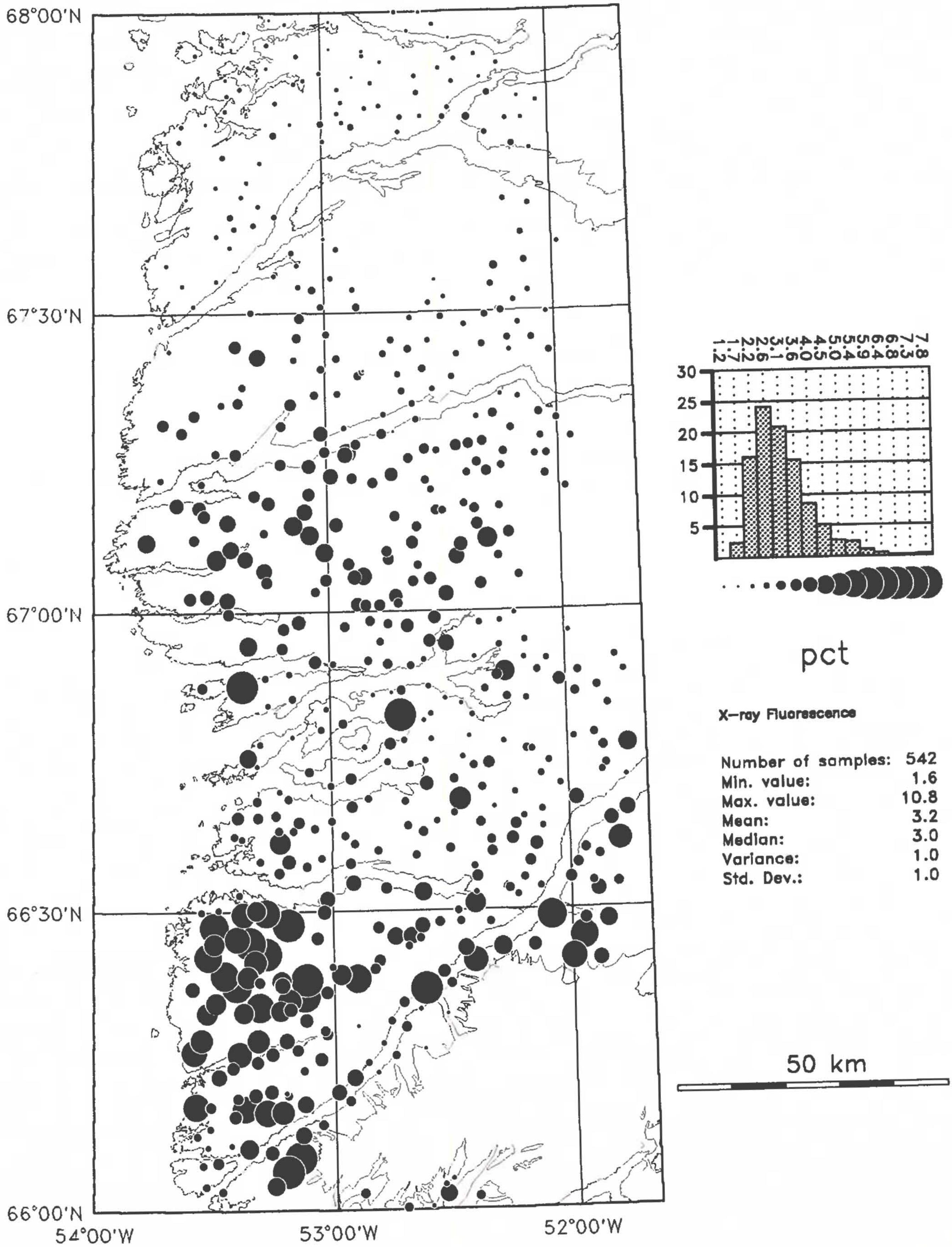

Fig. 8

CaO in stream sediment

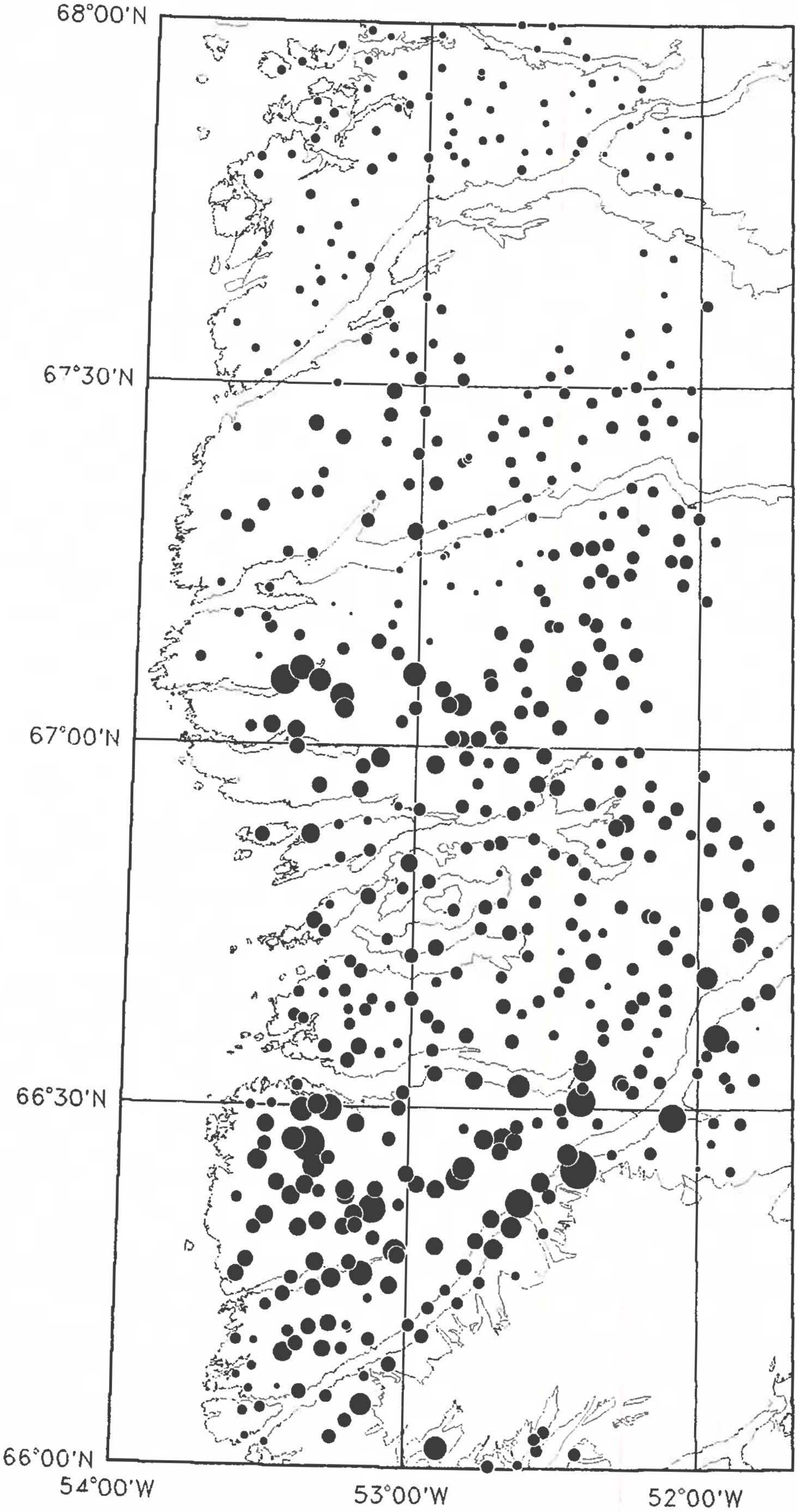

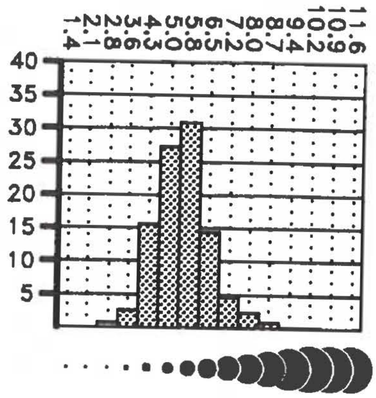

pct

X-ray Fluorescence

Number of samples:	542
Min. value:	2.8
Max. value:	9.8
Mean:	5.5
Median:	5.5
Variance:	1.0
Std. Dev.:	1.0

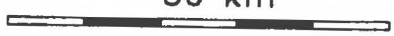

Fig. 9

Na2O in stream sediment

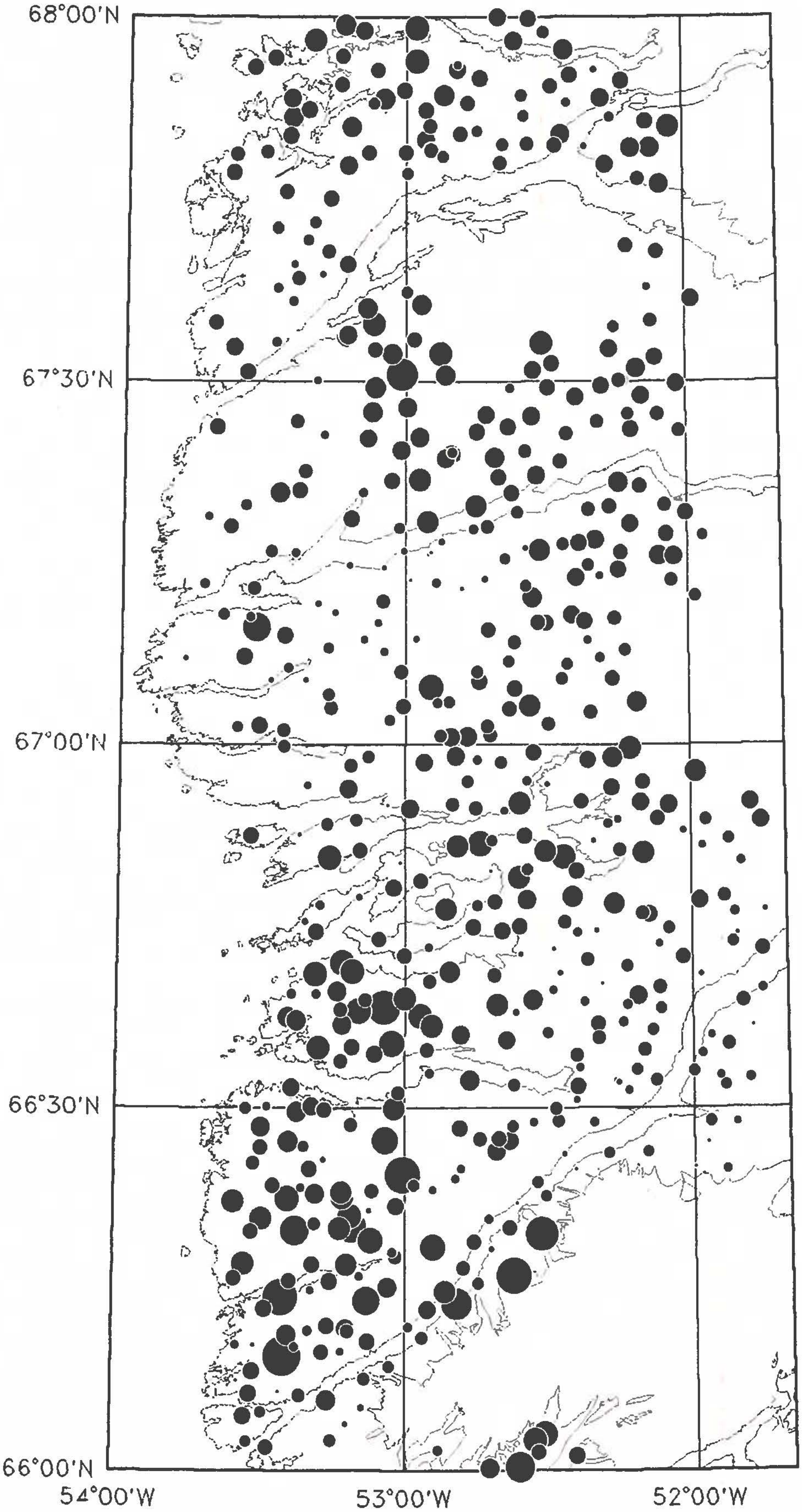

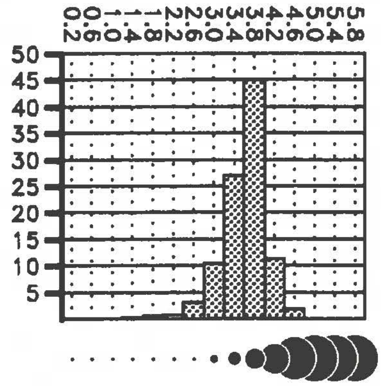

pct

X-ray Fluorescence

Number of samples:	542
Min. value:	1.6
Max. value:	4.8
Mean:	3.6
Median:	3.7
Variance:	0.2
Std. Dev.:	0.4

50 km

Fig. 10

K20 in stream sediment

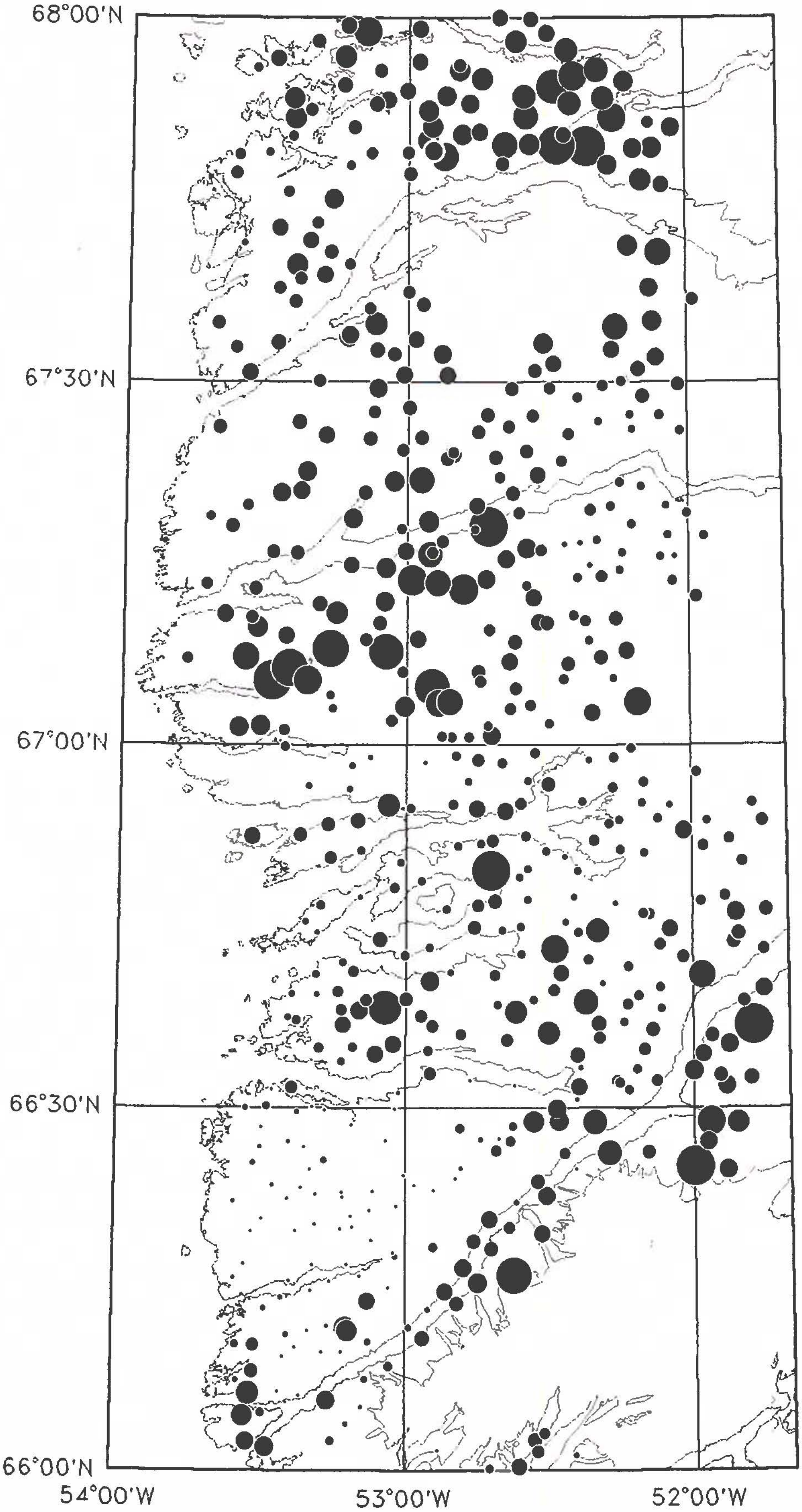

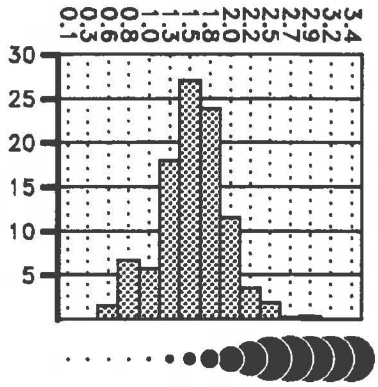

pct

X-ray Fluorescence

Number of samples:	542
Min. value:	0.5
Max. value:	5.4
Mean:	1.6
Median:	1.6
Variance:	0.2
Std. Dev.:	0.4

50 km

Fig. 11

P205 in stream sediment

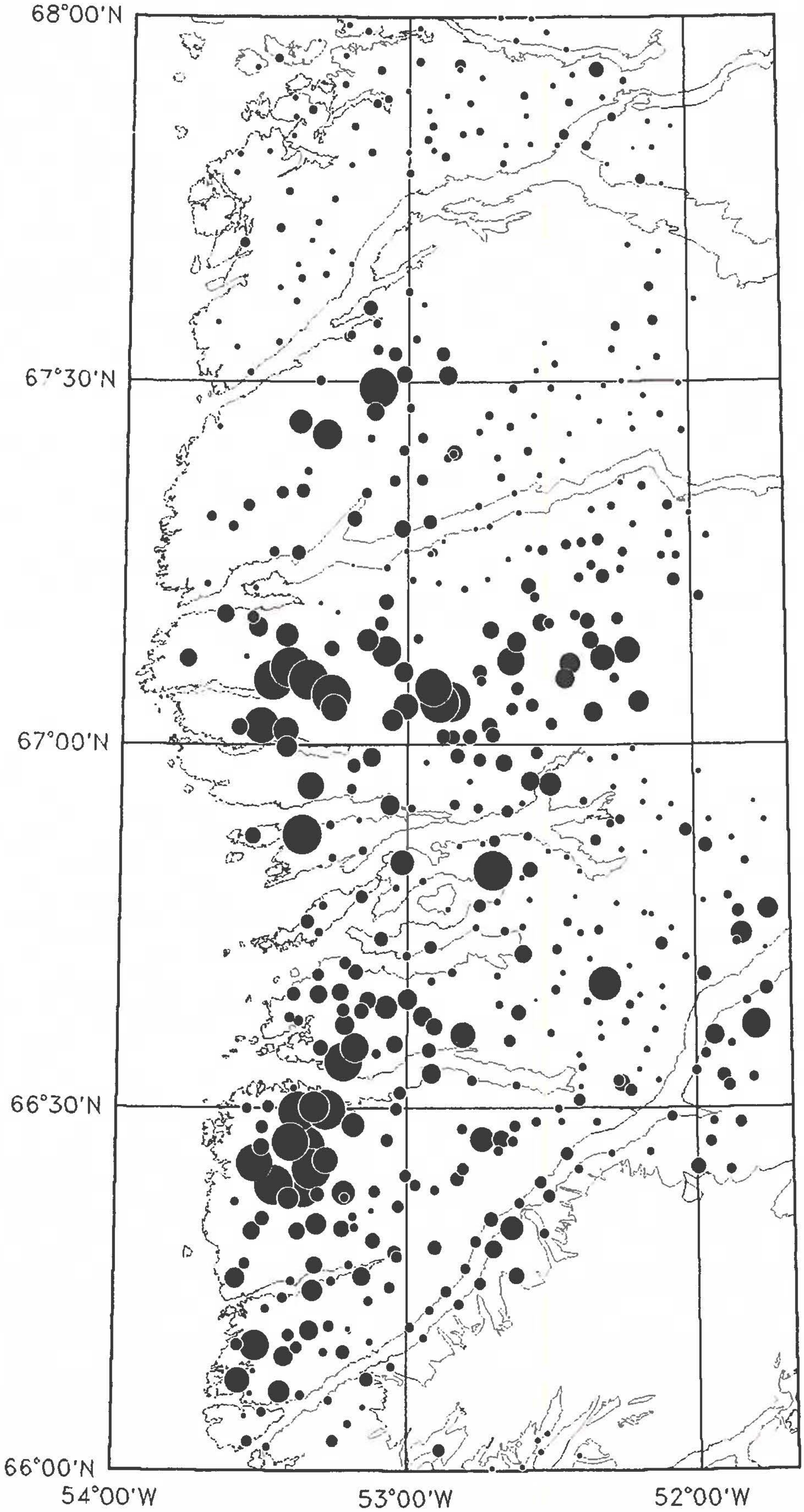

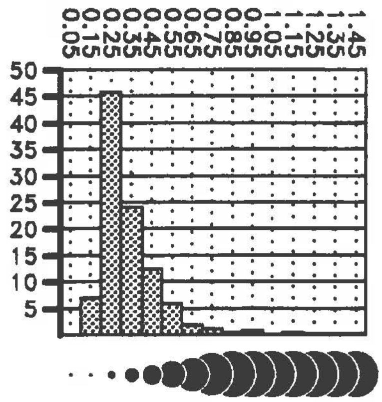

pct

X–ray Fluorescence

Number of samples:	542
Min. value:	0.13
Max. value:	2.45
Mean:	0.35
Median:	0.29
Variance:	0.05
Std. Dev.:	0.22

50 km

Fig. 12

As in stream sediment

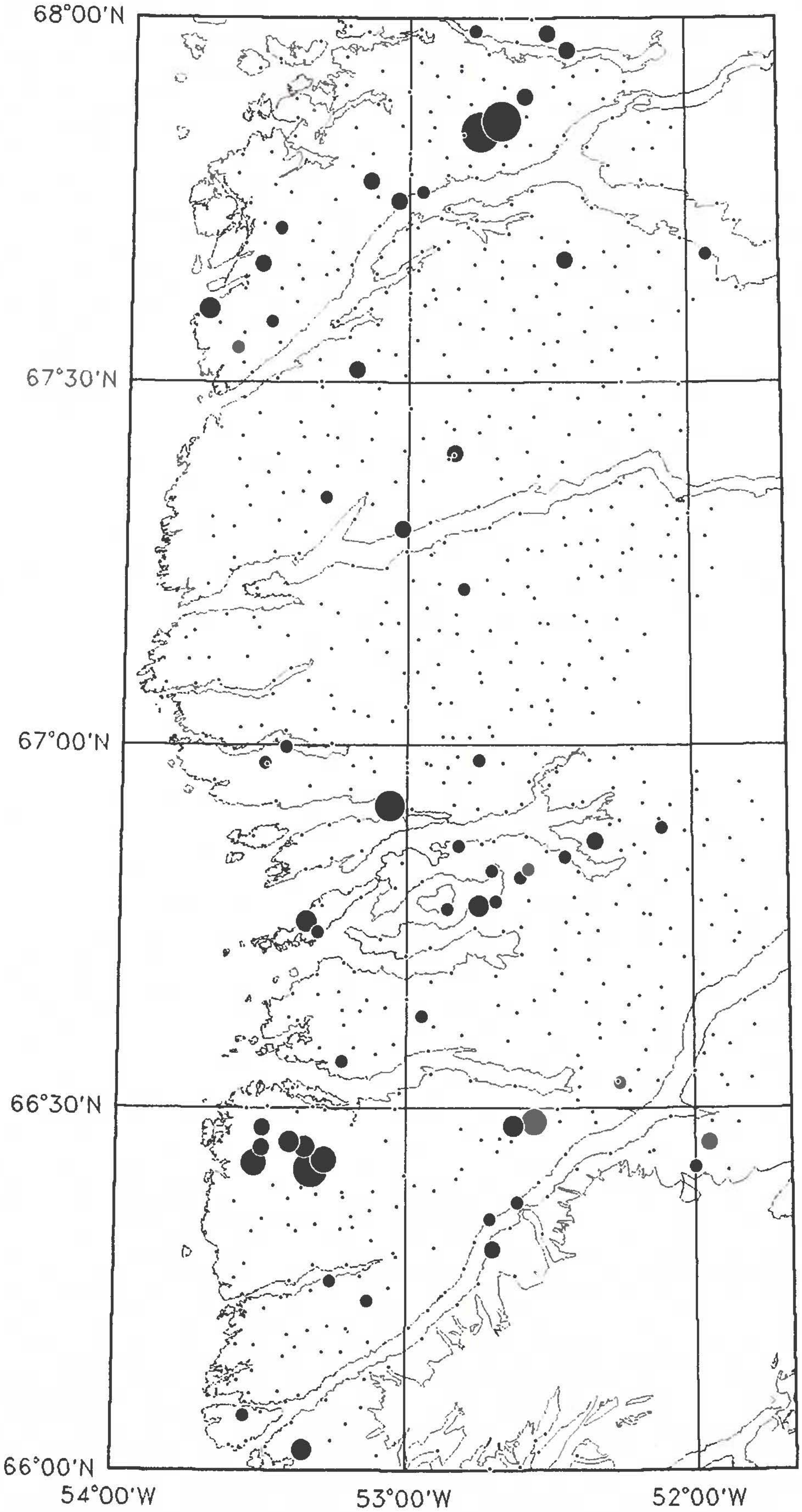

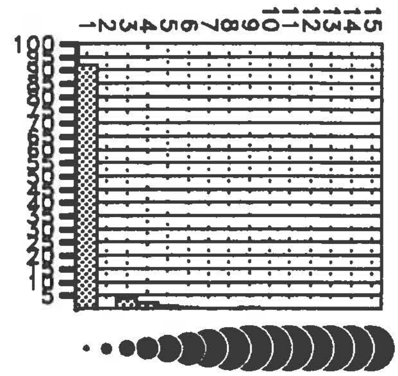

ppm

Instrumental Neutron Activation

Number of samples:	712
Min. value:	0
Max. value:	8
Mean:	0
Median:	0
Variance:	1
Std. Dev.:	1

50 km

Fig. 13

Au in stream sediment

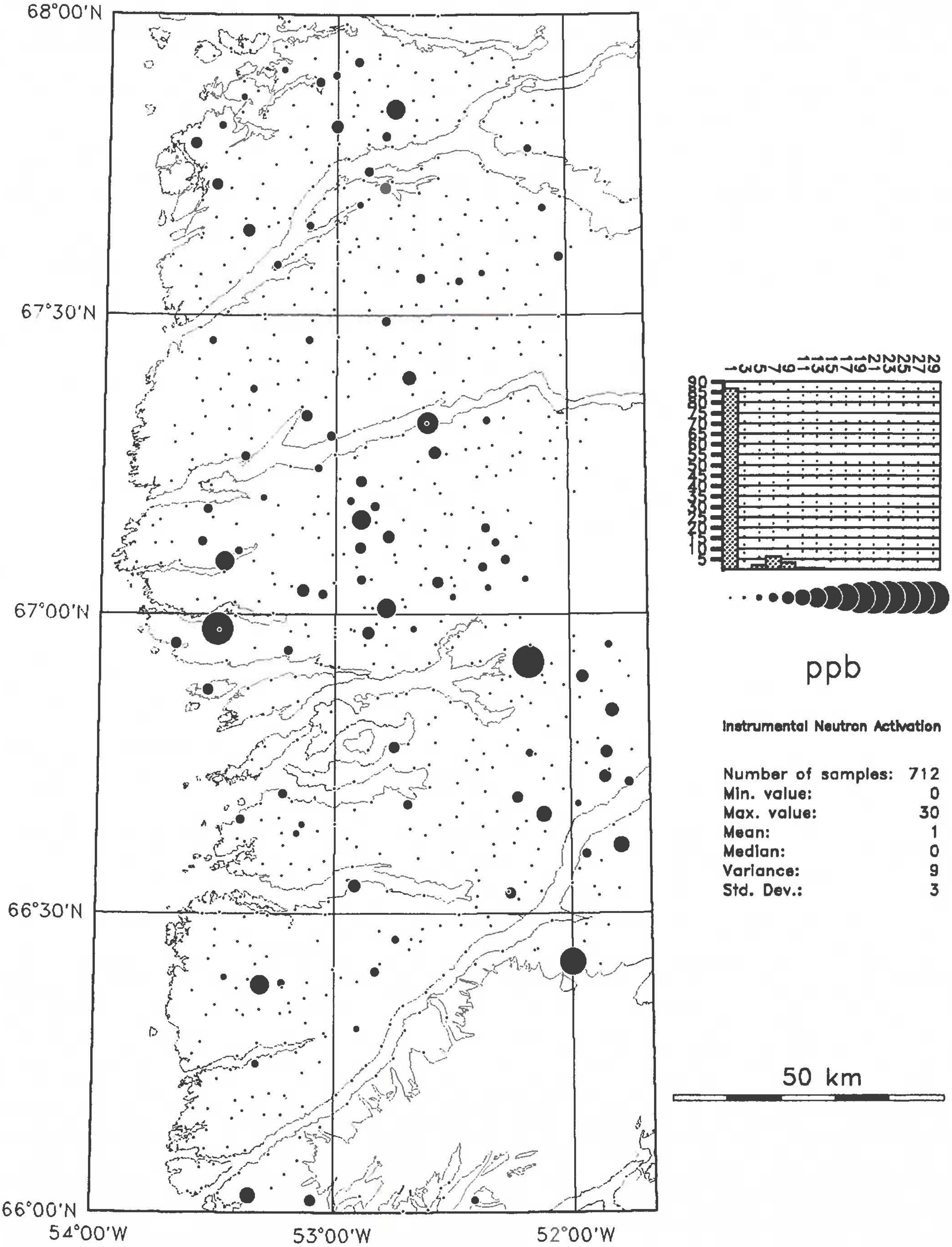

Fig. 14

Ba in stream sediment

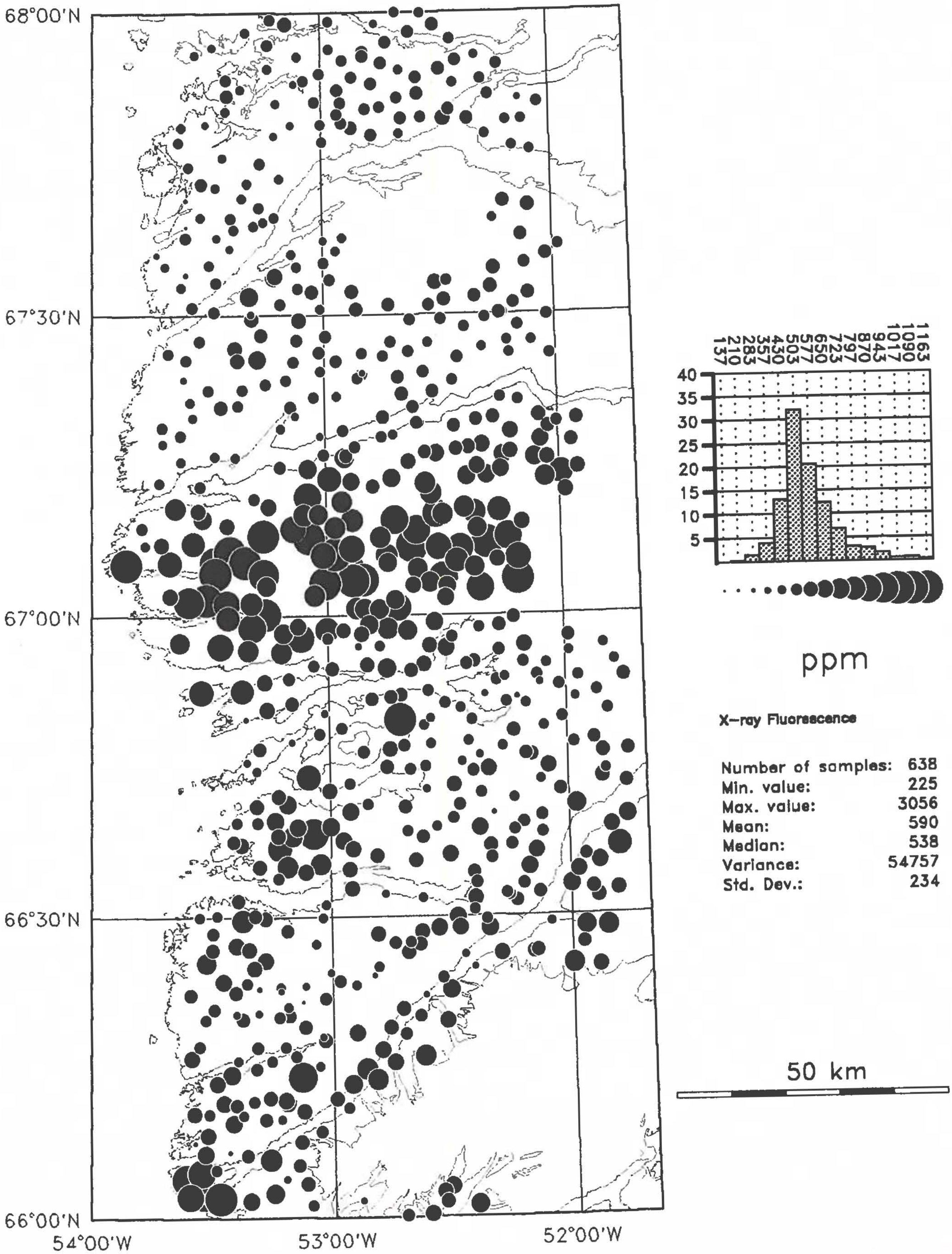

Fig. 15

Br in stream sediment

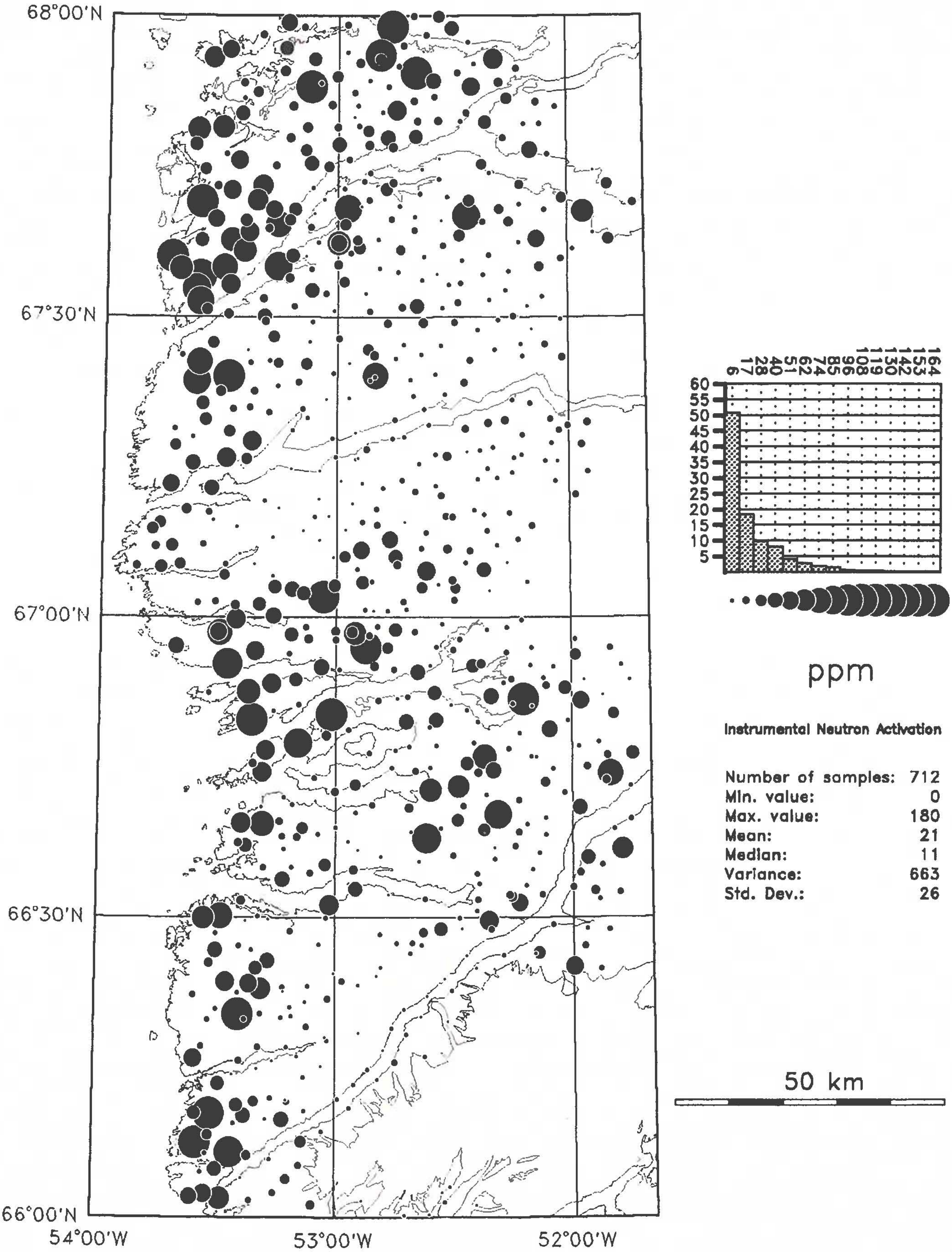

Fig. 16

Ce in stream sediment

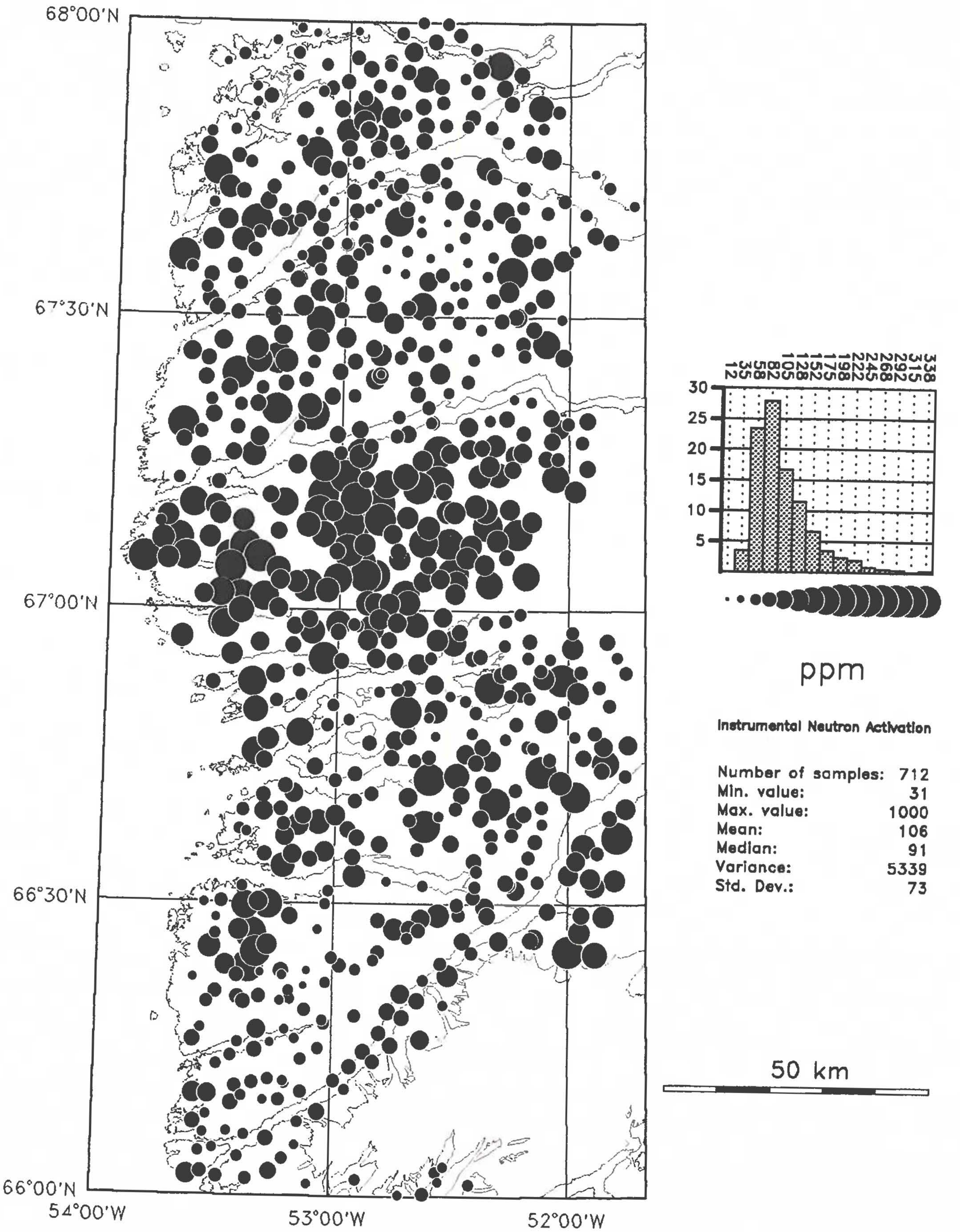

Fig. 17

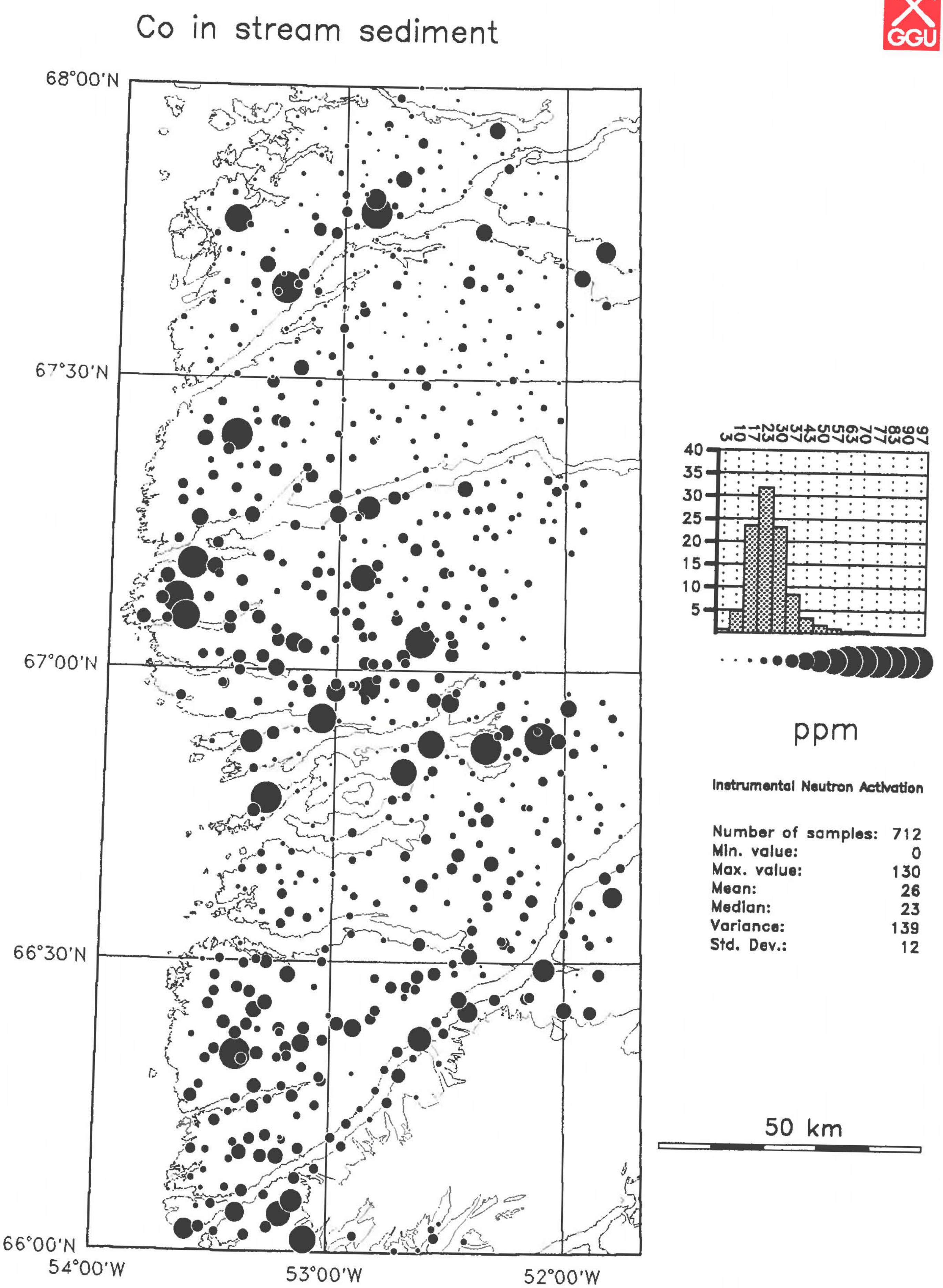
Co in stream sediment
68°00'N
67°30'N
67°00'N
66°30'N
66°00'N
54°00'W
53°00'W
52°00'W
3 10 17 23 30 37 43 50 57 63 70 77 83 90 97
40 35 30 25 20 15 10 5
ppm
Instrumental Neutron Activation
Number of samples: 712
Min. value: 0
Max. value: 130
Mean: 26
Median: 23
Variance: 139
Std. Dev.: 12
50 km

Fig. 18

Cr in stream sediment

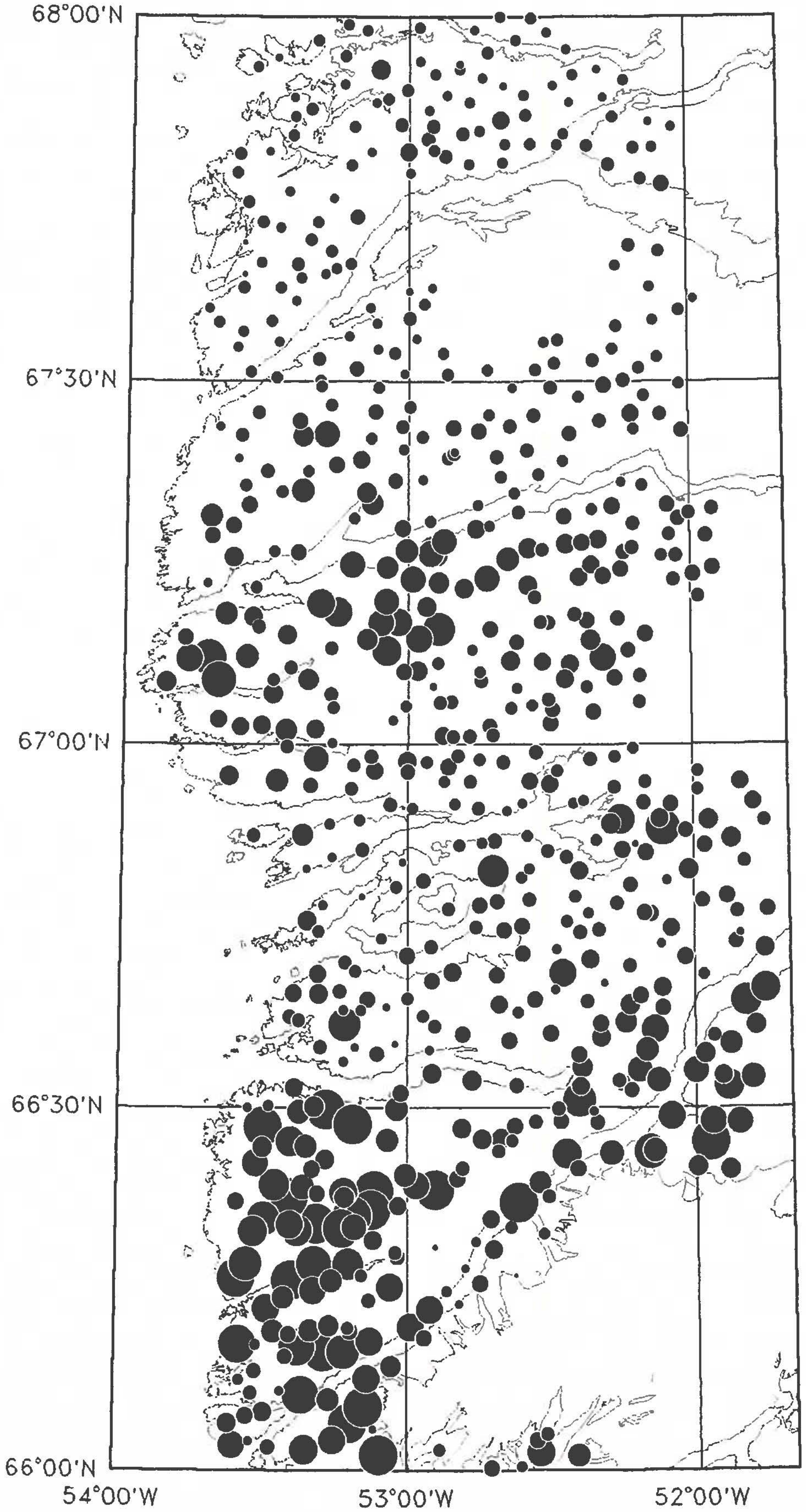

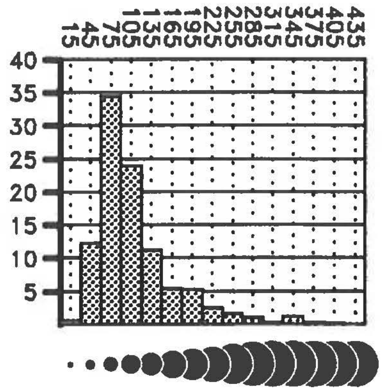

X-ray Fluorescence

Number of samples:	638
Min. value:	10
Max. value:	562
Mean:	112
Median:	92
Variance:	4594
Std. Dev.:	68

50 km

Fig. 19

Cu in stream sediment

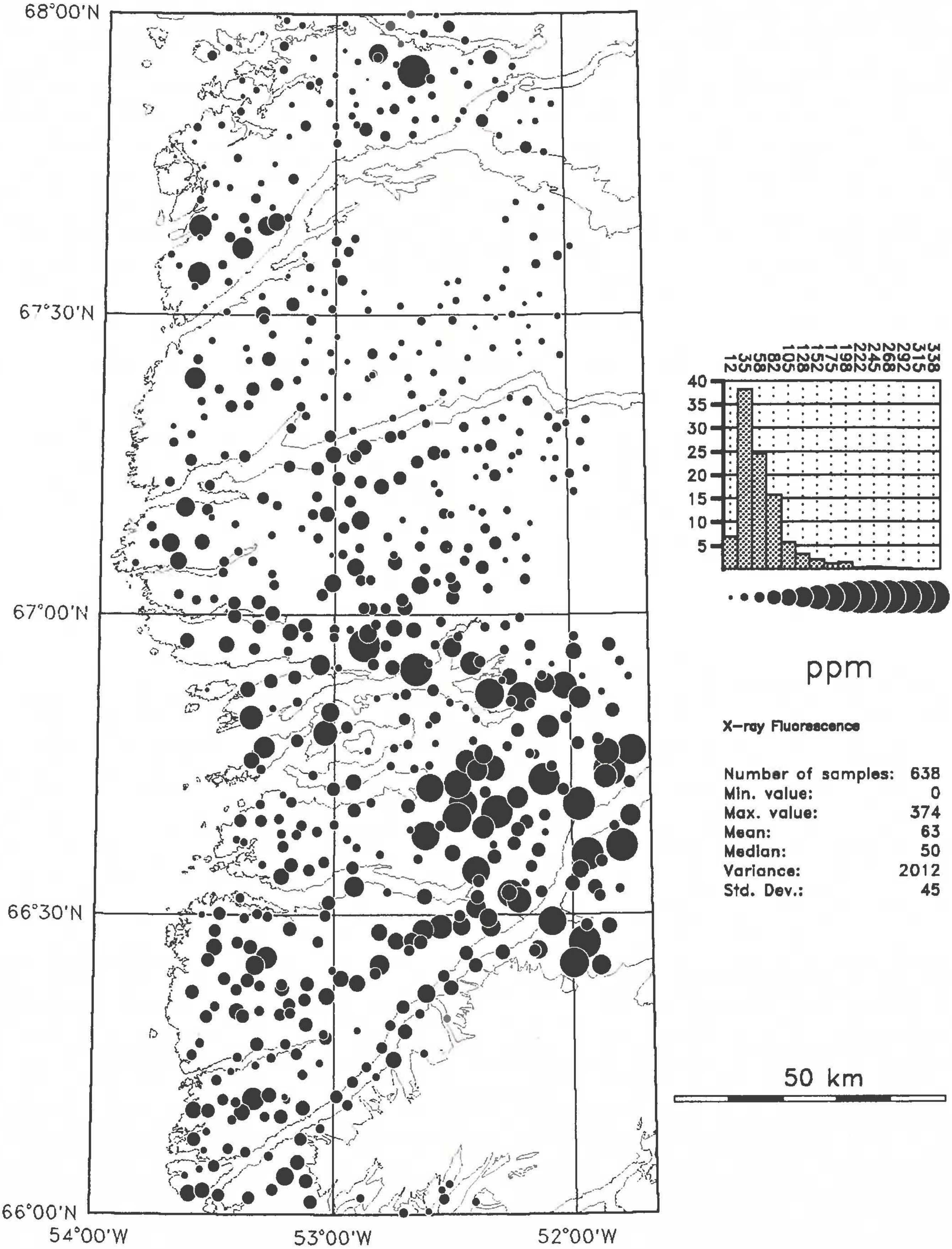

Fig. 20

Eu in stream sediment

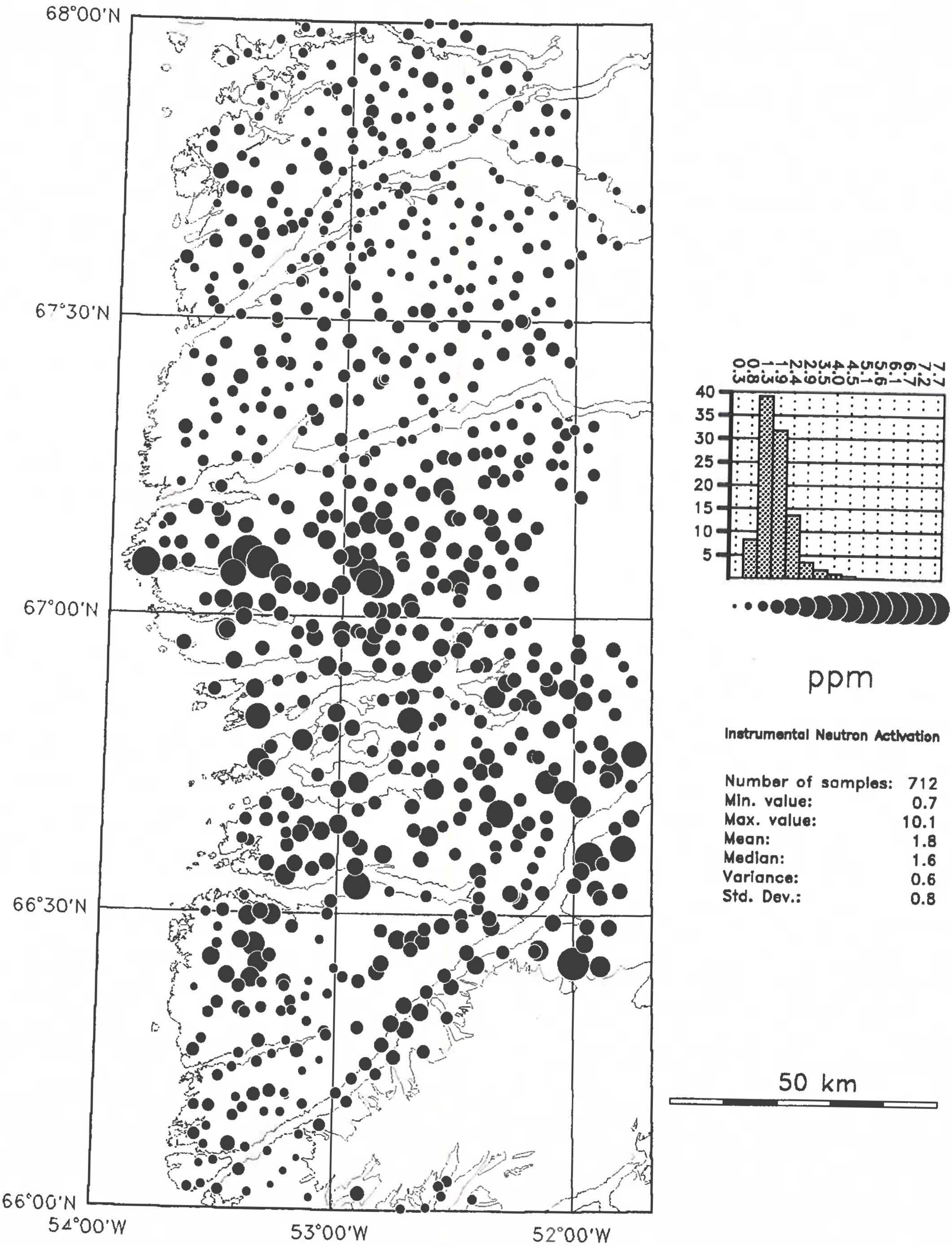

Fig. 21

Ga in stream sediment

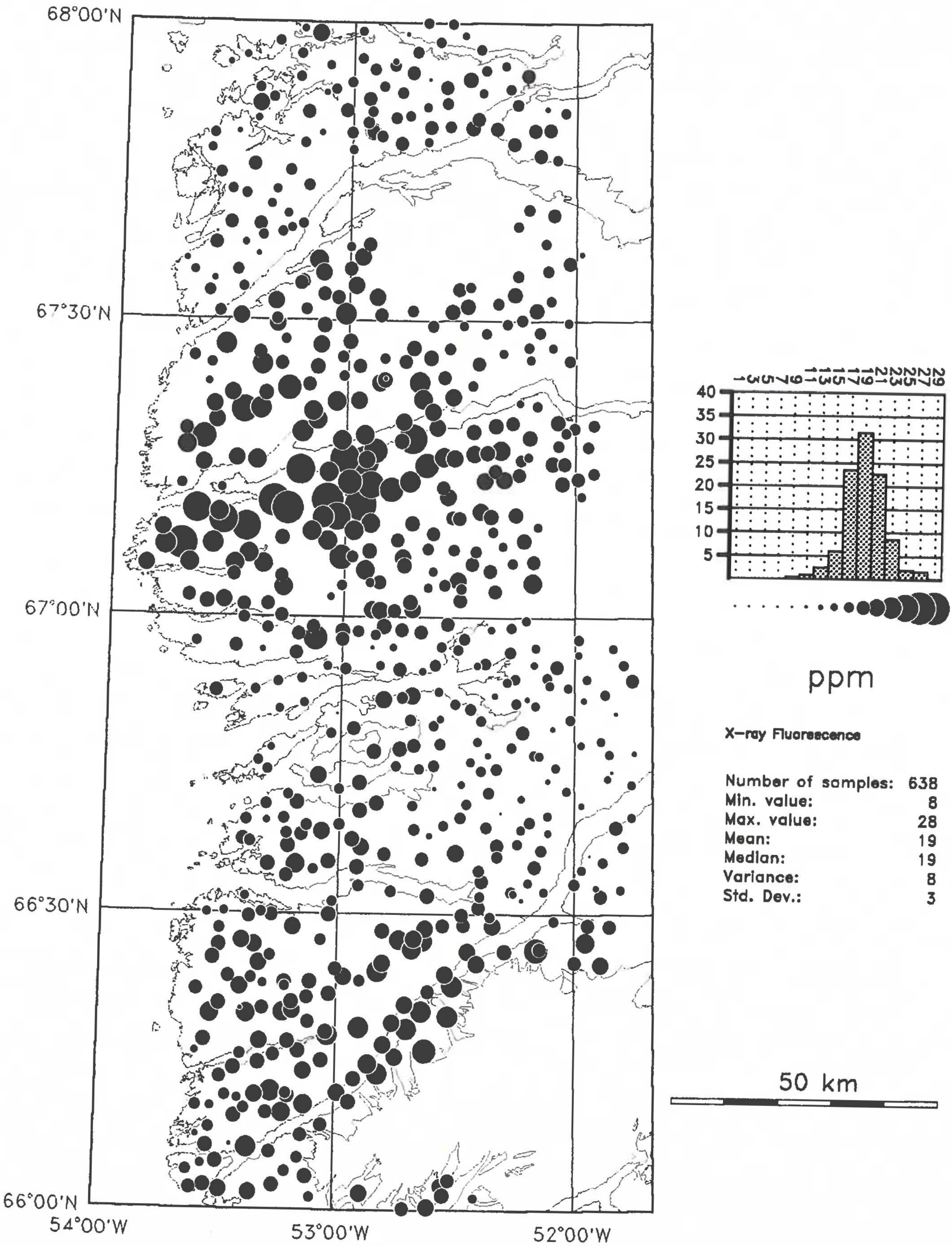

Fig. 22

Hf in stream sediment

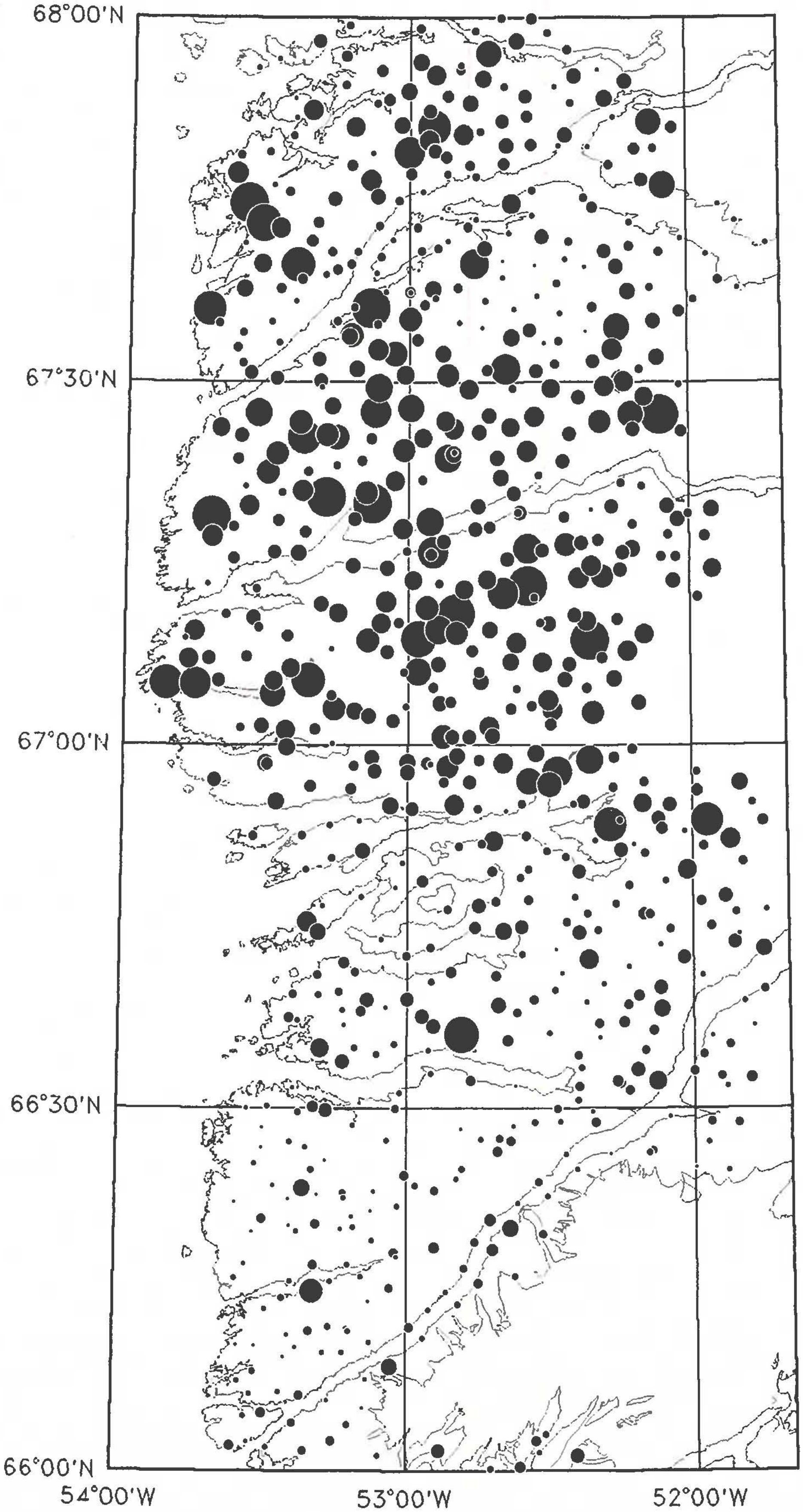

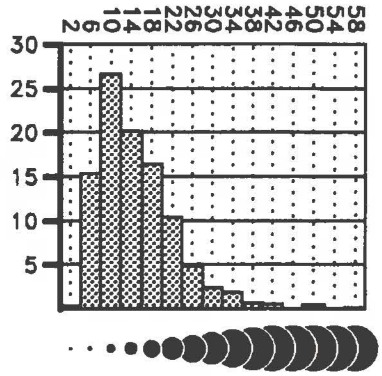

ppm

Instrumental Neutron Activation

Number of samples:	712
Min. value:	3
Max. value:	67
Mean:	15
Median:	13
Variance:	61
Std. Dev.:	8

50 km

Fig. 23

La in stream sediment

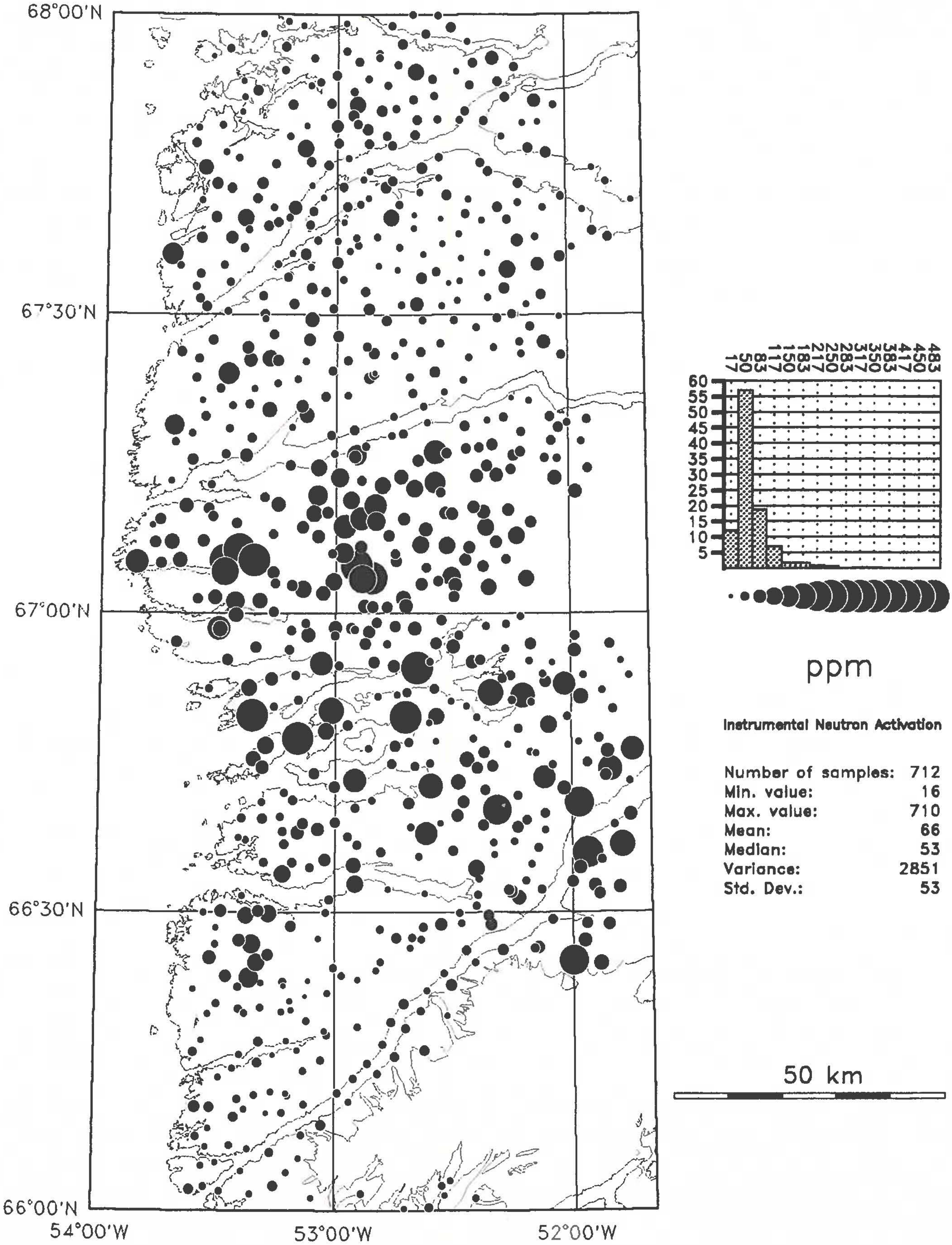

Fig. 24

Lu in stream sediment

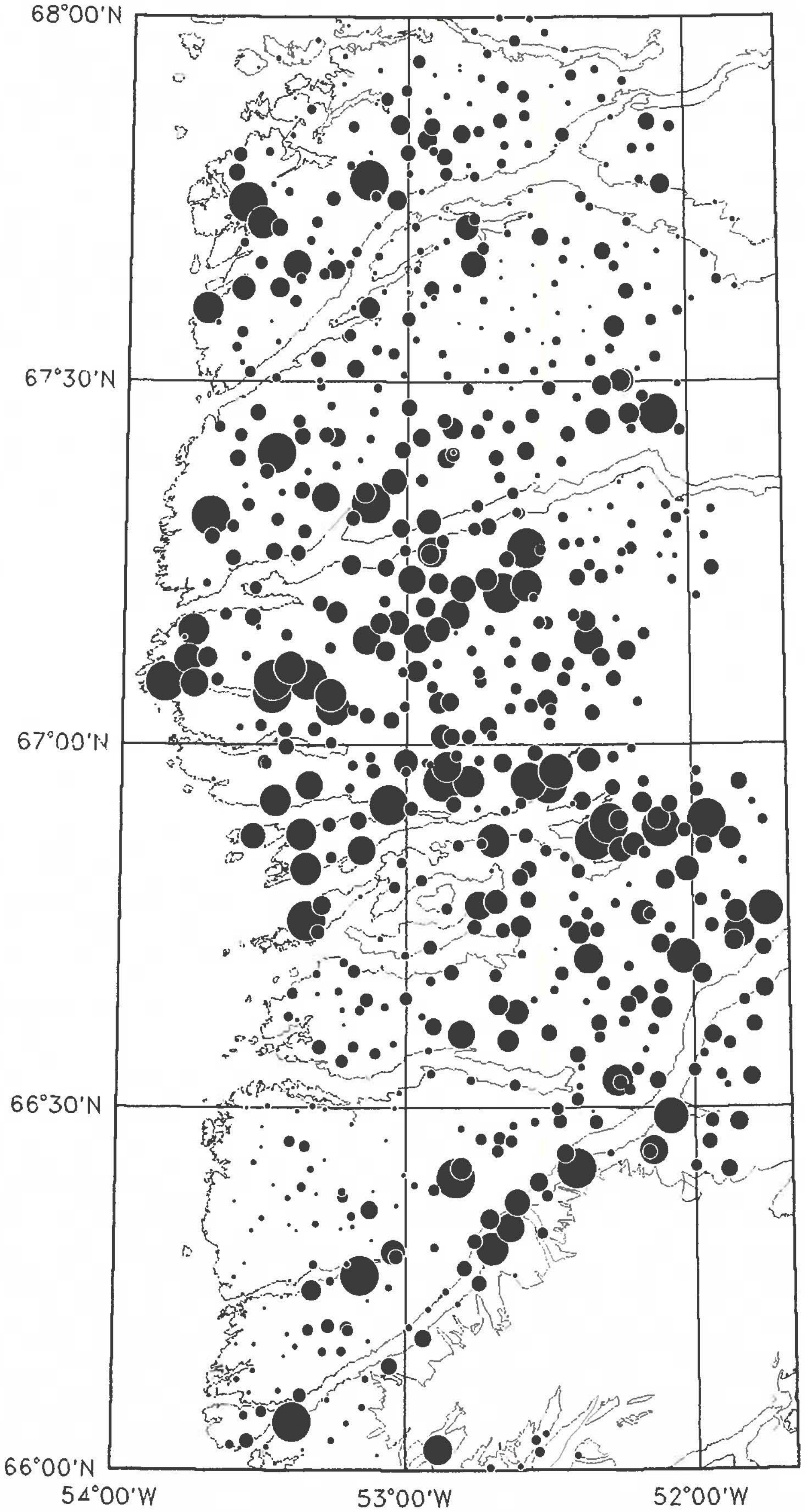

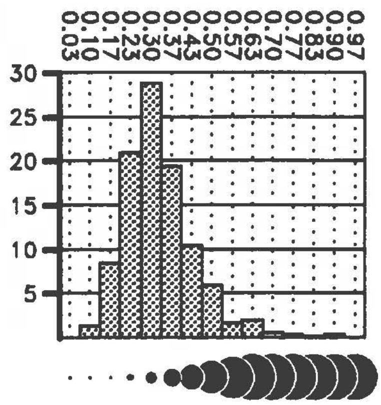

ppm

Instrumental Neutron Activation

Number of samples:	712
Min. value:	0.08
Max. value:	0.90
Mean:	0.33
Median:	0.31
Variance:	0.01
Std. Dev.:	0.12

50 km

Fig. 25

Mo in stream sediment

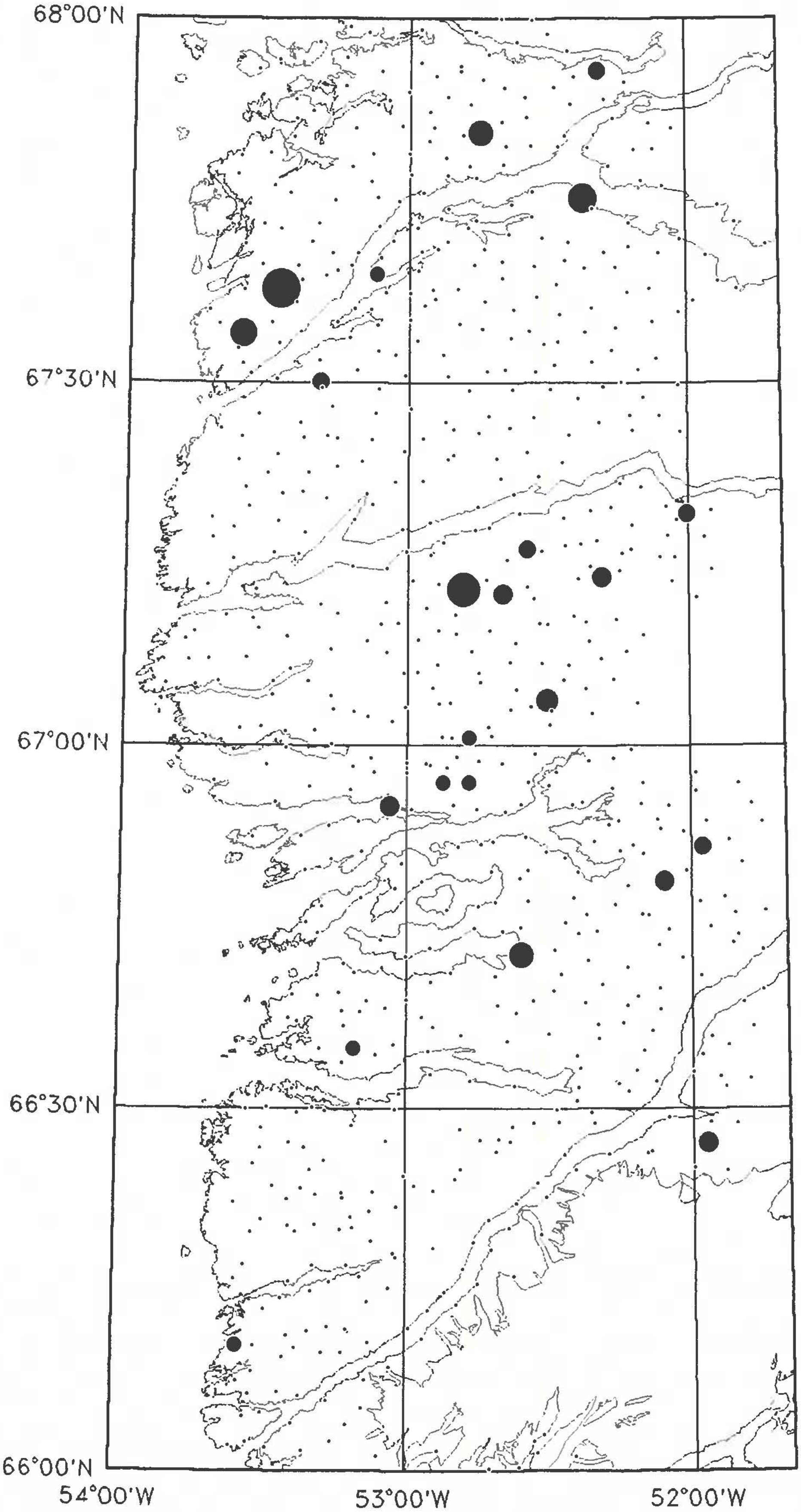

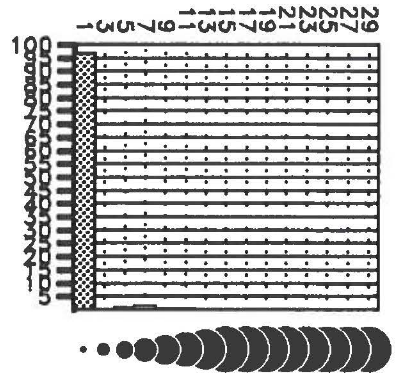

ppm

Instrumental Neutron Activation

Number of samples:	712
Min. value:	0
Max. value:	15
Mean:	0
Median:	0
Variance:	2
Std. Dev.:	1

50 km

Fig. 26

Nb in stream sediment

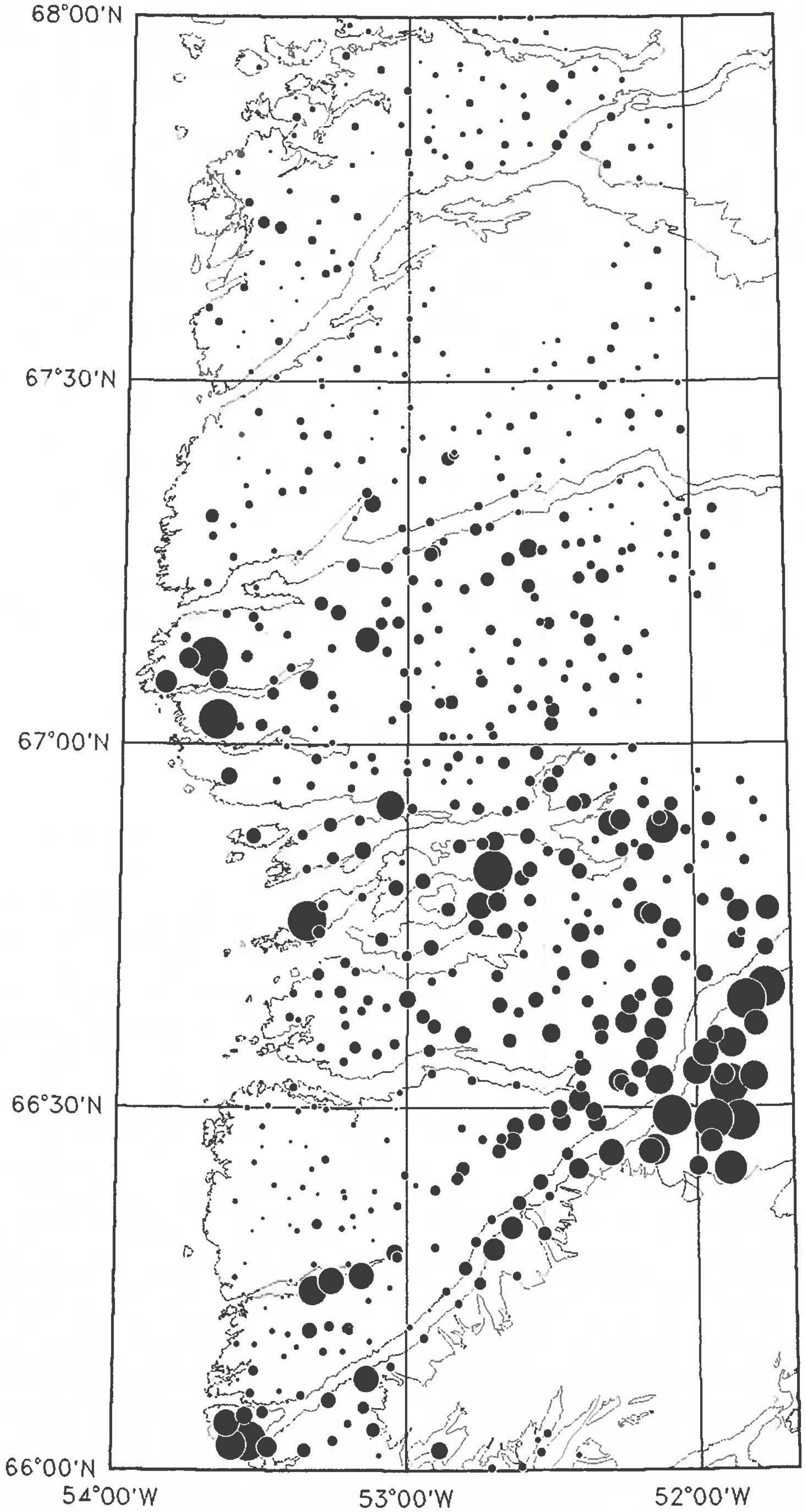

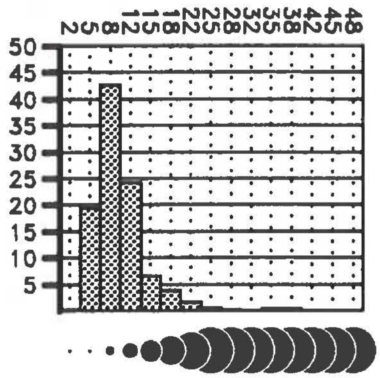

ppm

X-ray Fluorescence

Number of samples:	638
Min. value:	3
Max. value:	62
Mean:	10
Median:	9
Variance:	27
Std. Dev.:	5

50 km

Fig. 27

Nd in stream sediment

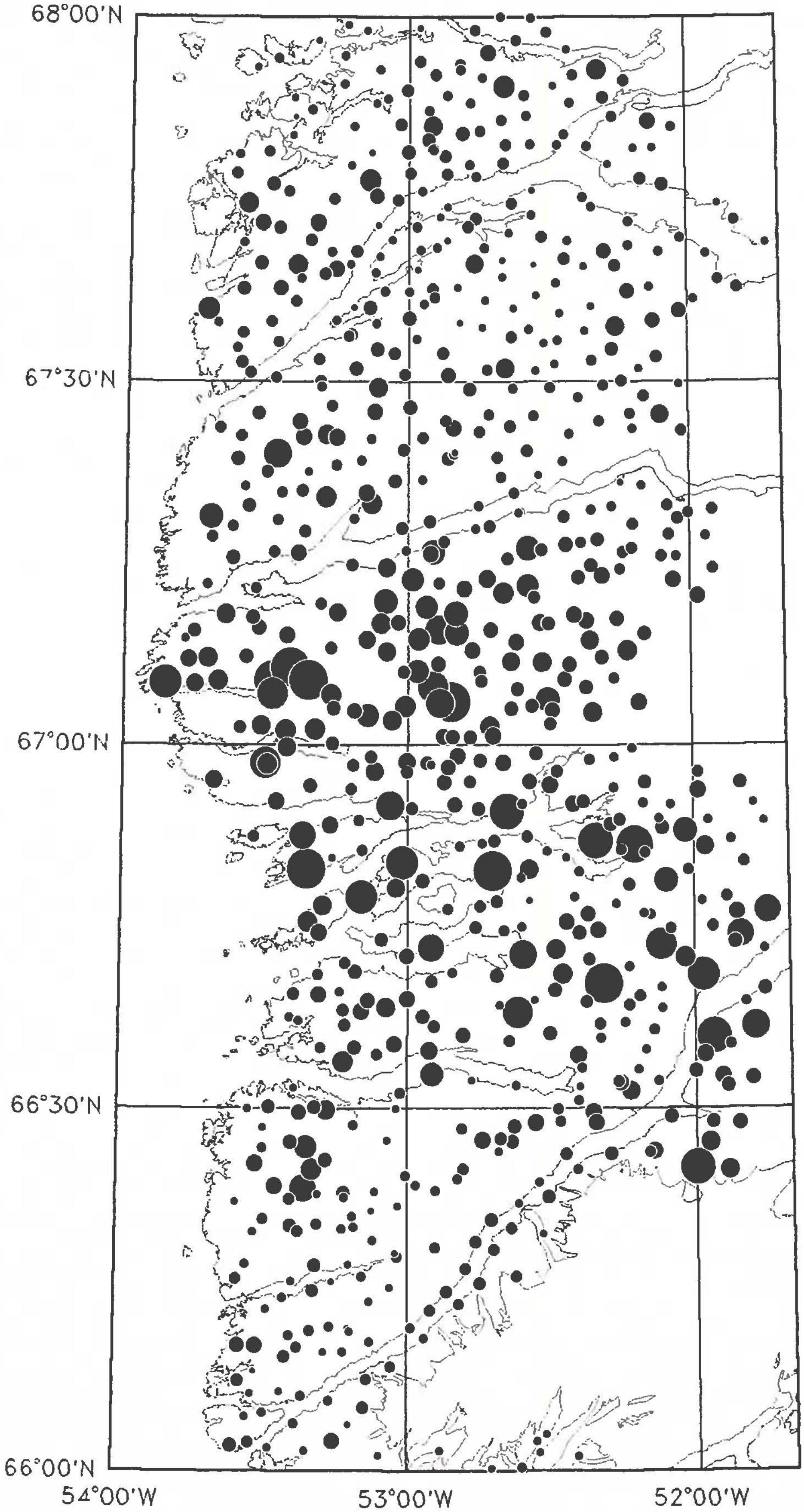

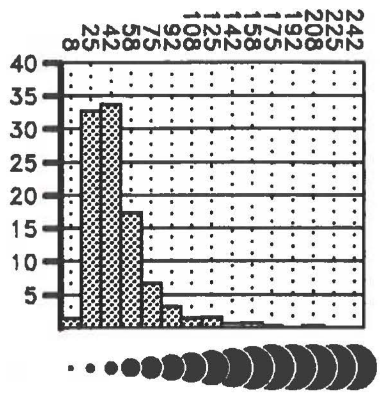

ppm

Instrumental Neutron Activation

Number of samples:	712
Min. value:	12
Max. value:	390
Mean:	48
Median:	41
Variance:	1053
Std. Dev.:	32

50 km

Fig. 28

Ni in stream sediment

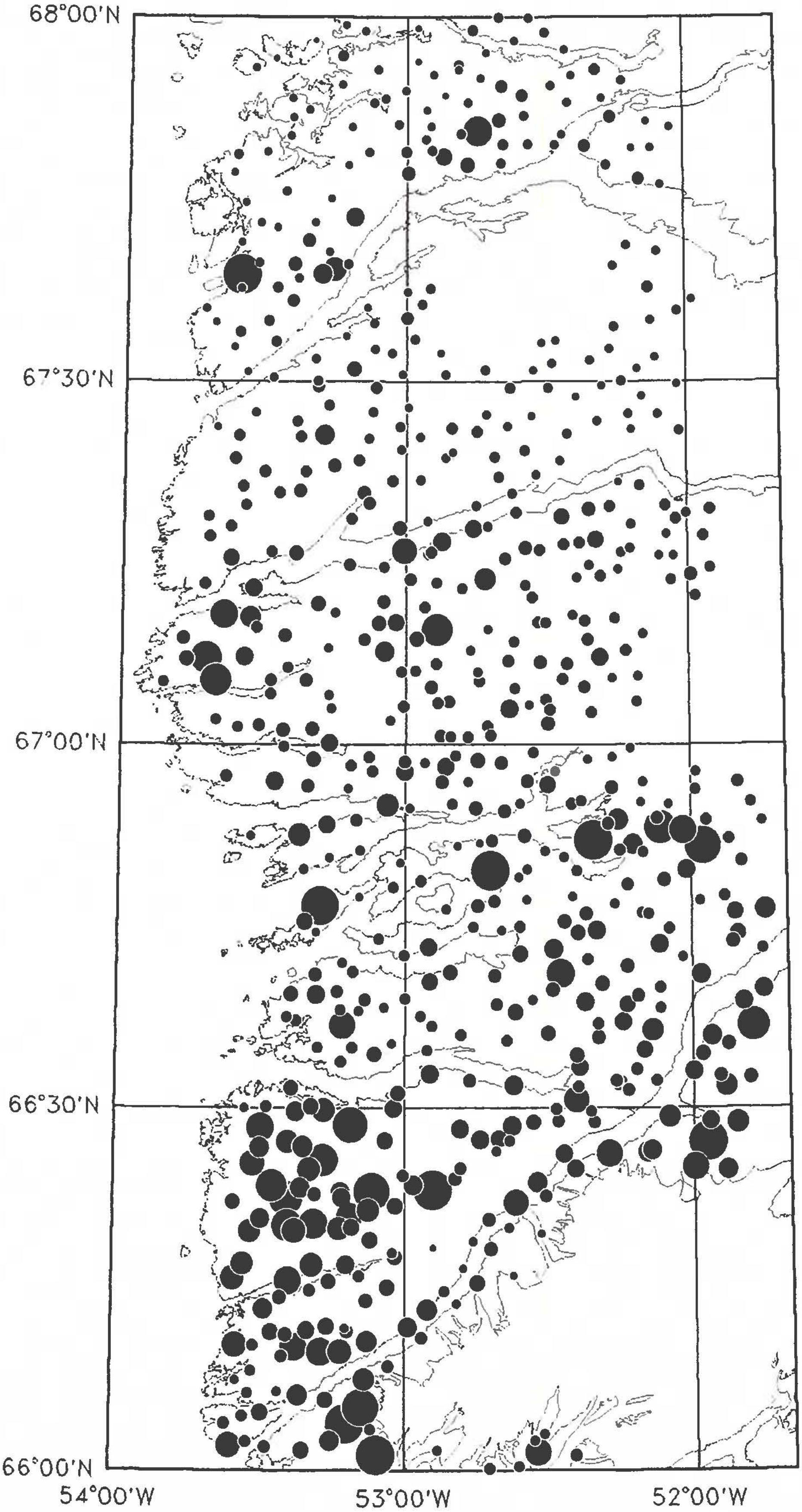

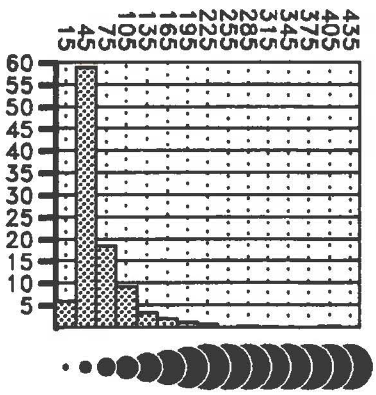

ppm

X-ray Fluorescence

Number of samples:	638
Min. value:	18
Max. value:	774
Mean:	64
Median:	51
Variance:	2363
Std. Dev.:	49

50 km

Fig. 29

Pb in stream sediment

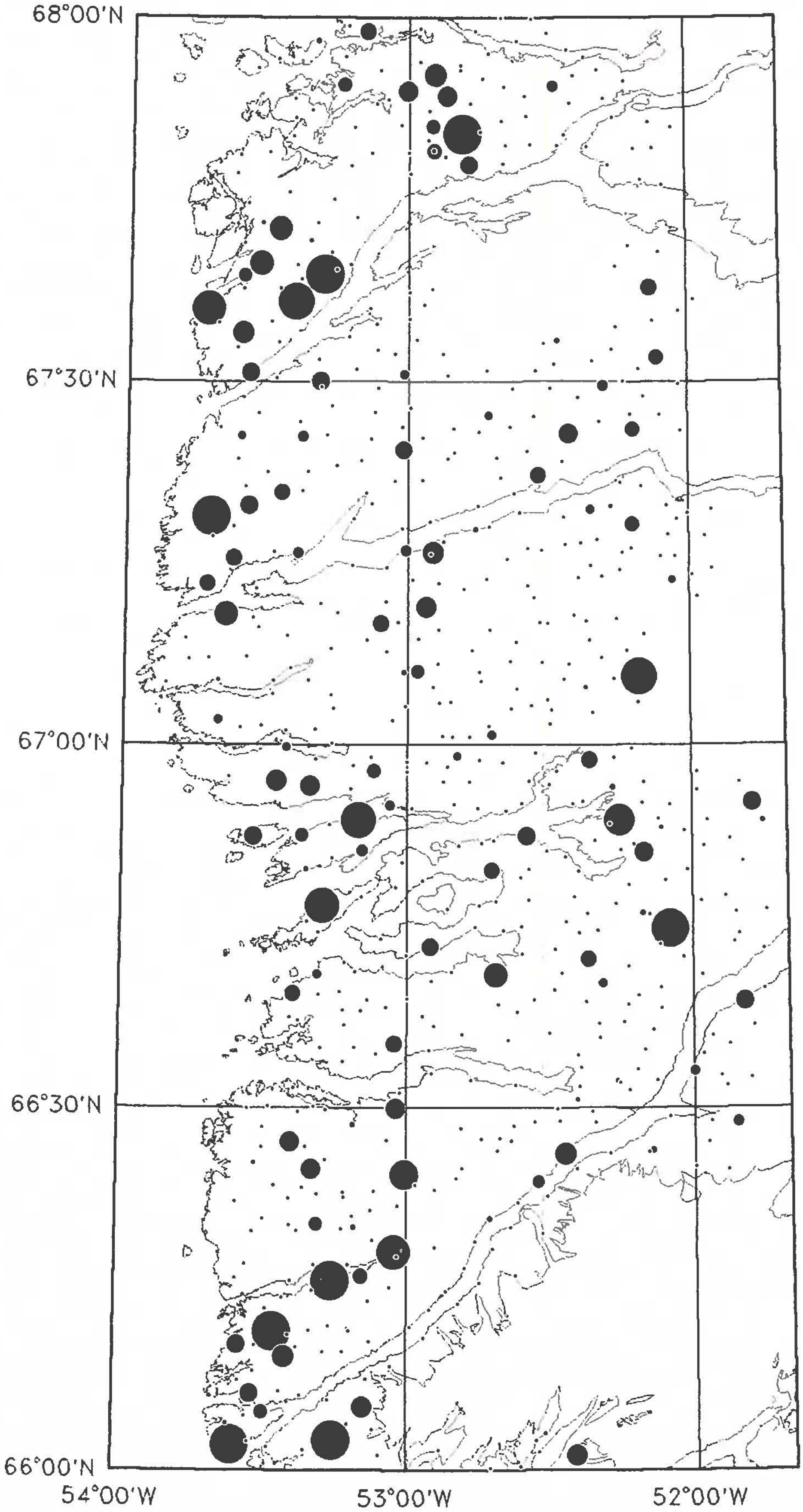

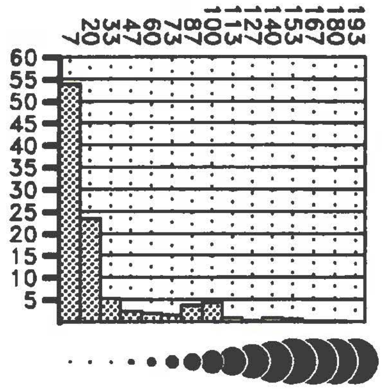

ppm

X-ray Fluorescence

Number of samples:	638
Min. value:	0
Max. value:	231
Mean:	24
Median:	13
Variance:	1201
Std. Dev.:	35

50 km

Fig. 30

Rb in stream sediment

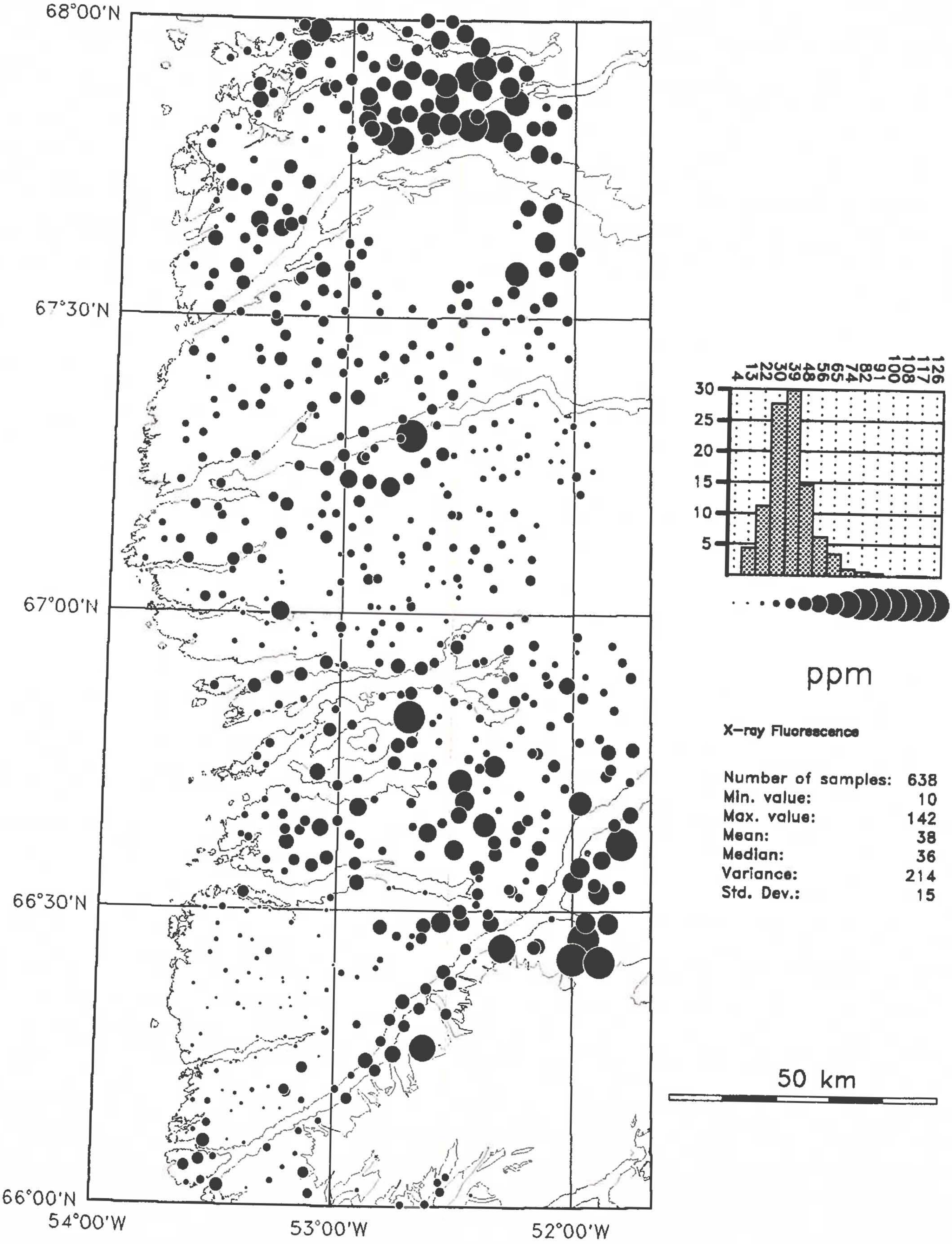

Fig. 31

Sb in stream sediment

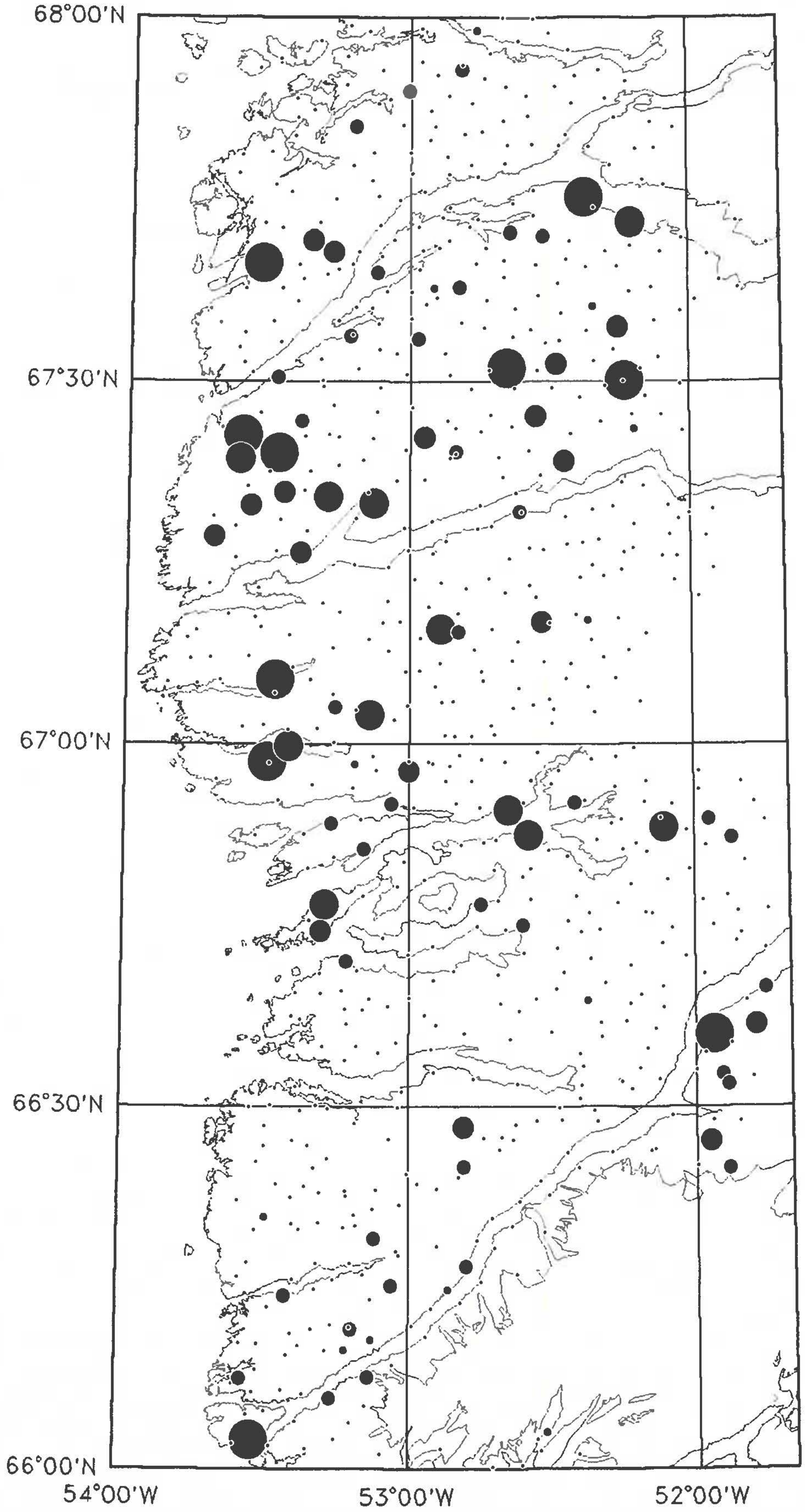

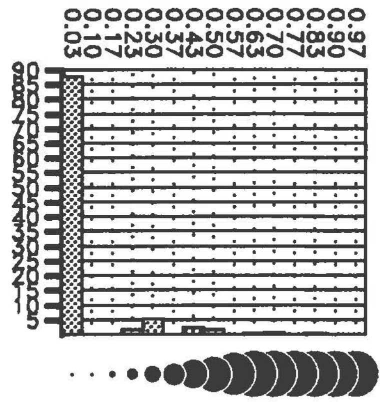

ppm

Instrumental Neutron Activation

Number of samples:	712
Min. value:	0.00
Max. value:	0.80
Mean:	0.05
Median:	0.00
Variance:	0.02
Std. Dev.:	0.13

50 km

Fig. 32

Sc in stream sediment

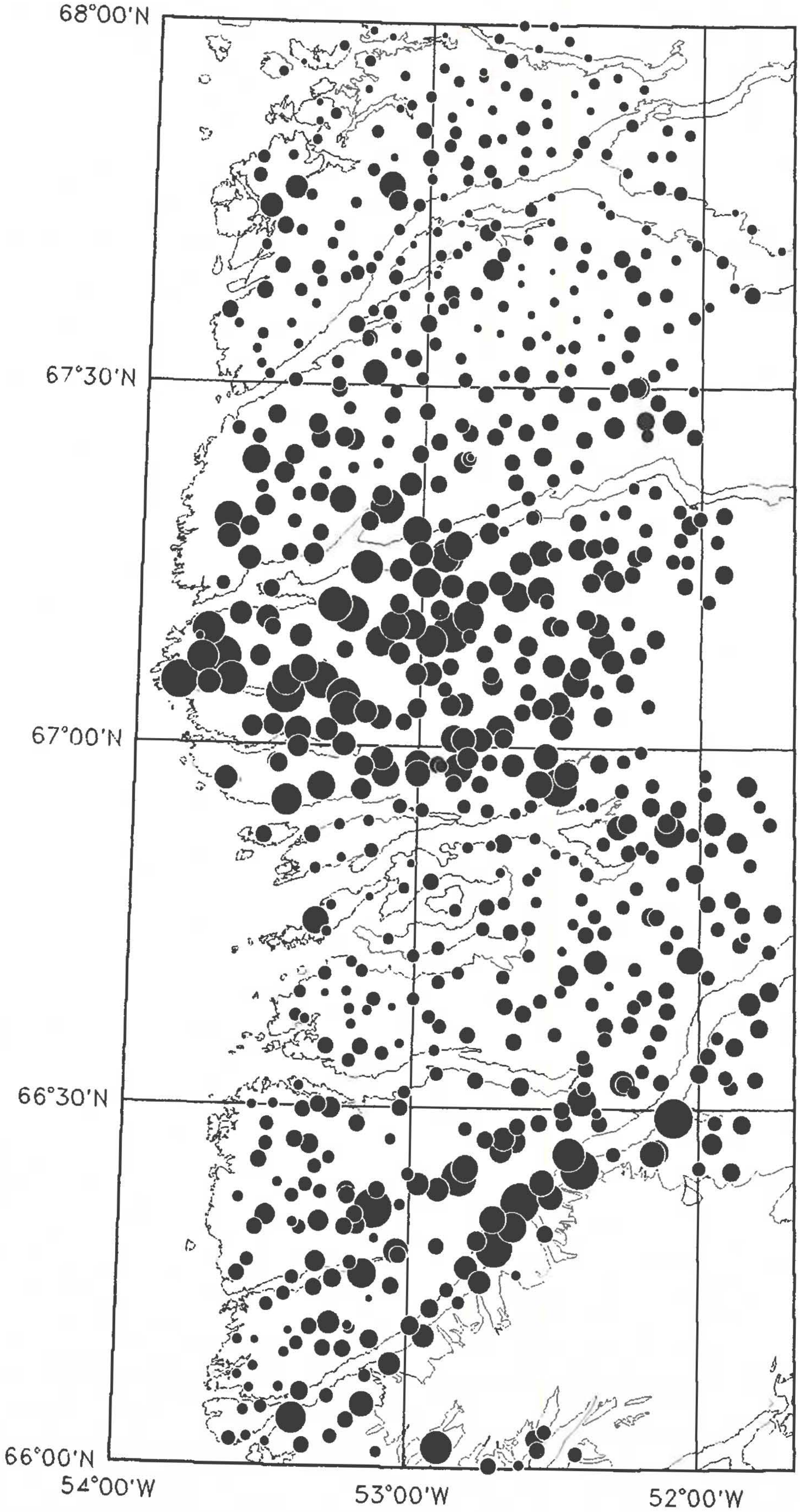

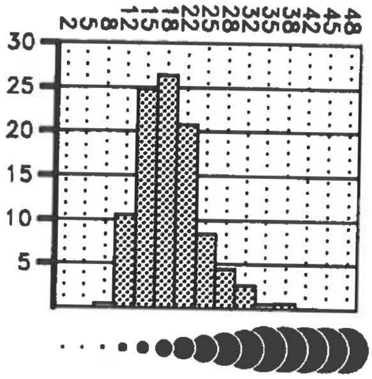

ppm

Instrumental Neutron Activation

Number of samples:	712
Min. value:	9
Max. value:	40
Mean:	19
Median:	18
Variance:	26
Std. Dev.:	5

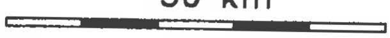

Fig. 33

Sm in stream sediment

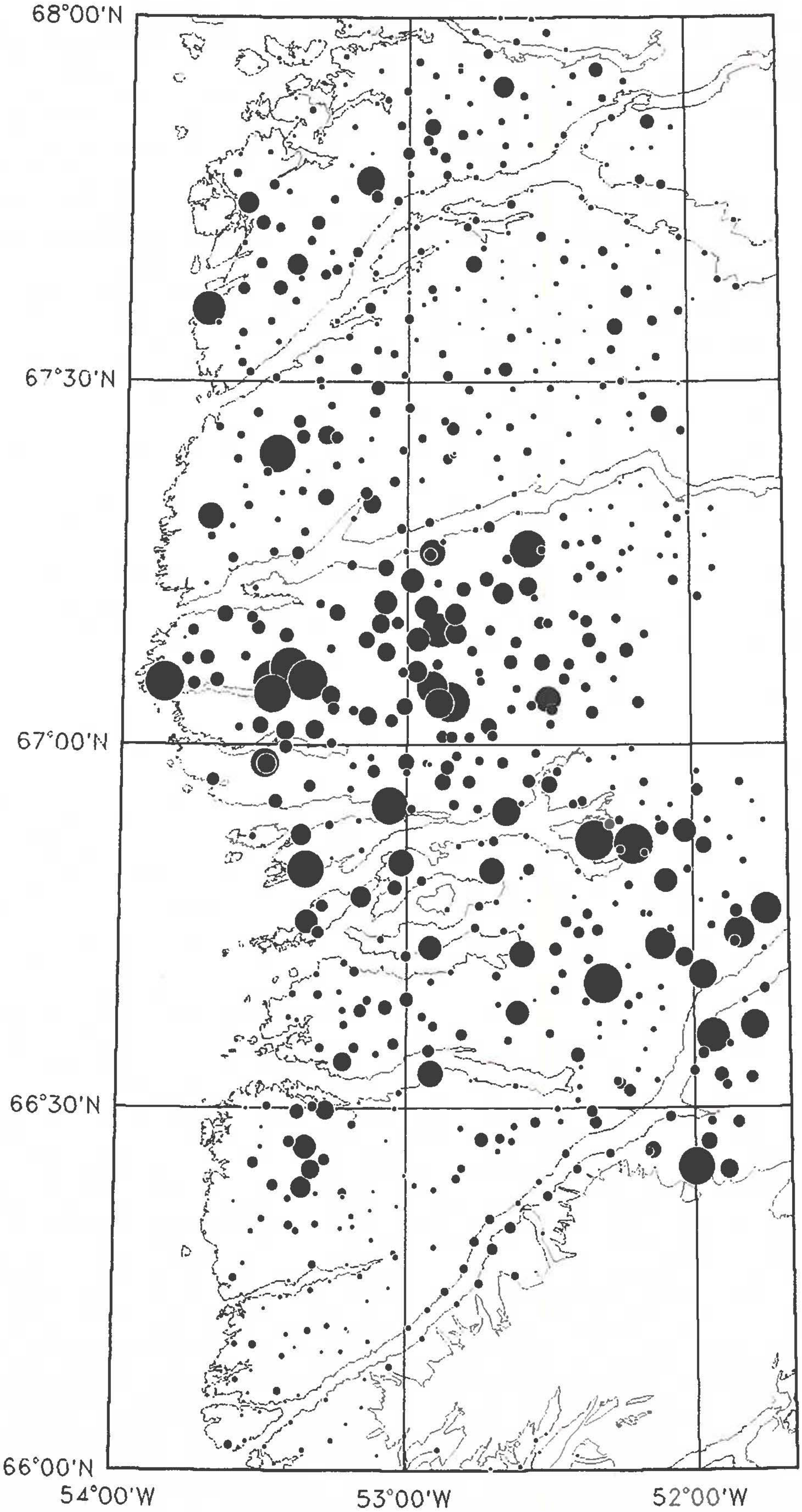

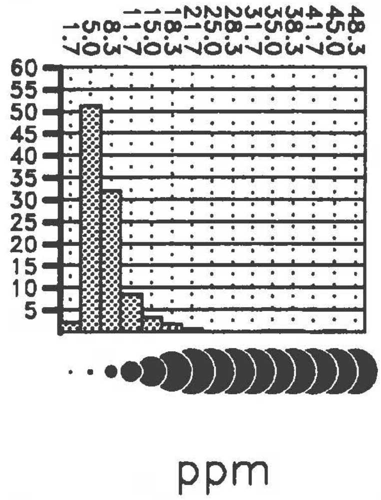

Instrumental Neutron Activation

Number of samples:	712
Min. value:	2.6
Max. value:	46.0
Mean:	7.3
Median:	6.4
Variance:	15.0
Std. Dev.:	3.9

50 km

Fig. 34

Sr in stream sediment

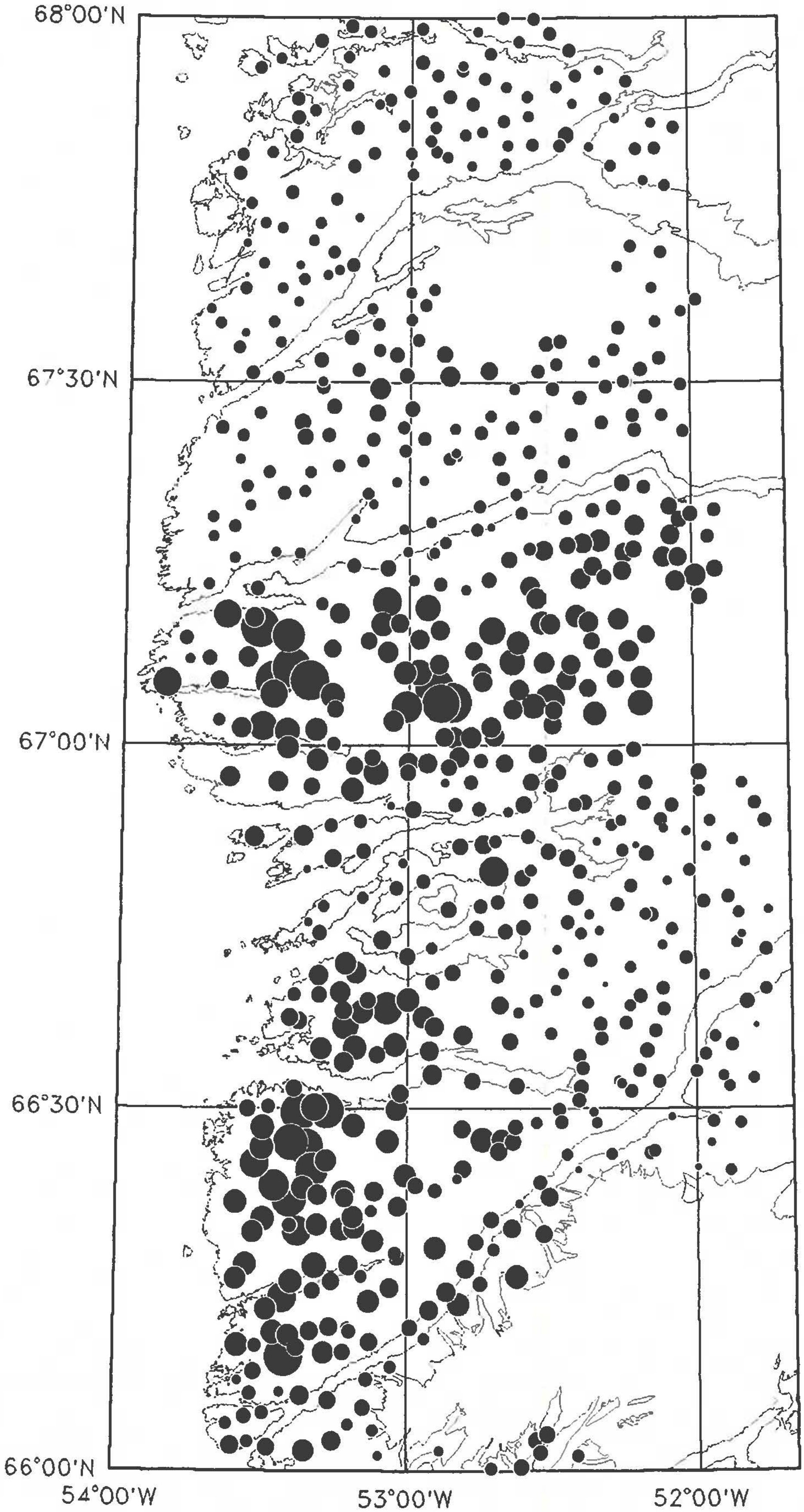

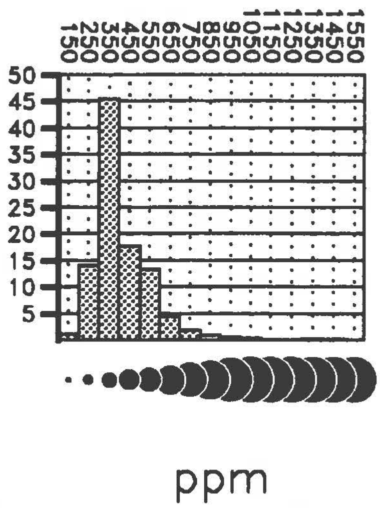

X-ray Fluorescence

Number of samples:	638
Min. value:	130
Max. value:	1962
Mean:	416
Median:	365
Variance:	30856
Std. Dev.:	176

Fig. 35

Th in stream sediment

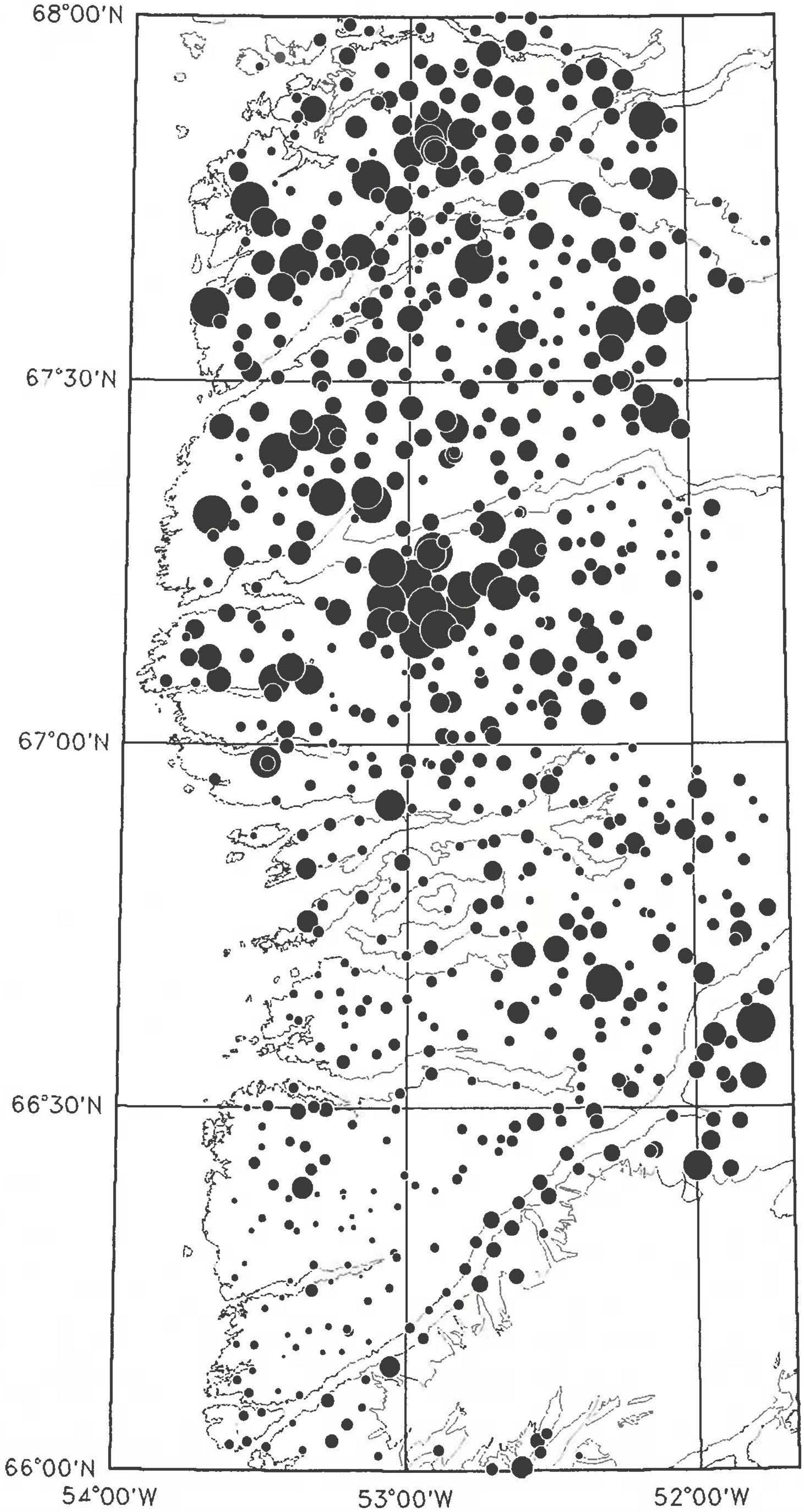

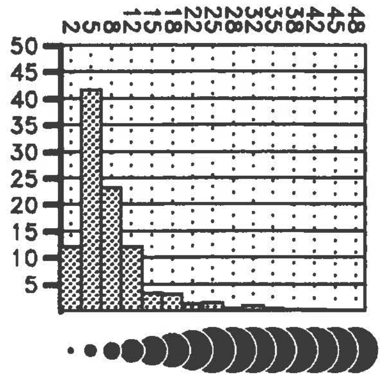

Instrumental Neutron Activation

Number of samples:	712
Min. value:	0
Max. value:	40
Mean:	8
Median:	6
Variance:	32
Std. Dev.:	6

50 km

Fig. 36

U in stream sediment

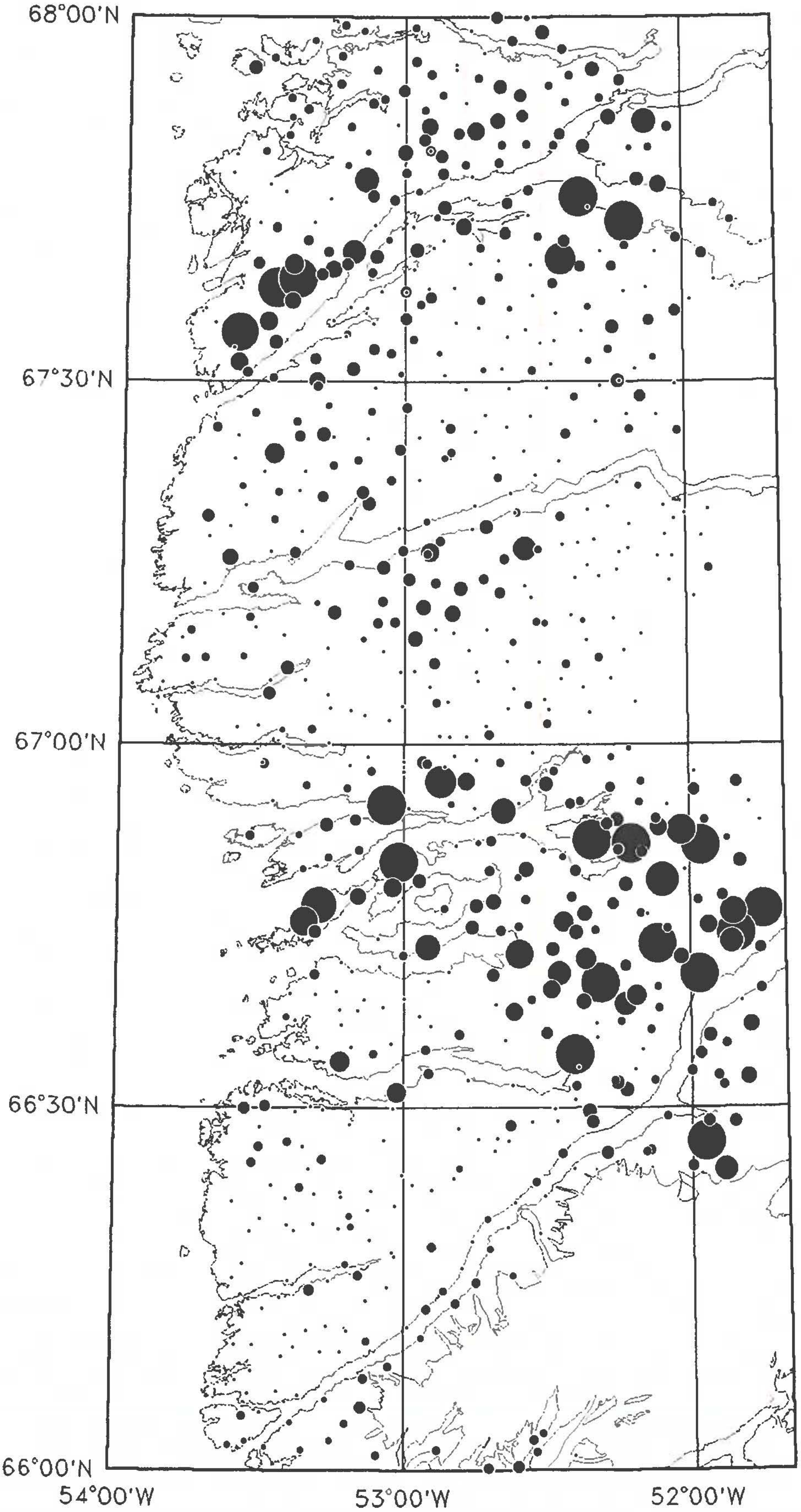

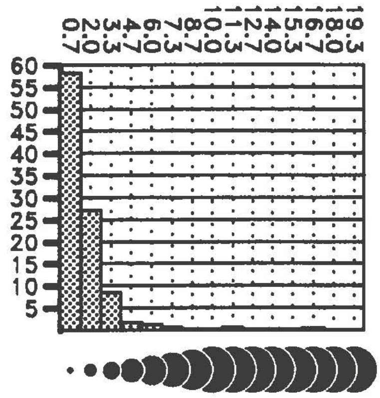

ppm

Instrumental Neutron Activation

Number of samples:	712
Min. value:	0.0
Max. value:	22.0
Mean:	1.5
Median:	1.0
Variance:	6.8
Std. Dev.:	2.6

50 km

Fig. 37

V in stream sediment

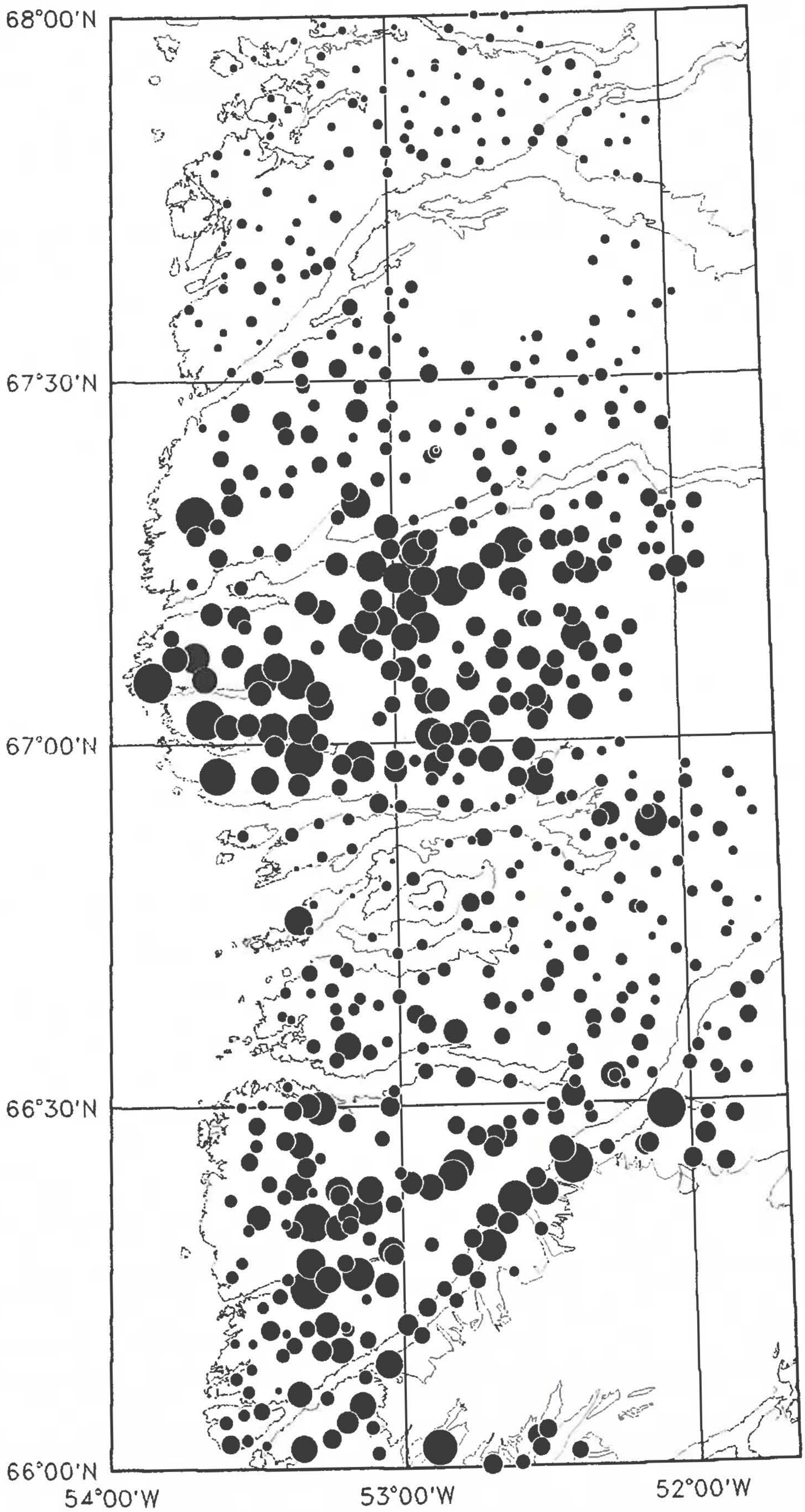

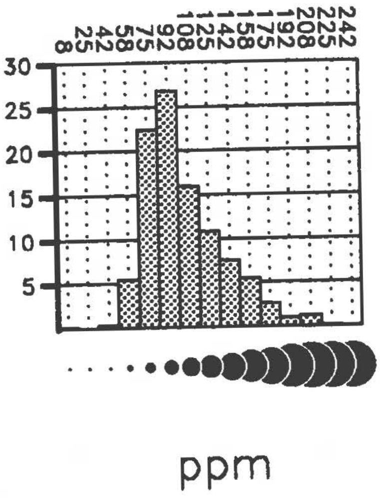

X-ray Fluorescence

Number of samples:	638
Min. value:	9
Max. value:	230
Mean:	104
Median:	96
Variance:	1025
Std. Dev.:	32

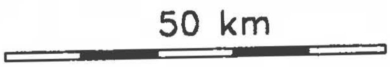

Fig. 38

Y in stream sediment

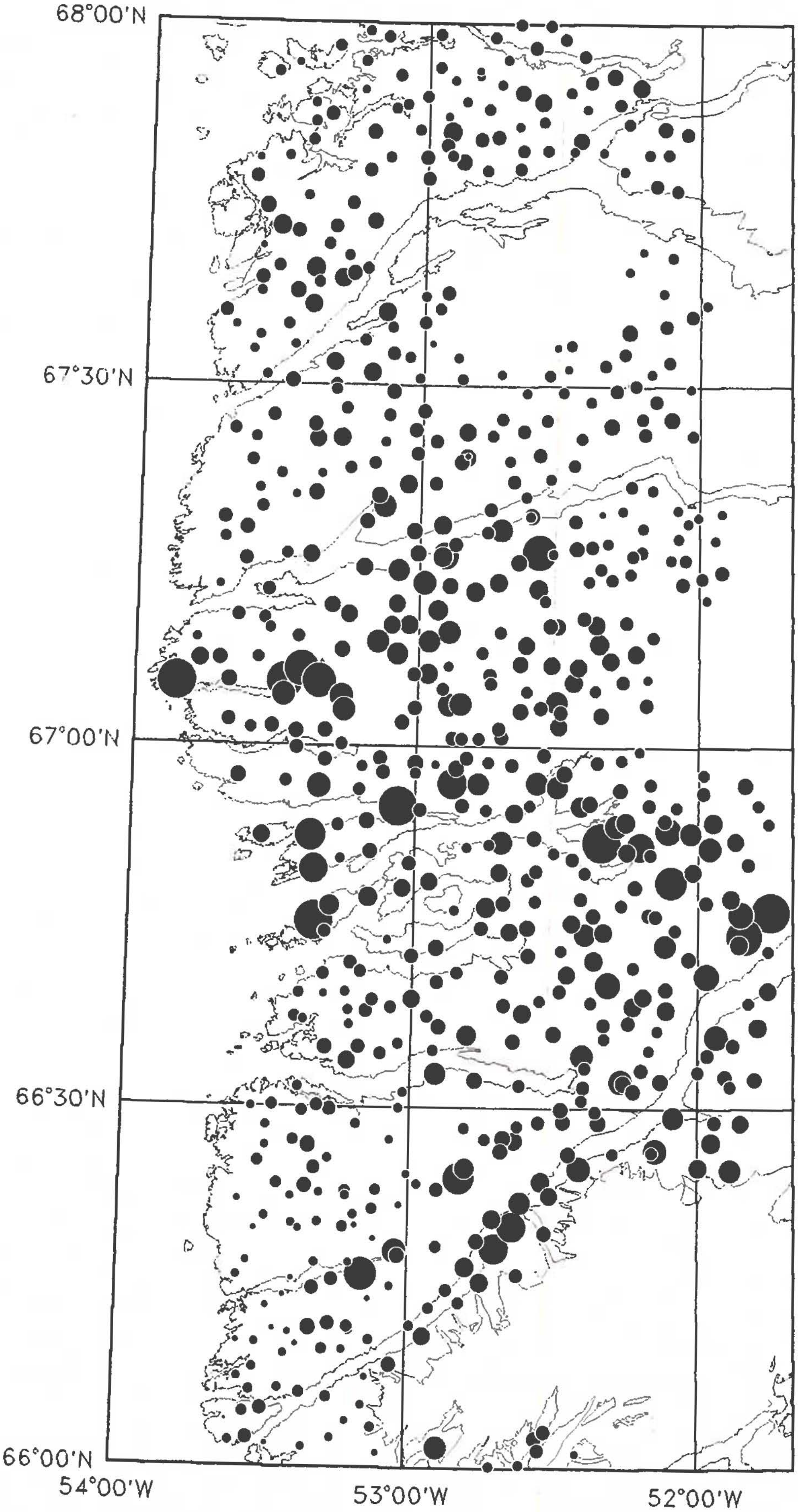

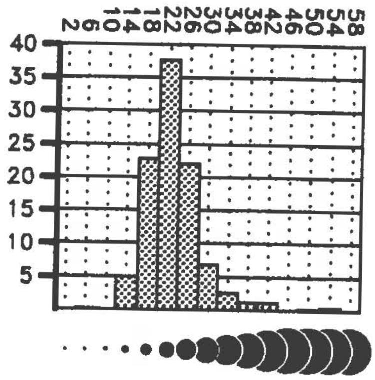

ppm

X-ray Fluorescence

Number of samples:	638
Min. value:	7
Max. value:	66
Mean:	23
Median:	22
Variance:	34
Std. Dev.:	6

50 km

Fig. 39

Yb in stream sediment

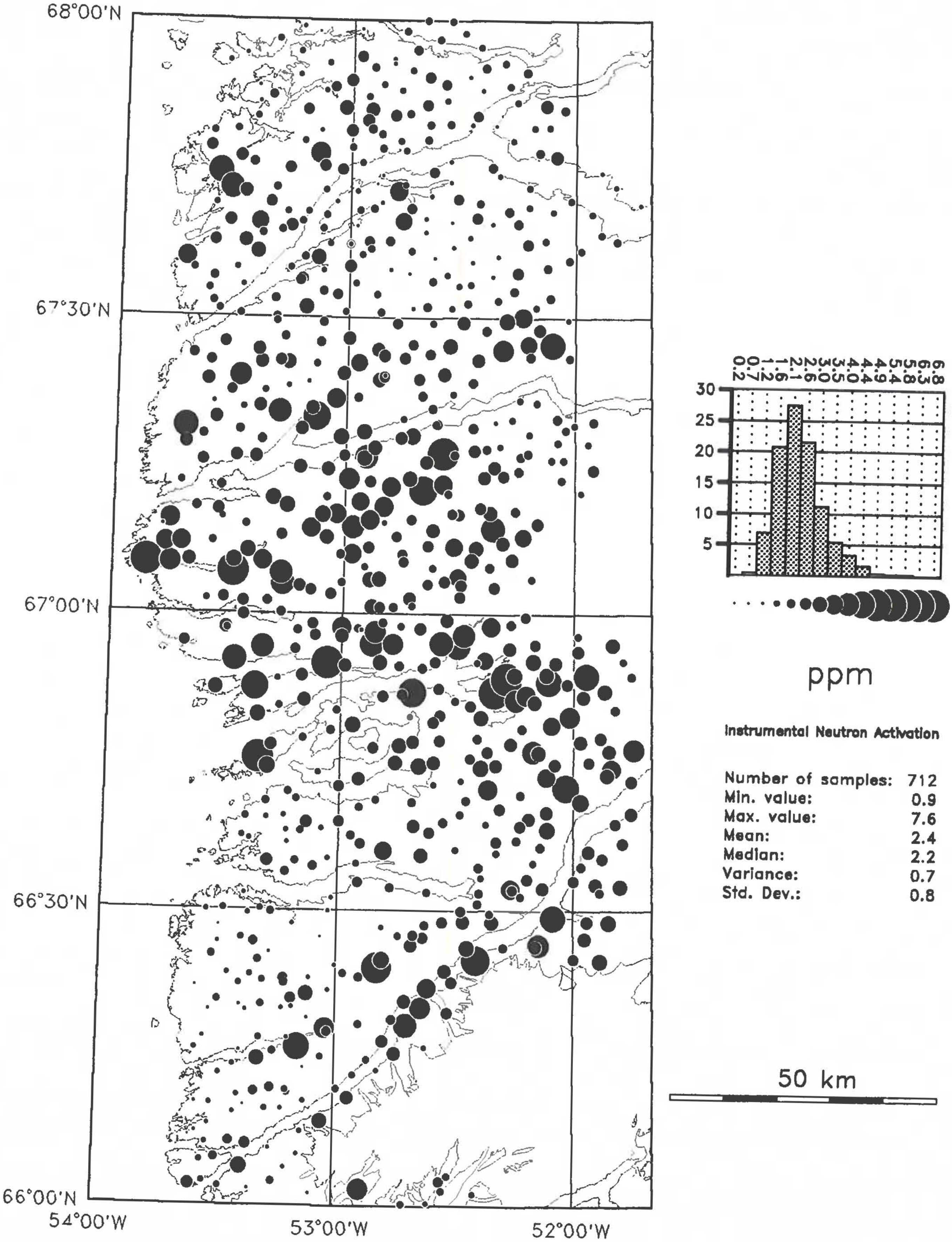

Fig. 40

Zn in stream sediment

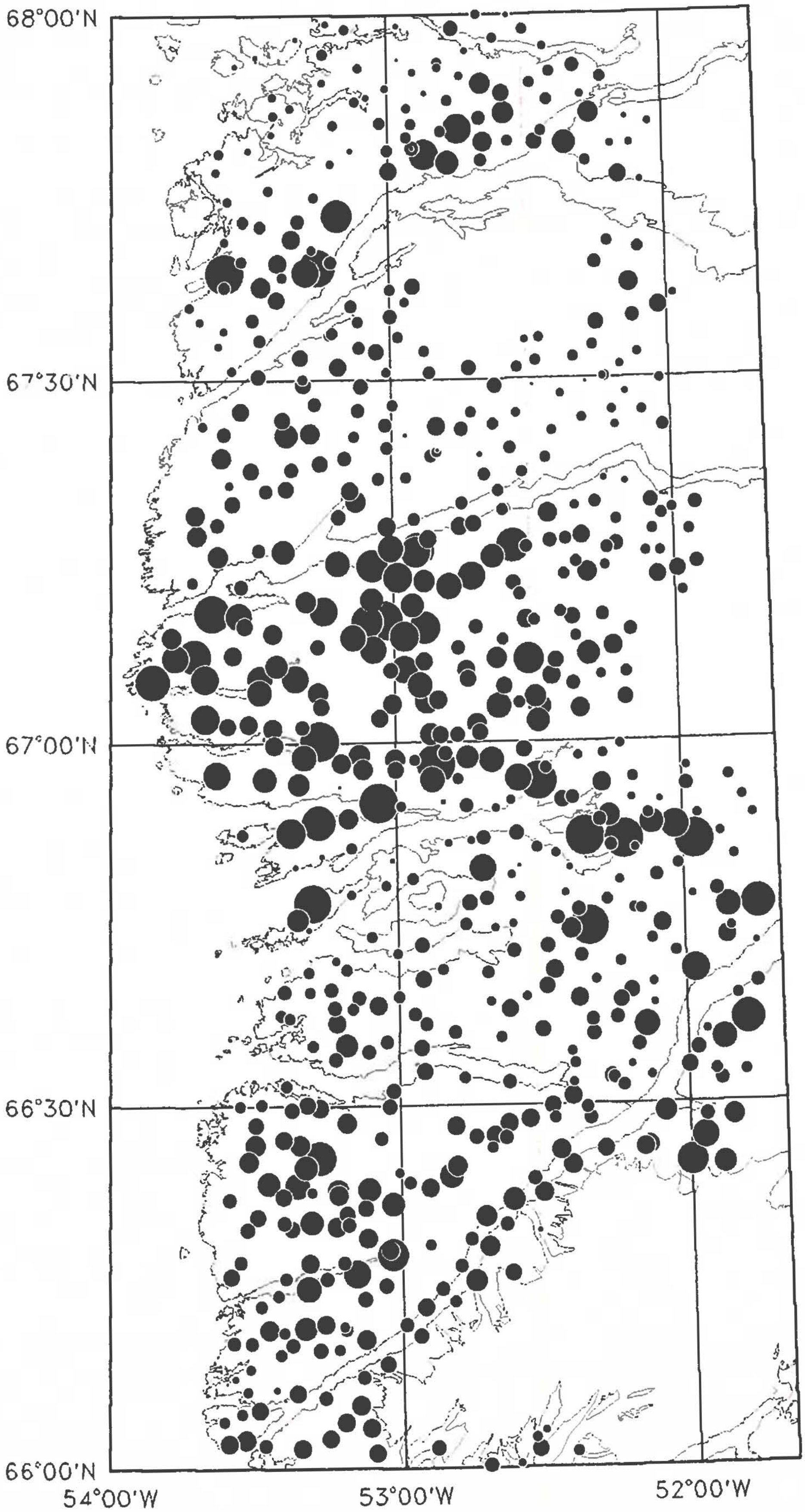

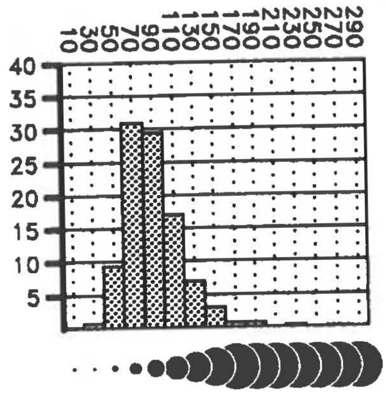

ppm

X-ray Fluorescence

Number of samples:	638
Min. value:	0
Max. value:	260
Mean:	89
Median:	85
Variance:	804
Std. Dev.:	28

50 km

Fig. 41

Zr in stream sediment

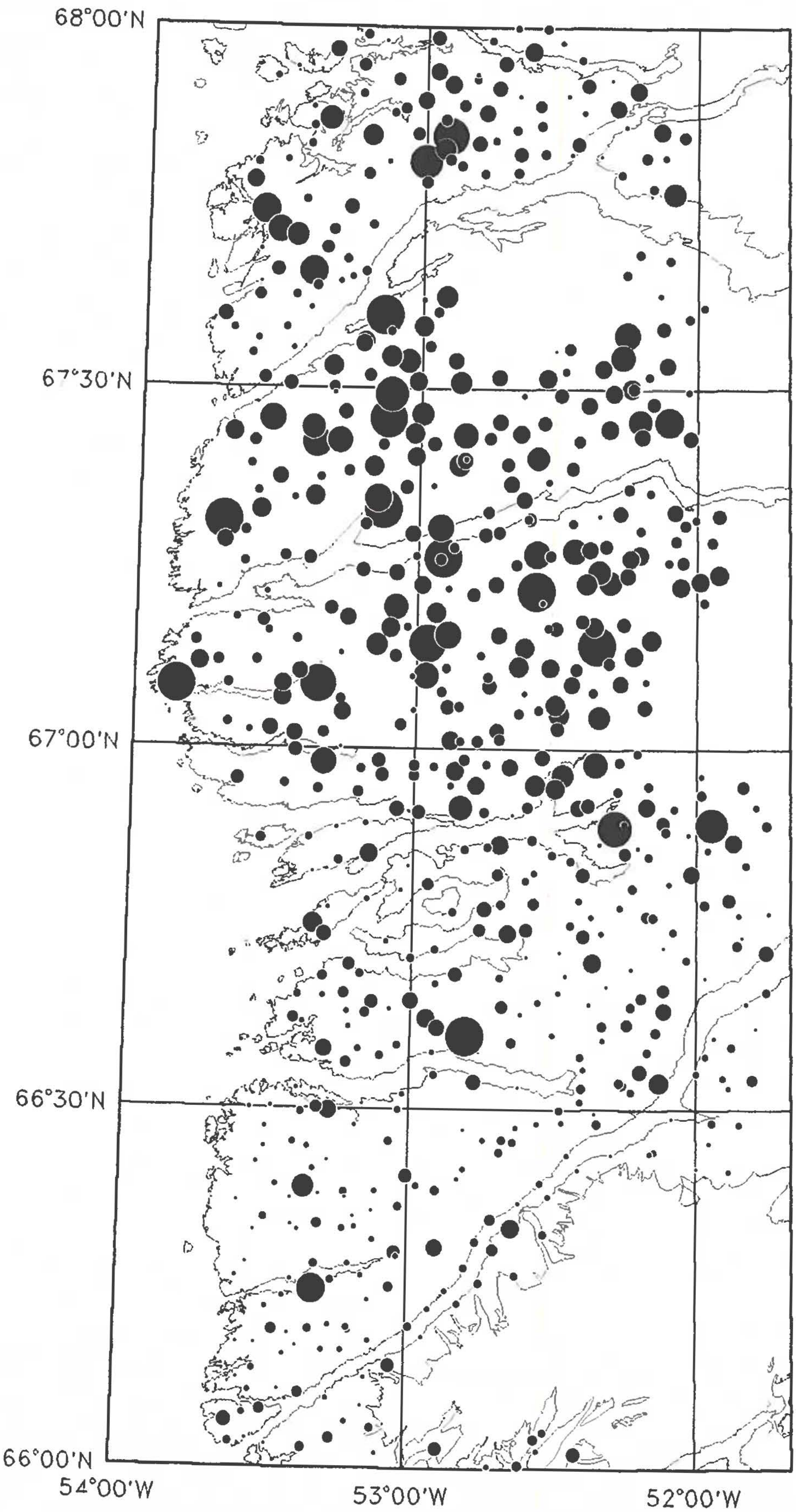

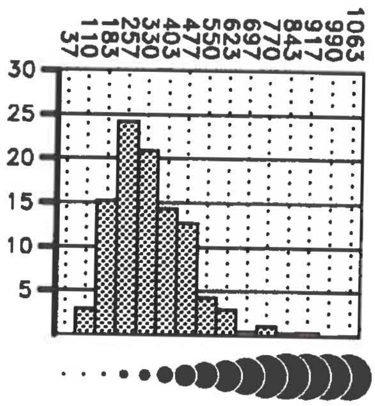

X-ray Fluorescence

Number of samples:	638
Min. value:	109
Max. value:	1167
Mean:	343
Median:	318
Variance:	20741
Std. Dev.:	144

50 km

Fig. 42

Total gamma-radiation

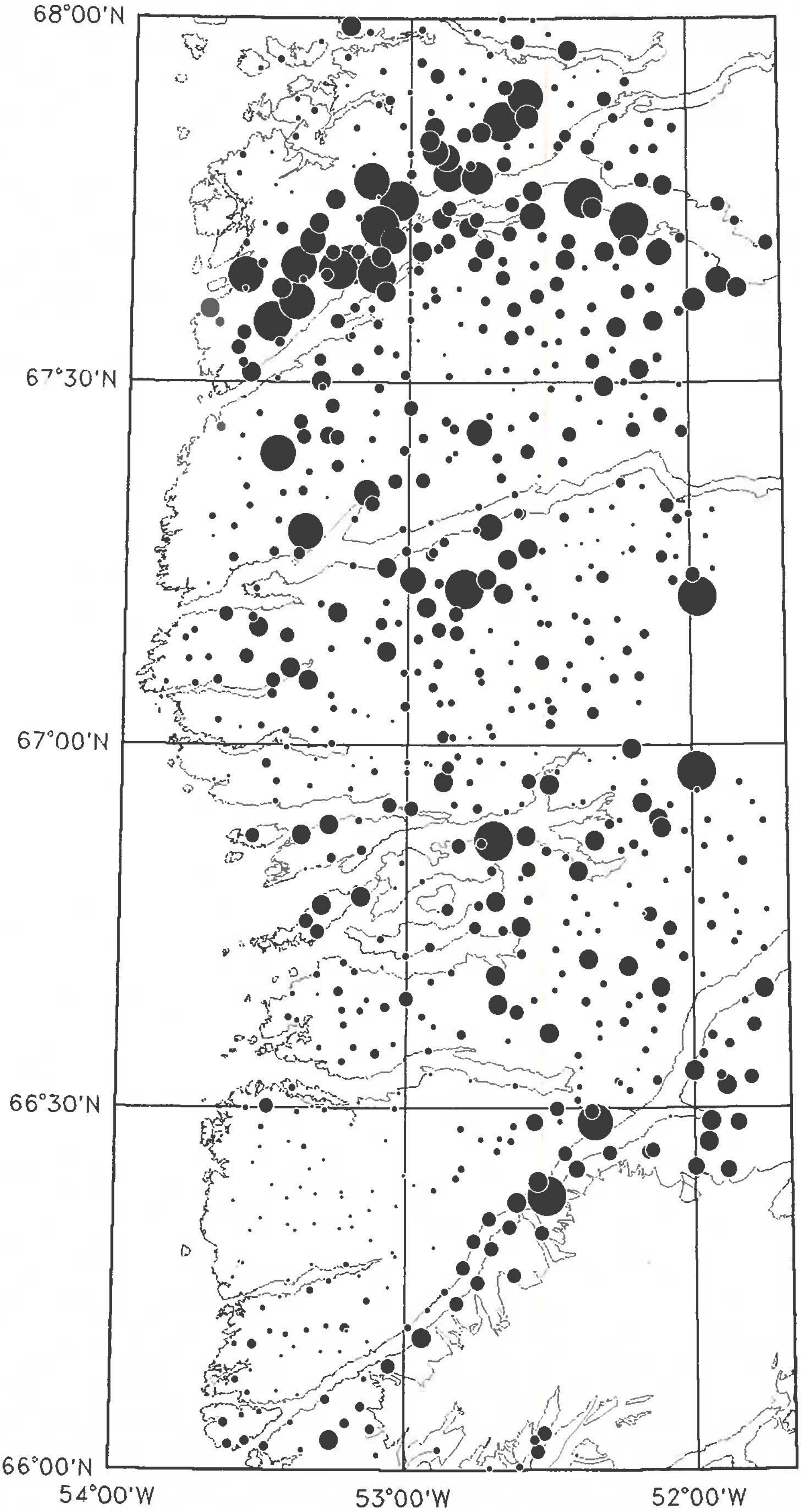

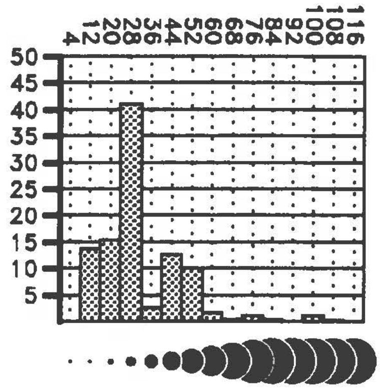

counts/sec

Scintillometry

Number of samples:	717
Min. value:	10
Max. value:	130
Mean:	31
Median:	25
Variance:	262
Std. Dev.:	16

50 km

Fig. 43

Conductivity of stream water

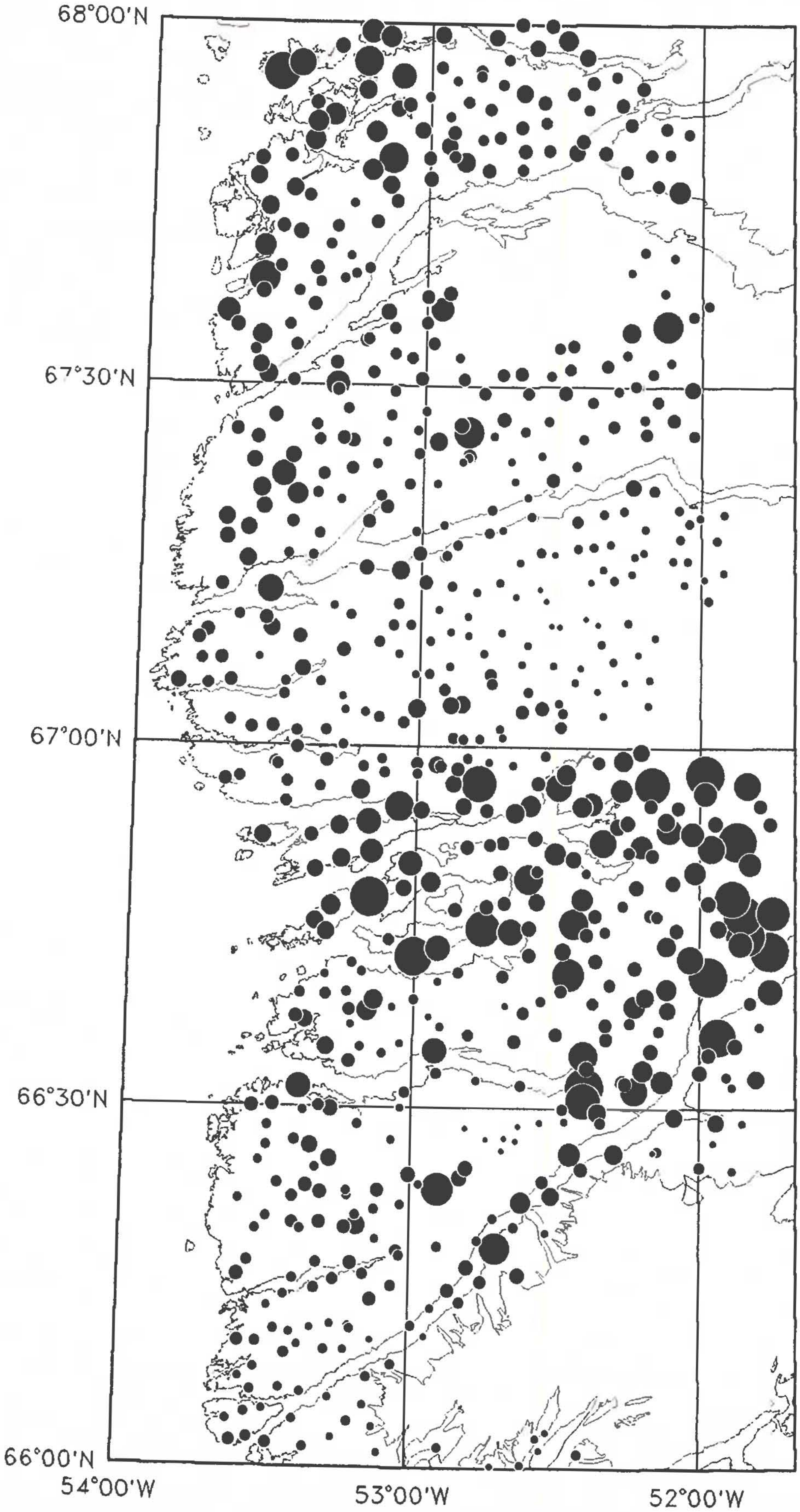

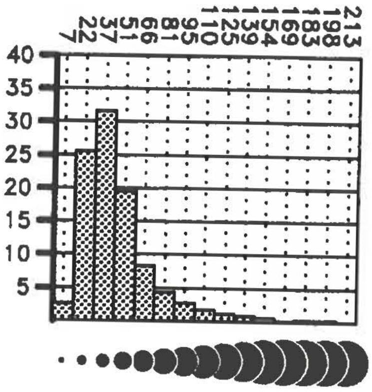

micro sievert

Number of samples:	665
Min. value:	9
Max. value:	246
Mean:	46
Median:	39
Variance:	922
Std. Dev.:	30

50 km

Fig. 44

Fluor in stream water

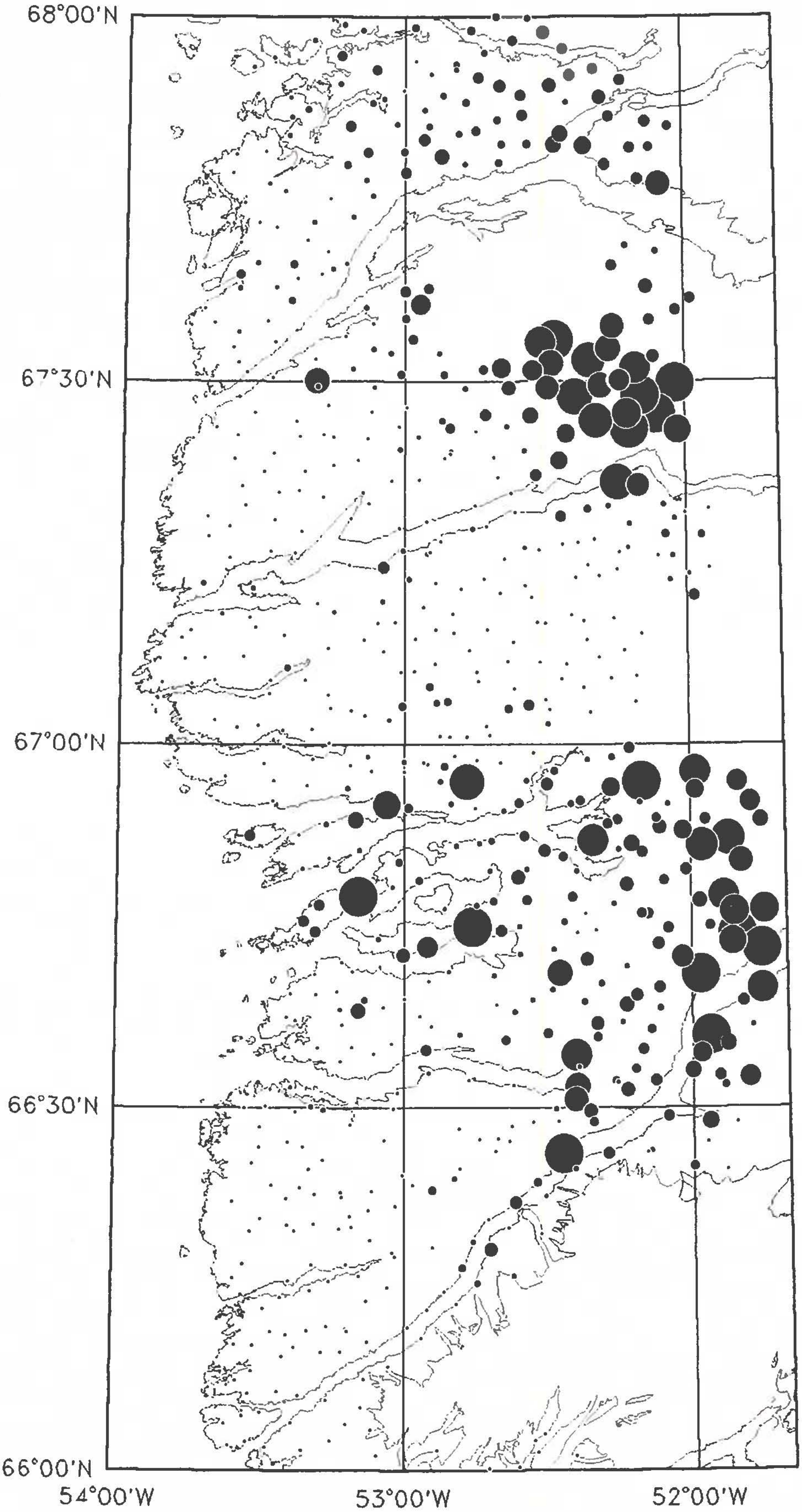

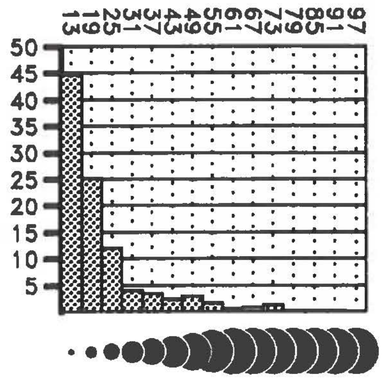

ppb

Ion sensitive electrode

Number of samples:	665
Min. value:	0
Max. value:	93
Mean:	12
Median:	11
Variance:	221
Std. Dev.:	15

50 km

Fig. 45

Stream sediment anomalies

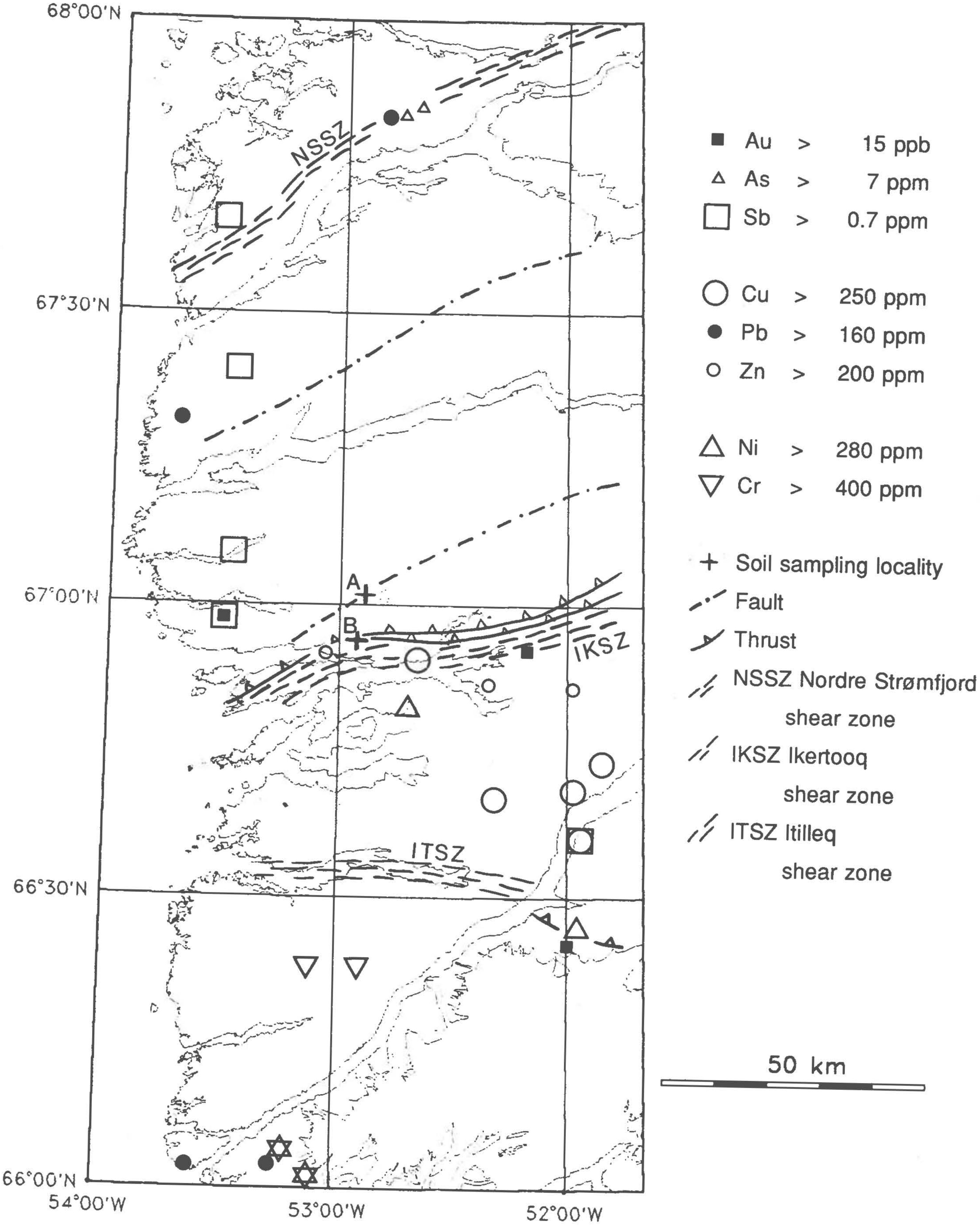

Fig. 46

Geochemical provinces

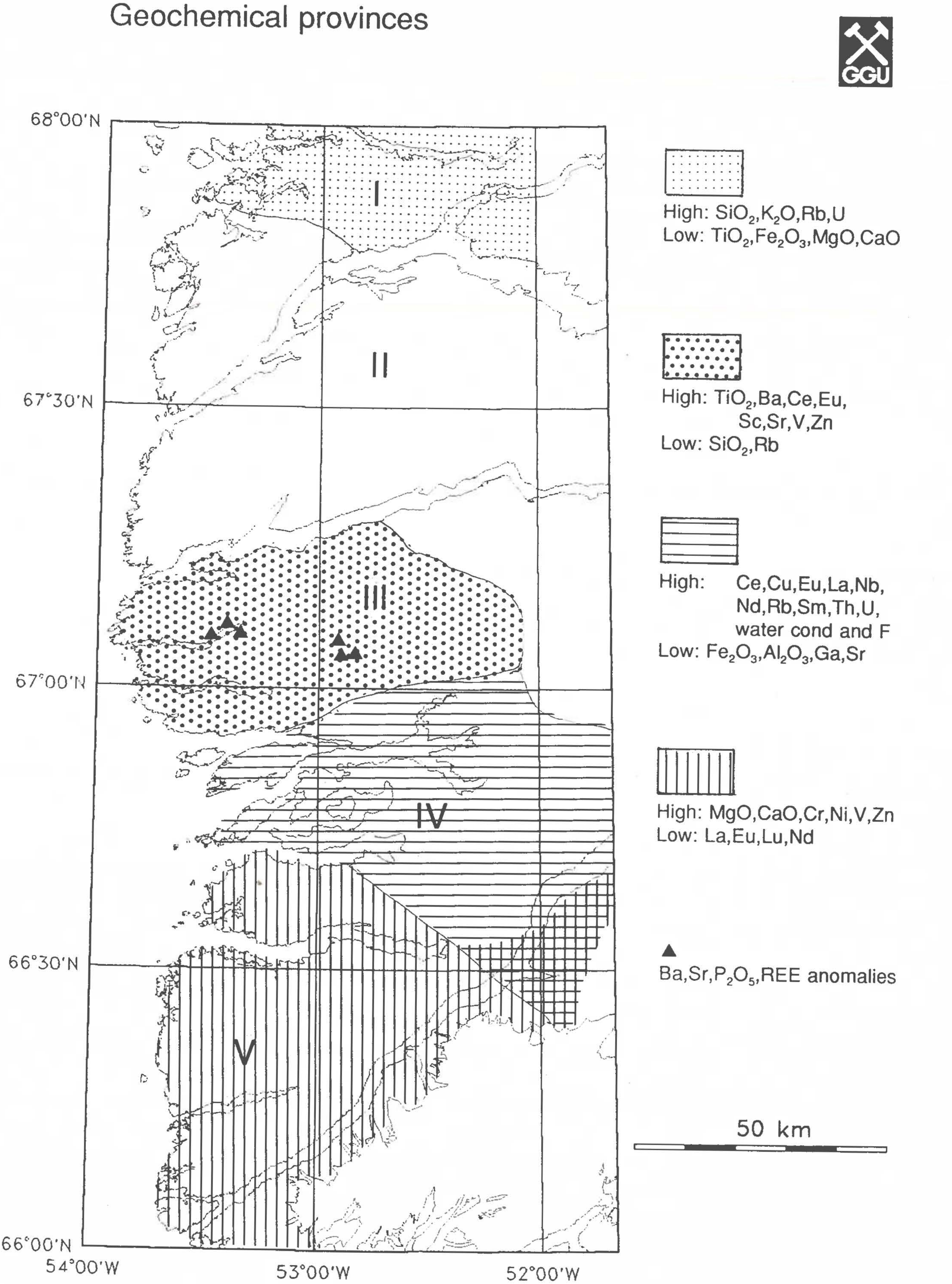

Fig. 47

ISSN 0903-7322